Assessment of Electrode Modifications for Vanadium Redox Flow Batteries

by

Caio Vinícios Juvêncio da Silva

B.Sc., Instituto Federal de Pernambuco, 2019

Thesis Submitted in Partial Fulfillment of the
Requirements for the Degree of
Master of Applied Science

in the
School of Mechatronic Systems Engineering
Faculty of Applied Sciences

SIMON FRASER UNIVERSITY
Spring 2022

Declaration of Committee

Name:	**Caio Vinícios Juvêncio da Silva**
Degree:	**Master of Applied Science**
Thesis title:	**Assessment of Electrode Modifications for Vanadium Redox Flow Batteries**
Committee:	**Chair: Helen Bailey** Lecturer, Mechatronic Systems Engineering
	Erik Kjeang Supervisor Professor, Mechatronic Systems Engineering
	Sami Khan Committee Member Assistant Professor, Sustainable Energy Engineering
	Woo Soo Kim Examiner Associate Professor, Mechatronic Systems Engineering

Abstract

Unlike traditional battery systems, vanadium redox flow batteries (VRFBs) have been gaining attention in the past years due to their advantages of flexible, scalable design and long-life cycle for energy storage applications. In these systems, porous electrodes such as carbon paper and carbon felts are often used due to their desirable properties including good acid resistance, high surface area, and reasonable cost. However, these materials may have drawbacks of poor reversibility and kinetics, which can affect the system overall performance. These limitations are related to interfacial phenomena at the electrode-electrolyte interface, which can be mitigated by improving wettability and active surface area. Among several approaches, thermal and chemical treatments are common in literature since these treatments can improve wettability, increase electrochemical active surface area, and can provide functional groups that are believed to facilitate vanadium redox reactions. Although different activation methods can improve electrode performance, there is a limited understanding and disparity between literature reports on how to assess the relevant properties in order to elucidate improvement mechanisms. Hence, this work aimed to systematically assess different modified electrodes so that impediments can be further understood, and reliable engineering solutions can be designed to mitigate such limitations. For that, a series of modified graphite felt electrodes were fabricated using different activation methods (thermal treatment, chemical treatment, and catalyst coating) and subjected to physical, chemical, and electrochemical characterization methods. The results revealed that wettability and electrochemical active surface area are the main physical and chemical properties that correlate to electrochemical performance improvements. More efficient electrodes can be achieved through thermal treatment by tuning process variables in order to enhance electrode properties. Moreover, performance can be further increased by combining thermal treatments and catalyst materials, though the main contribution in energy efficiency comes from the thermal activation process, which improved electrode wettability and consequently enhanced kinetics.

Keywords: Energy Storage; Vanadium Redox Flow Battery; Electrode; Activation; Catalyst.

Dedication

I would like to dedicate this thesis to all my family, in special to my mom Edilma Juvêncio, who has been my greatest inspiration and biggest support since day one. We did it, mom!

Acknowledgements

Foremost, I would like to appreciate and show my sincere gratitude and admiration to my advisor Dr. Erik Kjeang, for not only giving me the opportunity to work under his supervision, but also sharing many pieces of advice and passing along his enormous knowledge. I truly appreciate all the support, trust, and freedom he gave me during my research project so that I could become a more experienced researcher and engineer.

I would also like to express my appreciation to my NRC supervisor Dr. Vladimir Neburchilov, who was patient enough to guide me, teach me and pass along all his knowledge. I also appreciate all the encouragement for me to become more critical and proactive, having the freedom to suggest and try different approaches, no matter the outcome. The most important thing he taught me was how privileged we, as researchers, are to work with science and do what we love.

I would like to thank all my NRC coworkers who were extremely patient when I first joined the group and had so many questions. I want to thank Elizabeth Fisher, Shaochen Ding, Ken Tsay, Alison Plater, and Chaojie Song for all the support and for answering all my questions and helping me with my experiments.

I would also like to thank my FCReL colleagues, who also gave tremendous support. I want to thank Dr. Pei Pei for an incredible lab management and support in the lab. I want to thank two of my predecessors Drs. Omar Ibrahim and Marc-Antoni Goulet for all the knowledge and inspiration. I want to thank all the other graduate students and post-docs in the group, who may not work in the same research area as me, but also taught me important things.

I would like to thank the committee members Dr. Sami Khan and Dr. Woo Soo Kim for the constructive feedback and for all the academic advice throughout my graduate studies. I really appreciate your feedback and I believe it has enriched my research and helped my academic development.

Other than colleagues and coworkers, I would like to thank my friends who were the ones that saw both my success and my struggle, in especial Ana, Marcos and Renata.

I want to thank my friends from Brazil who, even though we are miles away, were always there for me. I want to thank my friends here in Vancouver who made me feel like home. I also want to thank my volleyball friends, especially Ted Lee, who introduced me to volleyball, which ended up being my getaway when I was too stressed about research and graduate studies.

Last, and far from be the least, I want to thank my family who has been my biggest supports and never doubted me, even when I did myself. My mom Edilma, who worked hard for me to get the best education and helped me to pursue my dreams. Thank you for believing in me.

Table of Contents

List of Tables

List of Figures

List of Acronyms

BET	Brunauer–Emmett–Teller
CA	Contact Angle
CE	Coulombic Efficiency
CF	Carbon Fiber
CNT	Carbon Nanotube
CTAB	Cetrimonium Bromide
CV	Cyclic Voltammetry
DMF	Dimethylformamide
EE	Energy Efficiency
EIS	Electrochemical Impedance Spectroscopy
ESS	Energy Storage System
FCReL	Fuel Cell Research Laboratory
GF	Graphite Felt
GFE	Graphite Felt Electrode
GONP	Graphene Oxide Nanoplatelet
HER	Hydrogen Evolution Reaction
LAC	Library and Archives Canada

MSP	Method of Standard Porosimetry
MWCNT	Multi-walled Carbon Nanotube
NASA	National Aeronautics and Space Administration
NRC	National Research Council Canada
RFB	Redox Flow Battery
rGO	Reduced Graphene Oxide
SAC	Special Active Carbon
SCE	Saturated Calomel Electrode
SEI	Sumitomo Electric Industries
SEM	Scanning Electron Microscope
SGL	SGL Carbon SE
SFU	Simon Fraser University
SoC	State of Charge
SSA	Specific Surface Area
UNSW	University of New South Wales
VE	Voltage Efficiency
VRFB	Vanadium Redox Flow Battery
WC	Tungsten Carbide

OCP	Open Circuit Potential
XPS	X-ray Photoelectron Spectroscopy

Chapter 1.

Introduction

This chapter summarizes the technical and scientific issues and opportunities related to Vanadium Redox Flow Battery (VRFB) systems, as well as the importance of this thesis for the electrochemistry field and commercial applications. Understanding the system limitations and how to assess them is essential to design better engineering solutions to achieve higher performances, which is the focus of this work. Hence, this chapter aims to provide an VRFB overview, discuss its challenges and present different modification approaches to mitigate interfacial limitations related to the electrode performance.

1.1. Problem Overview

Renewable energy resources, unlike fossil fuels, offer a near limitless supply of energy. However, there are times when renewable sources are not available. For instance, solar energy is unavailable during periods of cloud or darkness, and wind is not always available. Conversely, there are periods where natural energy is overly abundant: energy is wasted because, for instance, wind turbines cannot be turned off. To resolve these issues, energy storage solutions, such as batteries, have been proposed to store excess energy for use during periods when renewable energy sources may be otherwise unavailable.

For large-scale applications, energy storage systems such as batteries must present some desirable features. In terms of performance, they must be able to provide durability for charge and discharge cycles without losing capacity. In addition, storage systems must have high efficiencies and the ability to rapidly respond to changes in load or input. In terms of economy, they must have a considerable life cycle and reasonable cost [1]. Another desirable feature of a battery system is scalability, which is essential to

provide flexibility for demand uncertainties and be able to supply more energy to the system when needed. One type of batteries that is often considered is lithium-ion, however, they cannot withstand many cycling times without degradation [2]. Thus, among all different battery technologies, one promising solution that can meet many of these requirements would be the redox flow batteries (RFBs), which feature a flexible design and has an independent relationship between power and capacity [3]. Although different redox flow systems have been developed and implemented over the years, vanadium redox flow batteries are one of the technologies that have been receiving more attention because of their advantages such as fast-charging time, ability to deep discharge, and large-scale applicability [4].

In VRFB systems, electrodes are vital components having a great impact on the system's overall performance. Both electrodes (positive and negative) are made of carbon-based materials (*e.g.,* carbon felts, carbon cloths, and carbon papers) [5], since carbon materials have some advantages over other materials, such as reasonable cost, porous structure, and wide operation range [4]. However, these materials have some disadvantages like poor electrochemical activity and poor reversibility [2]. To address these drawbacks, several modification approaches have been studied in literature [6-9], including thermal and chemical treatments, which were firstly proposed by Maria Skyllas-Kazacos [11,17], heteroatom doping [12], KOH treatment [13], and the adoption of different electrocatalysts [14-16].

Thermal treatment is one of the most used methods for electrode activation, both in research and industry since it is a simple and cost-effective method to improve electrode performance. The main improvement mechanism provided by thermal activation is the introduction of functional groups onto the electrode surface. Thermal treatment process leads to the formation of different functional groups, such as phenolic (C-O), carboxylic or carbonyl groups (C=O, C-O-C), which can improve electrode wettability, as proposed by Skyllas-Kazacos [11]. Recent studies have reported that functional groups may increase the electrochemical activity of vanadium ions on the electrode surface, which can improve the charge transfer at the electrode-electrolyte interface [18,19]. Thus, in order to introduce these functional groups on the electrode surface, different thermal activation processes have been proposed, varying parameters such as temperature, time and atmosphere. Although thermal activation is often used in literature, there is still a debate whether improvements are due to functional groups or wettability improvements. Chapter

4 will evaluate the impact of different thermal treatment parameters, such as temperature and time, as well as aging and re-treatment process.

Another modification approach often presented in literature is the introduction of oxygen functional groups through chemical treatments. Chemical activation is also believed to improve electrode performance by introducing oxygen functional groups that can both improve wettability and reaction kinetics. However, little work has been done in order to understand the combination of thermal and chemical treatments, which can potentially have synergy and further improve electrode performance. Thus, Chapter 4 will also focus on understanding the impact of post thermal activation process on physical and chemical properties and how these changes correlate to electrochemical performance.

Besides thermal and chemical treatments, another activation method proposed in literature is catalyst deposition, which can improve both active surface area and charge transfer resistance. For that, catalyst selection is important, since, aside from increasing active surface area and improving kinetics, catalyst materials must not promote side reactions such as hydrogen evolution in the negative half-cell, as well as being stable in acidic media. Different parameters must be taken into consideration during ink formulation and coating process, such as catalyst particle size, electrical conductivity, stability, corrosion resistance, and others. Moreover, the catalyst deposition method must be selected in a way that catalyst particles are evenly distributed onto the electrode surface throughout the porous structure so that the active surface area can be enhanced without agglomeration and pores being blocked. Furthermore, catalyst cost and availability also play important roles in the catalyst selection. Hence, Chapter 5 will investigate catalyst selection and activity for the positive electrode and Chapter 6 will discuss catalyst selection for the negative electrode, assessing physical and chemical modifications and proposing improvement mechanisms for selected catalyst materials.

Pre-treatment cleaning is often proposed so that residual impurities from electrode fabrication can be eliminated. However, more work needs to be done in order to understand the importance of cleaning processes prior to thermal activation. Thus, Chapter 7 will investigate the impact of different solvents on cleaning the electrode surface and evaluate the impact of pre-treatment cleaning on different activation temperatures.

In literature, comparing results and understanding functional impediments may be somehow complex, since different electrode properties and test parameters can influence performance results. Hence, Chapter 8 will discuss different electrodes properties that can have impact during *in-situ* VRFB cycling tests. Both activation properties and cycling test parameters were taken into consideration and their correlations with performance results are discussed.

1.2. Motivation and Objectives

Vanadium redox flow batteries are becoming very attractive for energy storage applications because of their advantages such as flexible, scalable design and long-life cycle. However, improvements still need to be done to make this technology more cost-effective for large-scale applications. One way to improve the VRFB energy efficiency is to enhance the electrode performance. Although different approaches have been proposed in literature, there is still a debate on how these activation processes improve system performance and what the main improvement mechanism is. Hence, assessing electrode modifications is important to understand how activation methods impact different properties (physical, chemical, and electrochemical), and then elucidate the main mechanism for improving electrode performance in a complete VRFB cell.

The main objective of this thesis is to systematically assess electrode modifications such that reliable engineering solutions for VRFB systems can be designed and implemented. Other objectives are:

1. Investigate the correlations between physical, chemical, and electrochemical properties and their impact on electrode performance.
2. Investigate the impact of thermal treatment variables on electrode wettability and electrochemical performance.
3. Investigate and evaluate the impact of thermo-chemical combined treatments on electrode performance.

4. Understand the importance of pre-cleaning treatments prior to thermal activation.

5. Selection and deposition of electrocatalysts for both positive and negative electrodes.

1.3. Thesis Outline

This thesis focuses on understanding vanadium redox flow battery system limitations and proposing electrode modification methods to achieve robust systems with high performance. Moreover, functional impediments are proposed, taking into consideration different parameters so that electrode performance can be assessed. This thesis is divided into the following chapters:

Chapter 1 provides a problem overview and outlines research objectives, scope, and contributions.

Chapter 2 presents a literature review regarding VRFB systems and their limitations, as well as research progress and improvement opportunities.

Chapter 3 provides a description of the experimental approach adopted for electrode fabrication, characterization, and *in-situ* and *ex-situ* testing.

Chapter 4 presents the results and discussion related to thermal treatment, evaluating the impact of different activation parameters, as well as the combination of thermal and chemical methods and its influence.

Chapter 5 provides the results and discussion related to coated electrodes using both noble and non-noble metal catalysts materials for the positive electrode.

Chapter 6 presents the results and discussion related to activated electrodes using both metal and ceramic catalysts materials for the negative electrode.

Chapter 7 explains the importance of pre-treatment cleaning prior to thermal activation and its impact on physicochemical properties and electrochemical performance.

Chapter 8 provides a functional impediments analysis for different activation parameters that need to be taking into consideration for performance assessment.

Chapter 9 presents the conclusions and proposes future work for this study.

1.4. Findings and contributions

So far, the results from this thesis have been presented in two international conferences organized by the Electrochemical Society (ECS), which are listed below:

(1) V. Neburchilov, K. Tsay, K. Fatih, R. Neagu, O. Kodra, **C. Juvencio da Silva**, E. Kjeang, Efficient Catalysts for VO+2/VO2+ Redox Couples in Vanadium Redox Flow Batteries. ECS Meeting Abstracts - PRiME (2021). MA2021-02 101.

(2) V. Neburchilov, K. Tsay, K. Fatih, R. Neagu, O. Kodra, E. Kjeang and **C. Juvencio da Silva**, Highly Energy-Efficient Vanadium Redox Flow Batteries with Thermo-Chemically Activated Graphite Felt Electrodes. ECS Meeting Abstracts – PRiME (2020). MA2020-02 208.

Other than conference papers, peer-reviewed journal papers are planned to be prepared and submitted based on the results presented in this thesis.

Chapter 2.

Literature Review

This chapter provides a detailed literature review on different energy storage systems and their advantages and disadvantages, mainly focusing on vanadium redox flow batteries. It will cover VRFB history, applications, advantages and disadvantages, components, and limitations. Moreover, it will present a review on different electrodes modifications and approaches used in former studies to improve electrodes performance and overcome interfacial phenomena limitations. Lastly, it will discuss proposed improvement mechanisms and characterization tools used to assess these modifications.

2.1. Energy Storage Systems

Although electricity can easily be generated, transmitted, and transformed, efficient ways to store energy is still needed, especially for intermittent renewable energy systems such as solar and wind systems, which have been gaining much attention lately. Although different battery technologies have been proposed using different cell chemistry, they are often used for different applications, since each battery system has their own pros and cons. The main battery technologies often seen in ESS are listed below:

1. Lead Acid Batteries

This is one of the most mature systems and it has been used mostly in applications where a lot of power is needed, and weight is not necessarily a concern. Although lead acid batteries are considerably cheap with a high-power output capacity, some disadvantages like limited life cycle and low specific energy are the main limitation for this technology.

2. Lithium-ion Batteries

Lithium-ion batteries usage has been increased significantly over the past years. The popularity comes from their advantages such as high energy density, low cost, low-self discharge and cycling efficiency. While lead acid batteries have been used for automobile applications, lithium-ion batteries are the main candidates for electric cars application. However, some challenges still need to be overcome, such as safety concerns (over-heat and explosions), raw material resources (lithium availability), cost, scalability and high emissions associated with production and recycling.

3. Redox Flow Batteries

Redox flow batteries, also known as flow batteries, are not as mature as the other systems, but have been gaining a lot of attention lately due to their advantages over conventional energy storage systems. While conventional technologies offer limited power and energy, RFBs have decouple energy and power, which makes them attractive to stationary applications, since a flexible design and scalability are key features for these applications. For these systems, some disadvantages such as low energy density and safety concerns are the main concerns.

As abovementioned, these systems have different advantages and disadvantages regarding different systems specifications, such as life span, energy density and cost. A summary is presented below in Table 1 comparing different properties for these systems.

Table 1. Energy storage systems comparison [67]

	Lead acid	Lithium-ion	VRFB
Life span	2 years	3 - 5 years	**15 - 20 years**
Power and capacity	Linked	Linked	**Decoupled**
Depth of discharge	50%	80%	**100%**
Energy density	60 $Wh.l^{-1}$	300 - 400 $Wh.l^{-1}$	**18 – 45 $Wh.l^{-1}$**
Cost	600 – 1000 £ kWh^{-1}	120 - 300 £ kWh^{-1}	**200 – 400 £ kWh^{-1}**
Operational risks	Safe	Overheating (explosion)	**Hydrogen evolution (explosion)**

As shown in Table 1, VRFB systems offer some advantages over lithium and lead acid batteries such as life span and power capacity. However, VRFBs still need to overcome some limitations such as energy density and cost. Improving electrode performance is essential for those systems to operate at higher current density and reduce operational cost. Also, selecting proper catalyst materials that can hinder hydrogen evolution is important to reduce operation risks such as explosion, which can also impact system performance.

2.2. Redox Flow Batteries

Redox Flow Batteries are a promising system in the stationary energy storage field [4,5]. They were first studied by NASA in the 1970s for photovoltaic applications [6,7]. A few years later, in 1984, an all-vanadium redox flow battery was invented and developed

by researchers at the University of New South Wales in Australia (UNSW) [8,9,10]. Although there are several other types of redox flow batteries, vanadium batteries were the first commercialized systems for storage applications.

RFBs are electrochemical energy conversion devices (Figure 1) where the redox processes take place in the electrode-electrolyte interface using two different electrolytes. Both electrolytes are stored in external tanks and pumped into the batteries, which can be used to scale up the system if needed. Moreover, power and energy are decoupled. If the energy capacity needs to be increased, electrolyte tanks can be increased so more electrolytes can be stored. If power capacity needs to be increased, more cells can be added into the cell stack, since power and energy capacity are independent. Thus, the ability to increase the power capacity in this type of system makes applications in large-scale energy storage systems desirable [20].

Different RFBs have been proposed in literature, using different redox couples and mechanisms (see Figure 1). The main RFBs technologies are listed below.

- All Vanadium Redox System
- Vanadium-Bromine Redox System
- Iron-Chromium Redox System
- Zinc-Cerium Redox System

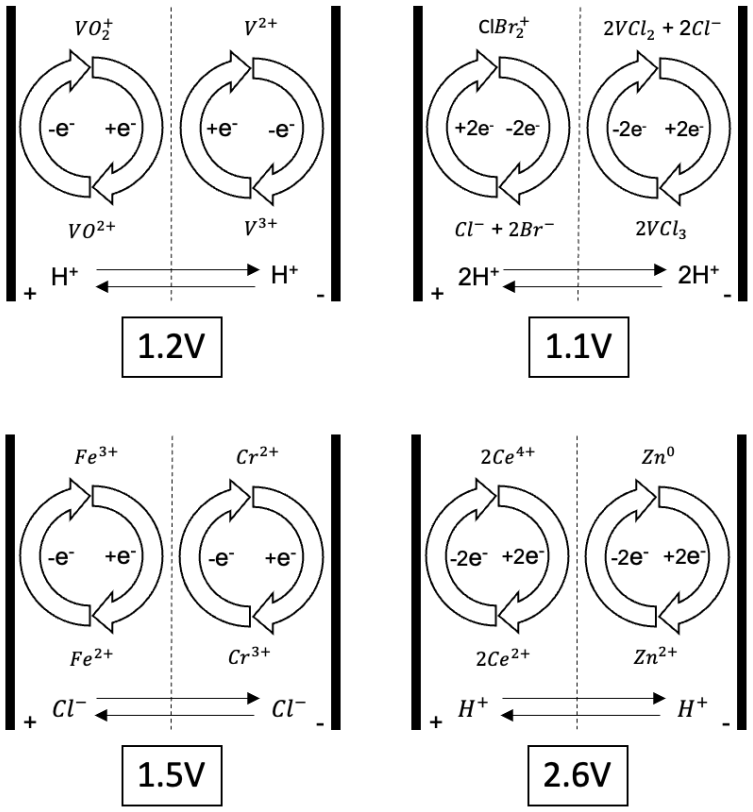

Figure 1. Different Redox Flow Battery technologies and their potential. a) All vanadium, b) vanadium/bromine, c) iron/chromium, d) zinc/cerium [21]

2.3. Vanadium Redox Flow Batteries

Whereas different redox flow systems have been proposed, vanadium redox flow batteries are receiving more attention because they have some advantages over the other flow batteries, especially since they use the same element for both electrolytes, which eliminates the crossover degradation and maintenance costs for electrolyte recovery. Although more efforts need to be done to make the system more efficient, VRFB systems have shown commercial progress and they have been used in several applications. Two different vanadium redox flow batteries were proposed in literature: all-vanadium and vanadium-bromide batteries. These systems are described below:

a) All Vanadium

In other systems, such as Iron/Chromium and Bromide/Polysulfide, the cross-over of the species and mixing of electrolytes is still a concern. The crossover of the elements affects not only the performance of the charge/discharge cycle and consequently the efficiency, but also the degradation of the system itself, which will lead to higher expenses with electrolyte separation and reactor recovery [22].

To solve this problem, a system where the same element is used (in different oxidation states) in both electrolyte composition was developed. As a result of that, crossover represents only a loss in system efficiency, but can be easily fixed by recharging the electrolyte, not requiring its removal or recovery.

In this type of system, vanadium is used in four different oxidation states: V(II), V(III), V(IV) and V(V). Where the pairs V(II) and V(III) are used in the negative electrolyte, and V(IV) and V(V) in the positive electrolyte, which generally exist in the form of VO^{2+} and VO_2^+. Electrochemical reactions for negative and positive electrolyte are captured below, respectively:

$$V^{3+} + e^- \rightleftarrows V^{2+} \qquad E^0 = -0.496 \text{ V vs SCE} \qquad (1)$$

$$VO_2^+ + 2H^+ + e^- \rightleftarrows VO^{2+} + H_2O \qquad E^0 = +0.750 \text{ V vs SCE} \qquad (2)$$

Both electrolytes have intrinsic colors that can be used to identify the oxidation state (Figure 2). Changing the oxidation state of vanadium causes the charge to be stored and released, and when these processes happen, there is a change in the pH of the system, also causing the electrolyte colors to change. Initially, V(II) has a purple color, and when it is oxidized to V(III), it becomes green, while V(IV) has an initial blue color, turning into yellow when it gets oxidized.

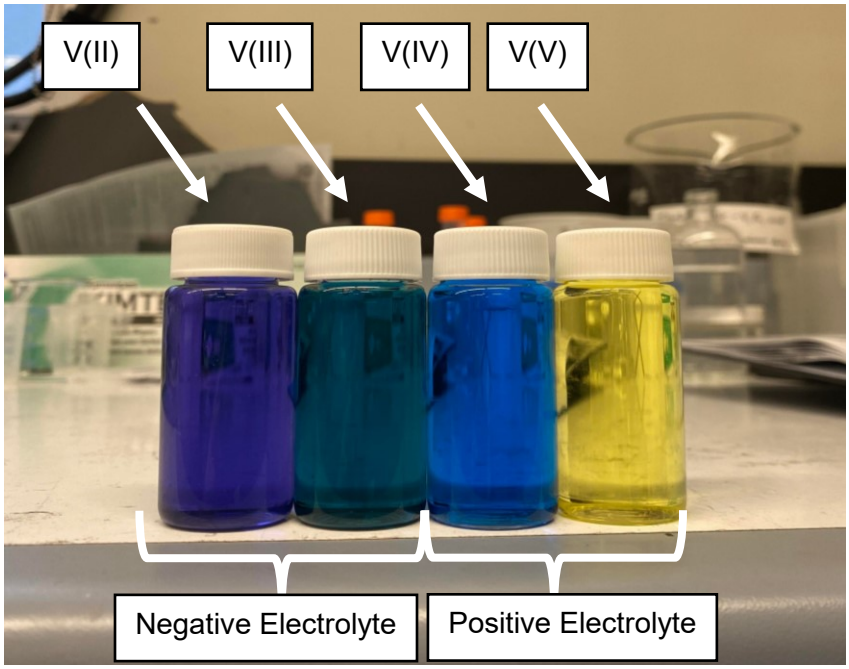

Figure 2. Vanadium Electrolyte and its different oxidation states.

b) Vanadium / Bromide

Since vanadium ions have limited solubility in the electrolyte, researchers have found that the solubility can be increased in the presence of halide ions [21]. In these systems, Br^- and Br_3^- couple are used in the positive electrolyte, and polyhalide ions Br^2Cl^- are formed in positive half-cell after oxidation. Due to the high solubility of vanadium bromine, the energy density of this system also increases significantly (35 - 70 Wh/L), when it is compared to the energy density of an all-vanadium system (25 - 35 Wh/L) [21]. Despite this improvement in energy density, other concerns may arise from the additive used, such as the emission of toxic bromine vapors. Therefore, to eliminate this issue, complexing bromine agents can be used to minimize or even eliminate emissions of bromine vapors [23].

2.3.1. History

VRFBs were firstly studied in early 1984, when Maria Skyllas-Kazacos and her co-workers from UNSW in Australia developed the system. Later in 1998, patent rights were bought by Australian Pinnacle Vanadium Redox Batteries Company and then Sumitomo Electric Industries (SEI) were the first ones to design cell stacks and make integrated systems under Pinnacle license. VRFBs were the first RFBs systems being commercialized for energy storage applications in 1996. Over the past years, VRFB system have made huge progress and applications have grown, where systems from kW to MW scales can be seen worldwide. Some of the systems and applications are listed below:

- Renewable Energy Dynamics Technology Ltd was responsible for installing a 5 kW system with a 5 hours storage capacity (60 kWh). This system is located at the University of Evora campus, and it is integrated with a photovoltaic system. The main goal for this system is to maximize the efficiency of photovoltaic generation and reduce energy costs [24].

- Pinnacle VRB company, with the support of the Australian Greenhouse Office grant, installed a 200 kW capacity storage system in Tasmania. The aim of this system was to reduce Hydro Tasmania's diesel expenses, which used this technology to gain insight into commercial VRB design and operation [25].

- Winafrique Technologies Ltd has installed two 5 kW systems. The systems were installed at two telecommunication stations in Kenya, with Safaricom Limited support. Traditionally, power was supplied from lead acid batteries and by diesel generators. However, due to the increased cost of fuel and equipment maintenance, and the concern about environment impacts caused by pollution, the company aroused interest in the use of renewable sources for power generation. Thus, connected to a solar or wind energy system, the VRFB system guarantees the power supply for up to 14 hours [26].

As it was shown above, VRFBs have potential to be used in large-scale energy storage applications. However, there are still some technical limitations that need to be overcome, especially performance improvements to reduce up-front capital cost for VRFB systems and make them more cost-effective.

2.3.2. Operation

In a typical VRFB system, vanadium compounds are dissolved in a sulfuric acid solution as electrolyte for chemical energy storage. In these systems, vanadium is used in four different states, as shown in Figure 2.

Before starting the cycling tests, both electrolyte tanks are filled with vanadium electrolyte (usually made of vanadium sulphate) with an average 3.5 oxidation state. The initial commercial electrolyte in the positive tank is oxidized to V(IV), while the other portion gets reduced to V(III) in the anolyte tank. Vanadium concentration is usually around 1.6M, while sulfuric acid concentration is around 2M for safety and handling concerns. The system operates in low temperatures (10 to 40^{o}C) to avoid vanadium precipitation in the electrolyte [134]. Figure 3 below illustrates a typical VRFB system.

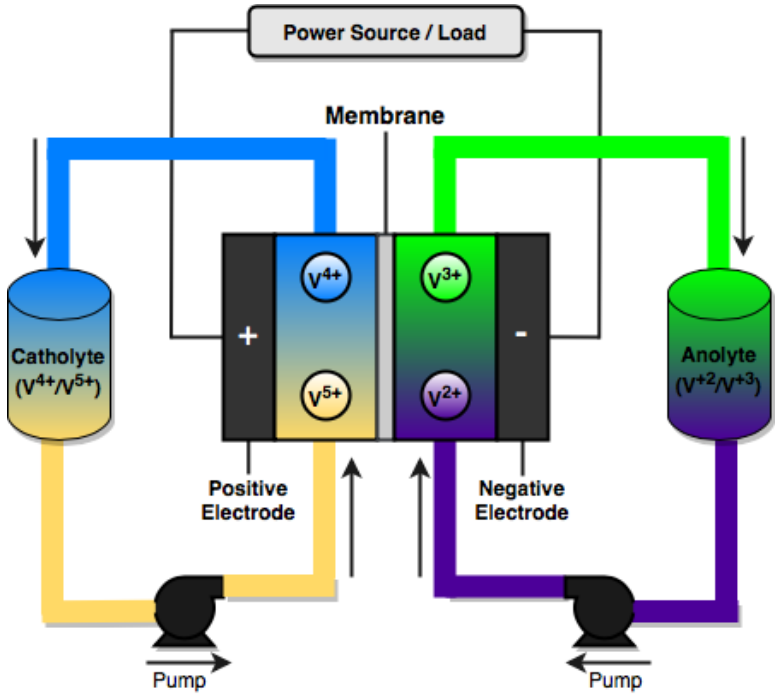

Figure 3. Vanadium Redox flow battery system and its components

In a typical operation, during charge V(III) electrolyte will be reduced to V(II), while V(IV) is oxidized to V(V). Conversely, in a discharge process, V(II) is oxidized to V(III) in the anolyte, while V(V) is reduced to V(IV) in the catholyte tank. To avoid electrolyte oxidation in the anolyte tank, an inert gas is purged to avoid air oxidation, while catholyte tank does not need to be purged, since only V(II) is impacted by air oxidation. Crossover and electrolyte imbalance may happen during long operations, which can be severe depending on the membrane material and tests parameters.

2.3.3. Components

In a VRFB system, different components such as membrane, electrodes and electrolyte are essential for system operation and those are the main research areas often seen in literature. The main components are listed below.

Membrane

Membrane is the component that separates the two half-cells, avoiding electrolytes mixing. Besides avoiding crossover contamination, it must allow the passage of ions to promote the current flow [27]. Membranes can be classified as ion exchange membranes or cation exchange membranes, according to the type of ionic group used. Moreover, membranes can be classified as perfluorinated ionomers, partially fluorinated polymers, non-fluorinated hydrocarbons, and others [28], based on the chemistry composition. The main research focus for membranes is designing membrane materials that can reduce ionic conductivity, avoid crossover and electrolyte imbalance, and ensure chemical stability [140]

Electrolyte

Electrolyte is defined as a solution that conducts current through ionization [29]. In a vanadium redox flow battery system, two different electrolyte composition are used for each half-cell. While they used different vanadium oxidation pairs for each electrolyte, sulfuric acid is used as supporting electrolyte for both half-cells, which supports double redox reactions (reduction and oxidation), helping to balance the ionic charges. In addition, supporting electrolytes provide extra ions to increase solution conductivity and improving current flow [29]. The main research focus for electrolyte is the impact of different additives to enhance performance and stability [75].

Electrodes

In VRFBs, the electrodes are one of the most important components, and their properties have a great impact on system performance since the reactions take place at the electrode-electrolyte interface. Electrodes must present some properties such as high electrical conductivity, high surface area, good wettability, chemical stability, low cost, high porosity, and others [30].

Both positive and negative electrodes are usually made from carbon-based materials (Figure 4), such as carbon felts, carbon cloths, carbon papers, and others [17],

since carbon materials have some advantages over other materials, like reasonable cost, porous structure, and wide operation range [31].

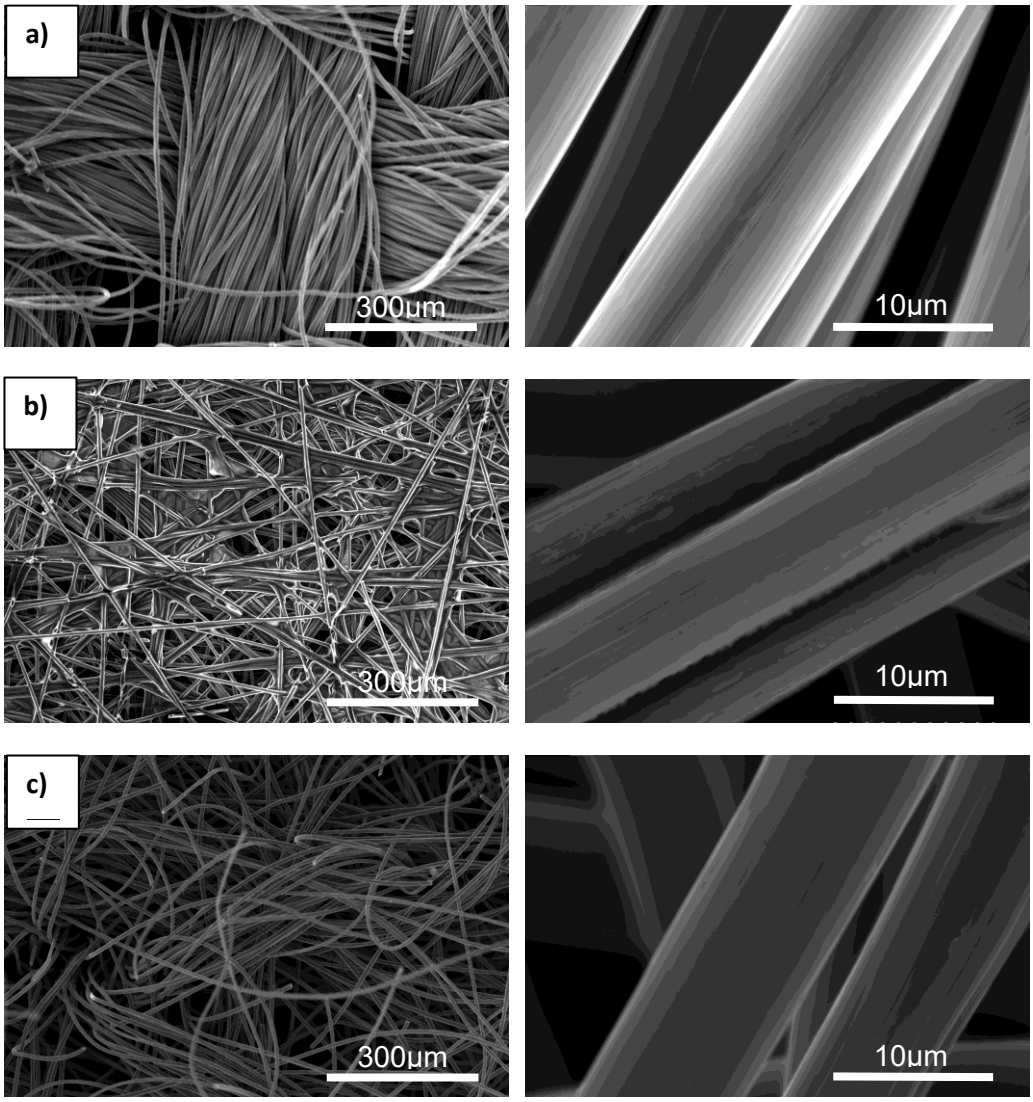

Figure 4. Common commercial materials used as electrodes for VRFB systems: a) carbon cloth, b) carbon paper, and c) carbon felt.

Although carbon-based electrodes are commonly used for VRFB applications, these materials have some disadvantages including poor electrochemical activity and poor

reversibility [2]. Interface phenomena challenges pose limitations to both performance and battery life cycle, which can also have an impact on operational cost. Understanding these limitations and proposing better solutions are the main goal for different electrodes research as well as for this work.

2.4. Test Parameters

For VRFB cycling tests, a single cell is charged and discharged at a specified current density using a potentiostat that can apply a load to the system. For *in-situ* measurements, performance is usually assessed by calculating several parameters such as energy efficiency, voltage efficiency and coulombic efficiency, which are the main criteria to quantify performance and for samples comparison. These parameters are defined below:

Energy Efficiency (EE) is defined as the ratio between the energy provided by the system when the cell is discharged, and the energy supplied to the system when the cell is charged. That is:

$$\eta_{EE} = \frac{\int P_{discharge}.(t)dt}{\int P_{charge}.(t)dt} \quad (3)$$

Where $P_{discharge}$ is the power delivered by the system during discharge, while P_{charge} is the power supplied to the system during charge, and t is the time. Energy efficiency is often used to understand the stability of the system.

Coulombic Efficiency (CE) is defined as the ratio between the current extracted during discharge process and the current provided during charging process.

$$\eta_{CE} = \frac{Q_{discharge}}{Q_{charge}} = \frac{\int i_{discharge}.(t)dt}{\int i_{charge}.(t)dt} \quad (4)$$

Where $Q_{discharge}$ is the charge extracted from the single cell, Q_{charge} is the charge supplied to the system during charge, $i_{discharge}$ is the current during discharge and i_{charge} is the current during charge. Coulombic efficiency is often used to evaluate the performance of the membrane or the effect of side reactions.

Voltage Efficiency (VE) is defined as the ratio of the cell voltage during discharge and voltage during charge. It can be interpreted as a polarization measurement since it integrates ohmic and polarization losses during cycling. In other words:

$$\eta_{VE} = \frac{\int V_{discharge}.(t)dt}{\int V_{charge}.(t)dt} \quad (5)$$

Where $V_{discharge}$ is the voltage of the system during discharge, V_{charge} is the voltage of the cell during charge.

In literature, voltage efficiency is often calculated as the ratio between the energy and coulombic efficiency. However, this is a simplified approach since pump losses are neglected. For this approach, we have:

$$\eta_{VE} = \frac{\eta_{EE}}{\eta_{CE}} \quad (6)$$

While coulombic efficiency is often used to evaluate membrane performance, voltage efficiency is used to understand and evaluate electrode performance.

2.5. Electrochemistry of VRFB

2.5.1. Cell reaction

Standard potential for a VRFB system is described below:

Negative: $V^{3+} + e^- \rightleftarrows V^{2+}$ E^0 = -0.496 V vs SCE

Positive: $VO_2^+ + 2H^+ + e^- \rightleftarrows VO^{2+} + H_2O$ E^0 = +0.750 V vs SCE

Overall: $V^{3+} + VO^{2+} + H_2O \rightleftarrows V^{2+} + VO_2^+ + 2H^+$ E^0 = +1.246 V vs SCE

2.5.2. Nernst Equation

The Nernst equation is used for the calculation of the cell's non-standard potential. The redox reaction, indicating the anodic and cathodic reactions, is shown in Equation 7.

$$E = E^0_{cell} - \frac{RT}{nF}.ln\frac{[V^{+3}]_S.[VO^{+2}]_S}{[V^{+2}]_S.[VO_2^+]_S.[H^+]_S{}^2} \quad (7)$$

Where E^0, R, T, n, F and stands for standard cell potential, gas constant, cell temperature, number of electrodes involved in the reaction, Faraday constant respectively.

The corresponding Nernst equation is used to calculate the VRFB's open circuit cell voltage. The subscript S denotes surface quantities. A calculation using typical concentrations is shown in [32]. Although it may seem tempting to increase the cell voltage, the stability window of water must be considered. Recall, the use of aqueous solutions is a key benefit of VRFBs. For discharging, the standard cell voltage of 1.26 V is

near the extent of the stability window of water (1.23 V) [33], which permits the use of aqueous electrolytes.

2.5.3. State of Charge (SoC)

SoC can be described as the relative amount of accessible charge stored in the electrolyte. It can range from 0% to 100%, where 0% being the bottom of charge and 100% represents the top of charge. Thus, at the bottom of charge, we have 100% V(III) concentration and 0% V(II) for the anolyte, and 100% V(IV) and 0% V(V) for the catholyte, and the opposite at 100% SoC (top of charge). SoC can also be used to determine species crossover, since SoC is related to cell voltage. In a determined cell voltage, reading a different SoC can be an indication of crossover and unbalanced electrolyte. The state of charge can be calculated from the species concentration, and it can be seen below.

$$SoC_{Anolyte} = \frac{C_{V^{2+}}}{C_{V^{2+}} + C_{V^{3+}}} \tag{8}$$

$$SoC_{Catholyte} = \frac{C_{VO_2^+}}{C_{VO_2^+} + C_{VO^{2+}}} \tag{9}$$

2.5.4. Electrode Kinetics

Besides Nernst equation, Tafel and Butler-Volmer equations are often used in literature to study electrode kinetics. The first equation is Butler-Volmer, which can be derived from the overpotential relationship:

$$J = J_o \left[\frac{c_O^s}{c_O^b} e^{\left(\frac{-\alpha F \eta}{RT}\right)} - \frac{c_R^s}{c_R^b} e^{\left(\frac{(1-\alpha) F \eta}{RT}\right)} \right] \tag{10}$$

Where C_o is the concentration for the oxidized species, C_R is the concentration for the reduced species, b stands for bulk and s for surface, α is the transfer coefficient and η is overpotential.

When studying kinetics parameters, it is preferable to avoid concentration gradients, and then ensure that both surface and bulk concentrations are kept the same. One way to achieve that is to mix solution (*e.g.,* rotating disk electrodes), so mass transfer limitations are negligible and hence the equation can be simplified to:

$$J = J_o \left[e^{\left(\frac{-\alpha F \eta}{RT}\right)} - e^{\left(\frac{(1-\alpha) F \eta}{RT}\right)} \right] \quad (11)$$

At small overpotential, the equation above can be further simplified to:

$$J = J_o . \frac{-F\eta}{RT} \quad (12)$$

Another equation used for kinetics studies is Tafel equation, which is a simplification of Butler-Volmer, and it can be used when overpotentials are considerably high (greater than 100 mV). At higher overpotentials, one of the terms in Equation 11 becomes negligible, and it can be simplified to:

$$\log j = \log J_o - \frac{\alpha F \eta}{2.3RT} \quad \text{for} \quad \eta\text{<-0.1V} \quad (13)$$

$$\log j = \log J_o + \frac{(1-\alpha) F \eta}{2.3RT} \quad \text{for} \quad \eta\text{>0.1V} \quad (14)$$

2.6. Interfacial Phenomena Limitations

Interfacial phenomena are critical not only for the system performance, but also for its life span and operational cost. A summary of the relevant phenomena at the VRFB electrode-electrolyte interface is shown in Table 2

.

Table 2. Impediments to performance at the electrode-electrolyte interfaces and their implications.

Component	Impediment	Type	Implications
Electrode	Surface area	Physical	Low current density
Electrode	Wettability	Physical	Low current density
Electrode	Charge transfer	Electrochemical	Slow kinetics
Electrode	Stability	Electrochemical	Lifetime
Electrode	Reversibility	Electrochemical	Slow kinetics
Electrode	Side reactions	Electrochemical	Low coulombic efficiency

For this thesis, the main limitations and impediments studied will be surface area, and wettability, while charge transfer and side reactions (hydrogen evolution) will also be discussed. For that, different approaches will be studied to tackle different limitations. While thermal treatment mainly improves wettability and active electrochemical surface area, catalyst materials can further improve charge transfer resistance and surface area while suppressing side reactions

2.6.1. Wettability

One of the main limitations of commercial graphite felt electrodes is their hydrophobicity. Commercial graphite felts are hydrophobic (Figure 5), and they have low active surface area. Wettability plays an important role in the electrode performance since pores need to be hydrophilic so electrolyte can penetrate as many pores as possible to increase the active electrochemical surface area and consequently improve electrode kinetics. Thus, different treatments have been proposed in literature to improve electrode's wettability [3,11,17]. The main two treatments are thermal and chemical treatments that can introduce desirable functional groups and make the electrodes hydrophobic. However, one main concern is stability, since these functional groups may degrade over time. Thus, providing a long-term solution for this problem is essential.

Figure 5. Commercial pristine graphite felt electrode hydrophobicity

2.6.2. Active Surface Area

Another drawback of carbon electrodes, such as graphite felt electrodes, is the low active surface area. Commercial graphite felt used in this work has a surface area of 0.4 m^2/g, which is lower compared to other electrodes. Increasing active surface area can improve kinetics, since more active sites will be available for the reactions to take place. Different modifications such as etching process have been proposed in order to increase

surface area and enhance electrode performance [17,107,114]. However, chemical treatments proposed in this work only introduced oxygen functional groups rather than etching and increasing surface area. Catalyst materials with high specific surface area (SSA), such as carbon supports are often used in literature since it uses the same material as the electrode (carbon) [157]. Thus, to enhance electrode active surface area, carbon supports will be used to achieve higher SSA so that kinetics is improved.

2.6.3. Side Reactions

During charging, as the standard reduction potential of the negative electrode (-0.26 V) is below that of the standard hydrogen electrode (0.00 V), this thermodynamically allows for the simultaneous parasitic evolution of H_2 [34]. Not only does hydrogen evolution consume charge, but it also covers active area and clogs pores. The Laplace pressure of the H_2 bubbles can be very high [80]. This coupled with large breakthrough pressures for small pores, makes pushing electrolyte through to unclog the hydrogen-clogged pores infeasible. When covered in these bubbles, electrodes have significantly lower coulombic and energy efficiencies and higher electrical resistances. Hydrogen evolution presents serious design concerns as it is both explosive and can lead to severe degradation of the load bearing capability of surrounding metallic components (hydrogen embrittlement). In order to mitigate H_2 evolution, catalyst materials such as Ti [137] and Bi [138] are proven to reduce hydrogen evolution rates (HER). Hence, selecting catalyst materials that can both be active and mitigate hydrogen evolution is crucial.

2.7. Research Progress

Different treatments, the majority of which are thermal and chemical, have been proposed in the literature to improve wettability and active surface area of VRFB electrodes. Thermal and chemical treatments introduce desirable functional groups (mainly oxygen and nitrogen) and significantly enhance wettability [17, 32, 34, 35]. For such treatments, stability is a major concern since these functional groups are part of the

redox reactions and degrade over time. Other solutions have also been proposed, such as acid treatment [36], thermal activation in air [37], heteroatom doping [38], KOH treatment [39], and the adoption of different electrocatalysts [40-42]. Recently, more attention has gone towards the structural design of the pore-network, offering an additional avenue for exploration [32, 43]. An abridged review of modifications that have been investigated is shown in Figure 6.

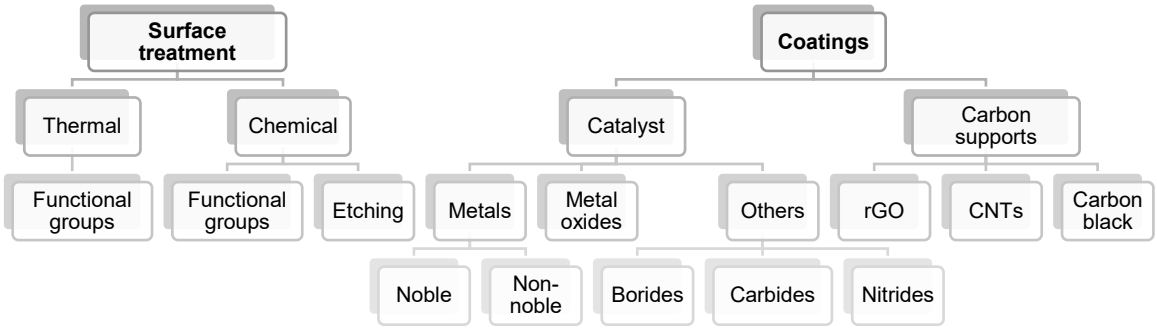

Figure 6. Different activation solutions proposed in literature.

Different modification approaches used in literature are listed below in Table 3, discussing their implications, improvement mechanisms and major drawbacks.

Table 3. Activation methods and their pros and cons.

Solutions	Type	Improvement	Drawbacks
Oxygen functional groups	Surface Chemistry	Wettability and kinetics	Stability
Nitrogen functional groups	Surface Chemistry	Wettability and kinetics	Stability
Plasma treatment	Surface Chemistry	Wettability	Stability
Metal catalysts	Coating	Wettability and kinetics	Cost
Metal oxide catalyst	Coating	Wettability and kinetics	Electrical conductivity
Carbon materials	Coating	Wettability, active surface area and kinetics	Agglomeration
Etching	Surface Morphology	Surface area	Strong acids
Micro-waved	Active Method	Wettability and surface area	Stability
Electrochemical pulse	Active Method	Wettability	Stability

2.7.1. Functional Groups

The impact of functional groups was first studied by Maria Skyllas-Kazacos in 1992, where a sample treated at 400°C for 30 hours showed a performance improvement due to oxygen-containing functional groups introduced via thermal treatment [11]. In addition to thermal activation, the impact of acid treatments on electrode surface chemistry and performance was also evaluated, where oxygen functional groups were reported to be the main improvement mechanism for the enhanced performance [17]. Besides oxygen-containing functional groups, different functional groups such as nitrogen [44,45,46,47,48,49,50,51,52,53,54], boron [55] and sulfur [56] were also studied, which are also believed to improve electrodes performance. These functional groups can be introduced to electrode surface through different methods such as thermal treatments, acid treatments, plasma jet and electrochemical treatments, where each treatment has a different impact on electrode performance due to changes in the physical and chemical properties of the electrode surface.

Although these treatments can enhance electrode performance, there is still a debate on whether oxygen-containing functional groups are beneficial for VO^{2+}/VO_2^+, V^{2+}/V^{3+} or both couples (see Table 4). As Skyllas-Kazacos discussed [11], C-O groups are believed to be associated with phenolic groups, while C=O groups are believed to be associated with both carboxylic and carbonyl groups. C-O groups were discussed to behave as active sites and have catalytic effects for VO^{2+}/VO_2^+. Kazacos also argued that improvements in hydrophobicity may be due to the increase of C-O groups. On the other hand, Dixon [51] stated that the enhanced performance of the electrodes was linked to the improved kinetics of the V^{2+}/V^{3+} mechanism. Due to the conflicting results and open debate, it is important to determine and understand how different functional groups (type and quantity) can impact the electrode performance.

Table 4. Impact of oxygen functional groups on electrode kinetics [34].

Impact on Electrodes				Reference
V^{2+}/V^{3+}	+	VO^{2+}/VO_2^+	+	11,57, 58, 59
V^{2+}/V^{3+}	+	VO^{2+}/VO_2^+	-	60, 61, 62

	Impact on Electrodes			Reference
V^{2+}/V^{3+}	Not mentioned	VO^{2+}/VO_2^{+}	+	63, 64, 65

Different treatments can impact electrode surface nature in different ways, introducing different types and amount of functional groups. Kim *et al.* [66] studied different surface treatments and their impact on surface nature and electrode performance. They reported that mild oxidation and plasma treatment can introduce more C-O and C=O functional groups to the electrode surface. Also, it was found that gamma-ray irradiation is the best approach to transform C=O into C-O (which is believed to be more beneficial to electrode kinetics). However, samples treated using gamma-ray irradiation method showed the lowest surface area compared to other treatments. Thus, it is also important to consider the balance between functional groups and surface area. Once there should be abundant active sites for the reactions to take place and also electrode surface nature must present favorable groups that can enhance electrode kinetics.

Also, studies have shown that the type of material is also important when making any conclusion about whether functional groups are benificial or not. Di Blasi et al [69] reported that carbon felt and carbon nanofiber showed a decrease in performance due to the increase of oxygen functional groups introduced by acid treatment. On the other hand, carbon paper and graphite rod has shown a enhanced performance due to the fact that the chemical treated cleaned the electrode surface and vanished oxygen species of the surface. Di Blasi also concluded that oxygen containing functional groups can be indeed benifical if they are introduced in a limited quantity, which he believes to be around 5%. In short, electrodes that contain too much oxygen will have a negative impact on its performance due to increased ohmic and charge transfer resistance.

A literature review was done to evaluate findings about the effect of functional groups. It was noticed that there is a lack of agreement on what funcional group is the most beneficial for performance improvement (see Table 5).

Table 5. Desirable oxygen species on electrode surface.

Reference	Treatment	Material	Electrode	Desirable functional group
11	Thermal	Graphite felt	Positive and negative	C-OH and C=O
17	Chemical	Graphite felt	Positive and negative	C-O-H and C=O
31	Chemical	Graphite felt	Positive and negative	C-OH
37	Thermal and chemical	Graphite felt	Positive	C-O
51	Thermal	Carbon felt	Positive and negative	C-OH
57	Thermal and chemical	Graphite felt	Positive and negative	O-C=O
70	Thermo-chemical	Graphite felt	Positive	C-OH
71	Chemical	Graphite felt	Positive and negative	C=O, COOH and C-OH
72	Thermal and chemical	Glassy carbon	Positive	No correlation
73	Thermal	Carbon felt	Negative	No correlation
74	Chemical	Graphite felt	Positive	C=O
76	Chemical	Carbon felt	Positive	C=O
77	Thermal	Graphite felt	Positive	C-OH
78	Chemical	Graphite felt	Positive	C-OH
79	Chemical	Graphite felt	Positive	C-OH
80	Chemical	Graphite felt	Positive	C-OH
83	Thermal	Graphite felt	Positive and negative	C-OH
86	Thermal and chemical	Carbon felt	Positive	C-O
87	Chemical	Graphite felt	Positive	-COOH
88	Chemical	Carbon cloth	Positive and negative	C-OH

It is important to mention that it is hard to determine and compare the impact of each treatment proposed and evaluate the impact of functional groups since different parameters were used, such as electrolyte compositions, electrode materials, membranes

type, current density and others. Moreover, there is a limited understanding on how to assess electrode properties that are impacted by different activation methods. Thus, conducting a proper assessment taking into consideration different physical and chemical properties and correlating them to electrochemical performance is essential to avoid misleading conclusions.

2.7.2. Thermal Treatments

Thermal treatment is a well-established approach for electrode activation, since it is a simple and low cost procedure to introduce as many oxygen funcional groups as other treatments. Thermal treatment for graphite felt materials was first proposed in 1992 by Maria Skyllas-Kazacos. Skyllas-Kazacos argued that thermal activation could introduce oxygen function groups that can behave as active sites for vanadium reactions and improve wettability. Also, it has been discussed in literature that, in addition to introducing desirable function groups, thermal treatment can clean graphite felt fibers that may contain chemicals left from the synthesis process.

Although Skyllas-Kazacos has proposed that the best combination of temperature and time would be 400ºC for 30 hours, it is common to see in literature different parameters combinations that is said to yield the best performance for different electrodes, since materials properties differ and they play an importante role to oxidation efficiency. Ghimire *et al.* [73] studied the optimization for thermal activation for negative electrodes and the impact of temperature and time for electrode properties such as charge transfer resistance, active surface area, oxygen amount and cell efficiencies. According to Ghimire's results, there is a limit in temperature and time where different properties reaches the optimical performance, which was also observed in Kasacos paper. Also, he noticed that a long thermal treatment forms C=O groups, while higher temperatures (750ºC) form C-O groups. Thus, he discusses that it is hard to conclude if both or only one functional group type are responsible for performance enhancement. Although he couldn't see any correlation between oxygen functional groups and performance, he was able to verify a clear correlation between double layer capacitance and cell performance. Therefore, other parameters should be taken into consideration when analyzing cell performance enhancement, treatments not only impact surface nature in terms of

functional groups, but also of physical properties like wettability. A summary is presented in Table 6 for different parameters, such as temperature, atmosphere, and time of the treatments.

Table 6. Thermal treatment modifications in literature and process variables.

Reference	Temperature [ºC]	Atmosphere	Time [h]
31	400	Air	4
37	450	Air	3
57	400	Air	6
75	400, 500, 610	NH_3/O_2	6, 12, 24 ,36
77	400	Air	10min, 15min, 20min, 30
78	, 600, 700, 800, 900	N_2	2
80	400	Air	30
81	500	Air	5
82	400	Air	30
83	500	Air	5
84	400	Air	30
85	100, 200, 300, 400	-	10, 20, 30
89	400	Air	25
91	340, 390, 415, 440	Air, N_2	2, 6, 12, 24
92	400, 450, 500, 550, 600	Air	9
93	400, 500	Air	3, 48
94	400	N_2, Air, 42% O_2	15, 30, 45
95	400, 450, 500, 550, 600	Air	-

As shown in Table 6, there is a divergence on what the best combination of parameters is to yield the best thermal treatment. Therefore, it is important to evaluate different thermal treatment parameters for the electrode material used, since the best combination for one electrode may not be the optimal for each electrode. For this work, different temperatures and times will be studied to understand those parameters impacts on different physical and chemical properties of graphite felt electrode.

2.7.3. Chemical Treatments

Skyllas-Kazacos also proposed chemical treatments as an alternative approach to improve electrodes performance by using different acids. It has been shown that, when treated with acids, electrodes could show an increase in functional groups content, which can improve wettability and reaction kinetics. In her paper, Skyllas-Kazacos used H_2SO_4 and HNO_3 as oxidizing agents, but other chemicals have been proposed in literature, such as H_2O_2, KOH, and others (Table 7). It is important to note that chemical treatments have been proposed with two main goals: introducing oxygen-containing functional groups and/or etching electrode surface.

Table 7. Chemical treatment modifications proposed in literature.

Reference	Modification / Reagent	Goal
17	H_2SO_4 / HNO_3	Functional groups
31	$KMnO_4$	Functional groups
39	KOH	Etching
59	H_2O_2	Functional groups
69	HNO_3	Functional groups
74	HF / H_2O_2	Etching and functional groups
80	Hummers method	Functional groups
96	$K_2Cr_2O_7$	Functional groups
97	Fenton reagent	Functional groups

Reference	Modification / Reagent	Goal
98	$KMnO_4$	Functional groups
99	KOH	Functional groups
100	K_2Cr2O_7	Etching
101	Cobalt acetate	Etching
102	H_2SO_4	Functional groups
103	Fenton reagent	Functional groups

One advantage of chemical treatments, compared to thermal treatment, is the fact that reagents can be used to introduce oxygen functions groups, but also is often used to modify electrode roughness and improve surface area. Since there is a debate whether functional groups or surface area has the greatest impact on efficiency improvement, combining both thermal and chemical treatments could have a synergetic effect for electrode modification because it can both improve surface area and introduce desirable functional groups on electrode surface.

2.7.4. Catalyst Materials

Metals

Metals (noble and transition) have been used in VFRB applications due to their good electrical conductivity and stability in acidic media [3]. However, some of these metals are not pratical as electrodes materials because of their high cost. Hence, metals have been combined with carbon materials as supports in order to improve electrode reversibility and charge transfer resistance. Some of the catalyst materials used in this work were already evaluated in other papers, so a literature review can be seen below showing the advantages and disadvantages of each material, as well as improvements achivements.

Iridium

Iridium is a highly conductive metal and and it is suitable for acidic media, being a good fit for VRFB application [3]. It was first studied by Kasacos [104], and it showed potential as a positive catalyst material. However, Wang and Wang [105] reported a decrease in efficiency due to increased cell resistance, which is believed to be caused by pores obstruction and oxygen evolution.

Tsai *et al.* [106] studied the effect of Ir on graphene, which has a higher conductivity than graphite. However, only *ex-situ* electrochemical tests were performed to determine the impact of Ir on graphene, which showed a smaller peak separation for Ir modified electrodes. Hence, more *in-situ* single cell tests are needed to evaluate Ir performance and suitability for VRFB systems.

Indium

Indium is often used in electrochemical applications due to its capability of reducing HER rate [3]. Indium was studied as catalyst material as cathode materials, while no reports were done in the negative electrode [107]. For cathode applications, it was found that a smaller catalyst loading is needed to be deposit on the electrode to achieve similar performances to Ir samples. Moreover, no degradation was seen after stability tests [107].

Bismuth

Although it is a heavy metal, bismuth is classified as a non-toxic metal and it is also less expensive compared to the other metal catalyst materials [3]. According to Gonzales *et al.* [108], modified Bi electrodes showed a good stability, where no degradation was observed after 100 cycles. Also, Bi was studied as an electrolyte additive and it showed performance improvements when added in anolyte, while it had no effect on the positive electrolyte [109]. Another stability test was performed by Suarez *et al.* [110], and even after 1,500 cycles, Bi modified electrodes showed no changes in *ex-situ* tests, while thermal treated electrodes degreaded after few cycles.

Liu *et al.* [111] studied the effect of Bi in both positive and negative electrolyte and it concluded that bismuth has no catalytic effect on the positive side. Liu also studied the impact of temperature on bismuth catalytic properties. He reported that even for low and high temperature, bismuth modified electrodes still has a better performance compared to pristine ones.

Antimony

Antimony has desirable properties such as corrosion resistance, low cost and also large overpotential for gas evolution [3]. It was also studied as electrolyte additive for the anolyte. However, it was shown that antimony was not completed removed from electrode surface after discharge, which can cause agglomeration and pores obstruction [112]. Compared to bismuth, antiomony modified electrodes has shown a lower performance.

Tin

Tin is relativily inexpensive and non-toxic metal and it was reported to improve electrode's wettability [3]. It was also studied as electrolyte additives, for both positive and negative electrolytes. However, improvements were more significant on the negative side compared to the positive side [113]. When compared to other additives, modified electrodes using tin as catalyst material showed a higher efficiency as bismuth modified electrodes.

Different metal catalyst have been proposed in literature for both anode and cathode materials. Thus, a summary can be seen below in Table 8, showing the advantages and disadvantages and impact on for both positive and negative electrodes.

Table 8. Catalysts materials summary – Advantages and disadvantages.

Reference	Catalyst	VO^{2+}/VO_2^+	V^{2+}/V^{3+}	Pros and cons
7, 104, 106	Ir	+	Not Informed	High oxygen evolution and pores obstruction
107	In	+	Not Informed	Reduces HER rate
108, 109, 110, 11	Bi	No effect	+	Good stability and can perform at high current densities (400 mA/cm^2)
112	Sb	No effect	+	Not completely remove after oxidation (agglomeration)
113	Sn	+ (minor)	+	Good performance compared to Bi

Bismuth is still one of the catalyst materials that can achieve good performances, even in high current densities. Other materials such as Iridium still need more deep understanding since improvements and disadvantages are still not clear as more *in-situ* tests need to be performed.

Metal Oxides

Metal oxides have also been widely used in literature as catalyst materials for VRFBs, specially due to their low cost compared to metal catalysts. These catalysts are abundatant and they are also stable in oxygen-evolving environments [3]. However, one disadvantage of metal oxides compared to metals is their low conductivity, which can be solved by combining metal oxides with another high electrical conductivy materials such as carbon materials (carbon nanotubes, graphene, rGO, and others).

WO_3

WO_3 catalyst has some advantages such as being stable in sulfuric acid environments and having a low cost compared to metal catalysts [3]. However, WO_3 is reported to has a low conductivity. Thus, it is combined with another material (usually a carbon support) to improve conductivity. Yao *et al.* [105] combined WO_3 with special active carbon (SAC), which has not only a good electrical conductivity, but also a high surface area. It was reported that both positive and negative modified electrodes showed improvements. Shen *et al.* [112] combined WO_3 with grafhite felt, which also showed improvements. Kabtamu *et al.* [113] used hexagonal tungsten nanowired doped with Nb, which was tested at a relatively high current density (160 mA/cm^2) and showed a good performance. Kabtamu *et al.* [114] also studied the combination of WO_3 and graphene, which has reported to have a synergistic effect with W-O-C bonds. Faraji *et al.* [115] studied modified electrodes with multi-walled carbono nanotubes (MWCNT), which has high surface area and carbonyl functional groups. Hosseimi *et al.* [116] studied nitrogen doped and WO_3 modified electrodes. Nitrogen was reported to increase hydrophilicity, which helps to better distribute the catalyst on the electrode's surface. Bayeh et al [117] studied a non-stoichiometric tungsten oxide $W_{18}O_{48}$, which is reported to have an advantage over WO_3 due to some oxygen containing defects with better catalyst properties.

SnO_2

Mehboob *et al.* [118] studied the effect of SnO_2 on both positive and negative electrodes, and he was able to show good performances when operating at high current density (150 mA/cm^2). Futher studies need to be done in order to better understand the role of SnO_2 as catalyst material, since the improvement mechanism was not fully explained.

TiO_2

TiO_2 has a good stability in acid media and it is reported to improve wettability [3] and it is often used in the negative electrode since it's believed to surpress hydrogen evolution [3]. Tseng *et al.* [113] studied the carbon black and TiO_2 composite electrode for the negative reaction and it showed that hydrogen evolution was inhibited. Tseng tested this electrode at high current densities and, compared to other metal oxides catalyst (CeO_2 and ZrO_2), it showed the highest VE at the same current density. Hou *et al*. [114] used the same approach to modify carbon paper electrodes, and it was shown a good improvement in the negative couple reaction. Vazquez-Galvan *et al.* [117] studied hydrogen treated rutile as a negative electrode and it also inhibited hydrogen evolution. Vasquez [144] also studied a nitrited modified electrode with TiO_2 and it was shown that nitrogen on the electrode surface can act as active sites for the reactions. Cheng *et al.* [116] compared rutile and anatese forms of TiO_2 and he reported that anatese has more catalytic effect towards the negative reaction, compared to rutile form.

Nb_2O_5

Nb_2O_5 has a good stability in acidic media and its catalyst properties were studied for both reactions (negative and positive) by Li *et al.* [118]. They noted that adding tungsten on the electrolyte helped the Nb_2O_5 distribution on the electrode surface. Although it has shown good performance at high current density, more studies need to be done to better understand the impact of Nb_2O_5 as catalyst.

Ta_2O_5

Ta_2O_5 has a good stability in acidic media, low cost and also a good adhesion on surface electrode [3]. Bayeh *et al.* [128] studied the effects of Ta_2O_5 on the positive electrode, and it was shown that Ta_2O_5 modified electrodes has abundant oxygen functional groups that can act as active sites for the positive couple reaction.

As it was shown, different metal oxides were tested and are believed to be a good fit for VRFB applications. Although different groups have shown advantages of using those materials, more studies need to be done in order to understand the main improvement mechanisms for them, since modification assessment for some electrodes is not fully explored. A summary can be seen in Table 9, comparing modified samples using different catalyst materials and their performance in *in-situ* cycling tests.

Table 9. VRFB performance comparison for diferente metal oxides activated electrodes proposed in literature.

Reference	Electrode	Catalyst	i [mA/cm^2]	CE [%]	VE [%]	EE [%]
105	Positive and negative	WO_3	60	95.1	81.8	78.1
112	Positive	WO_3	70	99.1	88.66	87.86
114	Positive and negative	WO_3	80	94.98	83.69	79.49
118	Positive and negative	SnO_2	150	96	78	75
119	Negative	TiO_2	200	90.0	73.0	65.4
120	Negative	TiO_2	100	97	75	73
122	Negative	TiN	200	-	-	84
123	Negative	TiO_2	100	97	84	81
124	Positive and negative	Nb_2O_5	150	97	77	75
125	Positive	Ta_2O_5	80	94.82	78.10	73.73

As shown in Table 9, activated samples were able to perform at higher current density and still show high energy efficiency. Among different catalyst materials, TiO_2 showed higher EE compared to other catalyst at higher current densities, which is believed to be caused by hydrogen evolution suppression.

Carbon Support

Carbon materials have been used as catalysts materials and support in VRFB applications due to their high surface area and electrical conductivity. They are mostly combined with other catalysts (especially metal oxides), though some studies showed the impact of carbon catalysts alone. Most of the studies have been focusing on carbon nanotubes, graphene, graphene oxide and reduced graphene oxided, which applications and milestone will be discussed below.

Carbon Nanotubes

Carbon nanotubes are widely used in fuel cell applications, but it has also been used as catalyst in VRFB application due to high surface area and also high electrical conducitivy. Li [162] studied three different types of MWCNTs (pristine, hydroxyl and carboxyl) as catalysts for the positive reaction. Li reported that carboxyl MWCNTs showed the best performance among the three modified electrodes, suggesting that carboxyl functional groups can act as catalysts for the positive reaction. Although it showed a better performance, carboxyl MWCNTs seems to have a poor adherence on the substrate. Thus, Wei [154] suggested a new approach using Nafion to enhance catalyst stability onto CF electrode's surface. Yang [158] stated that both methods used for Wei and Li are complicated and difficult, and he suggested a sucrose pyrolysis approach in order to deposit MWCNTs onto electrode surface. Wang *et al.* [159] introduced nitrogen functional groups on carbon nanotubes and he reported that it not only modified electrical properties, but also introduced defects sites on their surface. Gonzales *et al.* [37] compared the impact of both oxygen and nitrogen functional groups and he concluded that oxygen modified MWCNTs showed the best performance.

Graphene, graphene oxide and rGO

Graphene is considered as a good electrode material due to its high surface area and electrical conductivity, which can decreases contact resistance [157]. Gonzales *et al.* [155] studied graphene modified graphite felt using graphene oxide and it showed good

electrochemical performance. Moghim *et al.* [157] studied reduced graphene oxide as electrocatalyst and it showed a huge improvement on electrode resistance and also on $VOSO_4$ absortion. Graphene oxide was studied by Han *et al.* [163] due to the fact that graphene oxide nanoplates (GONPs) have a large amount of hydroxyl and carboxyl functional groups. GONPs modified electrodes proposed by Han *et al.* showed good electrochemical improvements towards both positive and negative reactions. However, no single cell experiments were done.

2.8. Proposed solutions

For this work, a comparative study of various activation treatments applied to the same VRFB architecture subjected to a full suite of diagnostics was done in order to establish their relative effectiveness and key underlying mechanisms so that a combined solution (Figure 7) can be proposed aiming for an optimal design for both positive and negative electrodes. For that, different impediments were tackled, such as active surface area and wettability, which can be drastically enhanced with the proposed solutions and seem to be the main parameters to improve electrode performance. Applying effective solutions can make VRFB operate at higher current densities and operational costs can be decreased, making it more competitive as ESS.

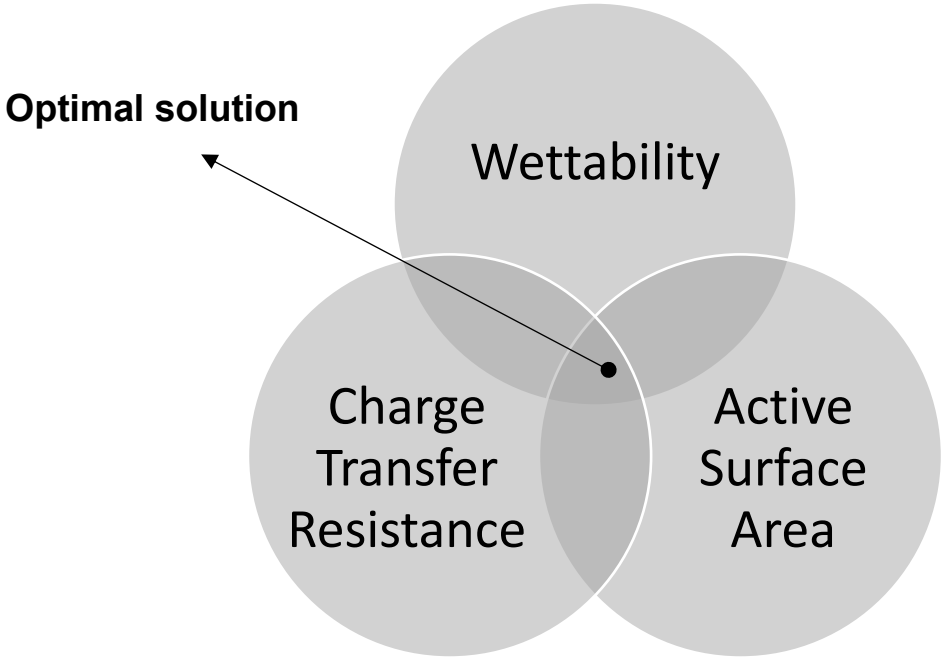

Figure 7. Proposed solution goal satisfying different electrode limitations.

The optimal solution aims to achieve higher performance by tackling different impediments, as shown in Figure 7. For that, both thermal activation and catalyst coating are used since each activation mechanism can provide different improvements. While thermal treatments can improve wettability and electrochemical active surface area by providing high concentration of functional groups that are active for both positive and negative redox reactions, catalyst materials with highly porous carbon supports can further improve active surface area and charge transfer resistance. Hence, the expected outcome for this combined solution is:

1) Higher energy efficiency (+15%).
2) Stability (less degradation in energy efficiency over 50 cycles)
3) Operation at higher current density
4) Maintenance cost and time are reduced compared to pristine, which is degraded overtime.

Chapter 3.

Experimental

In this chapter, materials, experimental techniques, and methodology are described for both *in-situ* and *ex-situ* physico-chemical and electrochemical characterization of VRFB electrodes. Tests conditions and parameters are detailed for different characterization tools. In addition, electrode, catalyst selection and modification processes (thermal and chemical treatments, pre-treatment cleaning and *in-situ* flow deposition) are described.

3.1. Electrode Selection

Graphite felt electrodes (GFE) GFD 4.65EA (SGL, Germany) were used in this study as this polyacrylonitrile (PAN) graphite felt material has been widely used in VRFBs. SGL graphite felt was also chosen because of desirable properties such as chemical resistance, high open porosity, high purity, and electrical conductivity. GFE properties can be seen in Table 10.

Table 10. Commercial graphite felt electrode properties. [68]

Properties	Units	GFD 4.65EA
Carbon fiber precursor	-	PAN
Bulk density	g/cm^3	0.09
Nominal thickness	mm	4.6

Properties	Units	GFD 4.65EA
Area weight	g/m^2	465
Open porosity	%	94
BET surface area	m^2/g	0.4
Electrical resistivity ⊥	Ω.mm	<5
Electrical resistivity II	Ω.mm	<3
Area-specific resistance* ⊥	$Ω.cm^2$	<0.15
Total impurities	%	<0.05

Note: II parallel to longitudinal direction of felt; ⊥ vertical to longitudinal of felt;
*compression to 80% of initial thickness

3.2. Thermal Treatment

The graphite felt samples were thermally treated varying two main parameters: temperature and time. To avoid unwanted aging effects and associated variability, samples were treated one day prior to *in-situ* and *ex-situ* tests. Samples were cut into the desired shape (3x3 cm), and then placed in a furnace which was programmed accordingly (Figure 8). Initial parameters such as time and temperature were selected based on Sun and Skyllas-Kazacos [11] study on thermal treatment impact and then tunned so that electrodes properties such as wettability could be improved. After treated, samples were placed in bags to avoid air contamination. The description of thermal treated samples is captured below in Table 11.

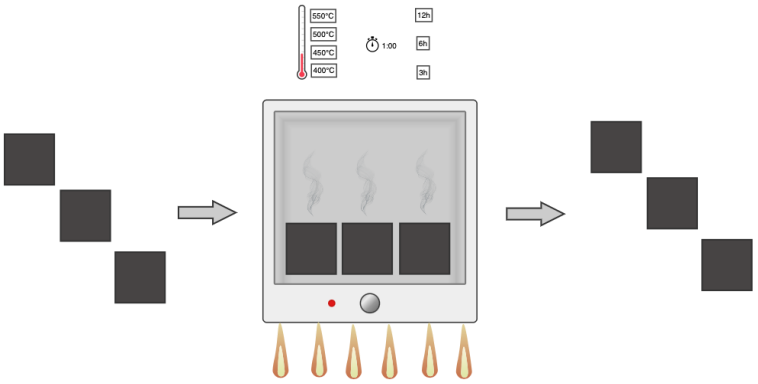

Figure 8. Thermal treatment scheme.

Table 11. Summary of thermally treated electrodes and their respective treatment variables.

Treatment	Sample	Temperature [ºC]	Atmosphere	Time [h]
Thermal Treatment	GF400	400	Air	6
	GF450	450		6
	GF5003h	500		3
	GF500	500		6
	GF50012h	500		12

3.3. Chemical Treatment

For thermal-chemical treatment, samples treated at 400ºC for 6 hours were used as baseline to evaluate potential further improvements in wettability, since GF400 electrodes were still hydrophobic. Thus, pre-treated samples were immerged in different oxidizing agents for 48 hours (Figure 9). After that, electrodes were washed until pH 7 was reached, and then dried in a vacuum furnace for 24 hours. To avoid air contamination, dried electrodes were kept in bags. Summary of electrodes descriptions and their respective treatments can be seen in Table 12.

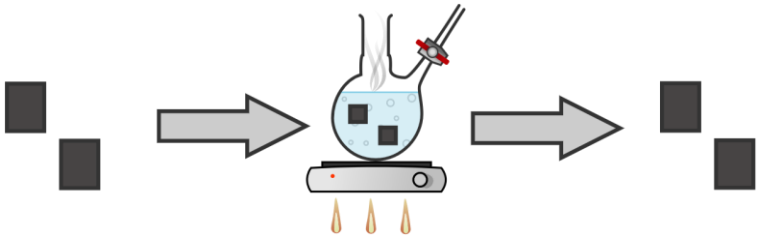

Figure 9. Chemical activation scheme.

Table 12. Summary of thermo-chemically treated electrodes and their respective treatments variables.

Treatment	Sample	Baseline	Oxidizing Agent
Thermal – Chemical Treatment	GF400 - 10H_2O_2	GF400	10% H_2O_2
	GF400 - 30H_2O_2		30% H_2O_2
	GF400 - HNO_3		10% HNO_3

3.4. Pre-cleaning Treatment

Before thermal treatment, a pre-cleaning process was done to eliminate potential chemicals residues that may be left after electrode synthesis process. Electrodes were cut either in 3x3 cm squares samples and they were place in a beaker. A reagent alcohol solution was firstly used for the pre-cleaning treatment. The beaker was filled until samples were fully emerged in the solution. Then, the beaker was sealed with parafilm and taken to ultrasonic bath, where they were ultrasonicated for 1 hour. After degassing, electrodes were dried at 100^{o}C on a hot-plate and then placed in the furnace for the thermal treatment (Figure 10). Solvent molecules are believed to have no impact on electrode surface since they are evaporated during thermal treatment.

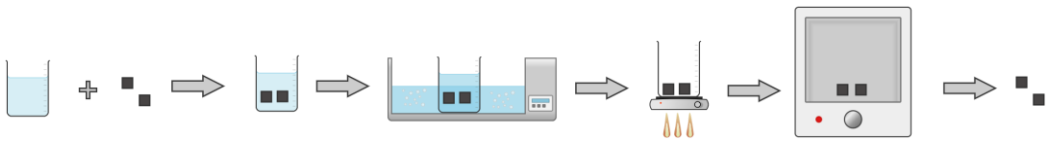

Figure 10. Pre-treatment process scheme.

3.5. Catalyst Materials Selection

Catalyst materials must present some desirable properties for both positive and negative electrodes, such as good electrical conductivity, high specific surface area, stability in acid, and others. In addition, anode and cathode materials must also prevent side reactions, and different catalyst can be used for each or both cells. For the positive electrodes, noble and non-noble metals were selected since they have high electrical conductivity and good acidic stability. Carbon supports were used to enhance SSA. For the negative electrodes, metal (mostly Bi) and metal oxides were selected due to the good acidic corrosion resistance and good electrical conductivity as well as being able to hinder hydrogen evolution.

3.6. Coating Process

For the coating process, a vacuum dip coating process was proposed. For that, catalyst ink was prepared beforehand using the selected ink formulation, and then poured into a beaker where sample was fully immersed and covered by parafilm. Then, the beaker was placed in a vacuum furnace where samples were kept under vacuum so that trapped air could leave the pores and ink could deeply penetrate electrode. After ink was fully soaked, samples were placed in a hot-plate and dried at 100ºC for few minutes (Figure 11). Dried electrodes were then labeled, and characterization analyses were carried out.

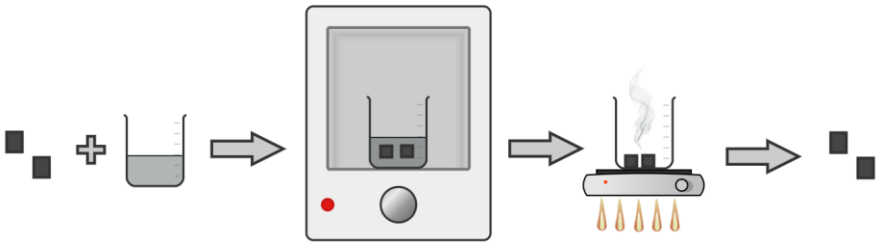

Figure 11. Dip-coating process scheme.

3.7. *In-situ* flowing deposition

For the flowing deposition method [135], carbon materials were sonicated in an ultrasonic probe to disperse catalyst particles into commercial electrolyte solution. Once catalyst was dispersed and VRFB tests were set-up, the dispersed electrolyte was placed in the electrolyte tank and flowed through the system for few minutes until the color was changed and deposition was achieved. Different parameters were taken into consideration and will be discussed later, such as flow rate, catalyst loading and material selection.

3.8. Catholyte and Anolyte Preparation

For *ex-situ* measurements in half-cells such as cyclic voltammetry and electrochemical impedance spectroscopy, catholyte and anolyte formulations were prepared. For positive electrodes assessment, a catholyte solution of 0.2M $VOSO_4$ in 2M H_2SO_4 electrolyte was prepared. Anolyte was prepared by charging initial catholyte solution, in a different concentration, oxidation state reached around 2.5. For negative electrodes assessment, an anolyte solution was prepared using a 1.6M $VOSO_4$ in 2M H_2SO_4 electrolyte, and then charged in 1.4V for few hours. In order to confirm the final solution state of charge, titration was performed and SoC values were calculated (Figure 12).

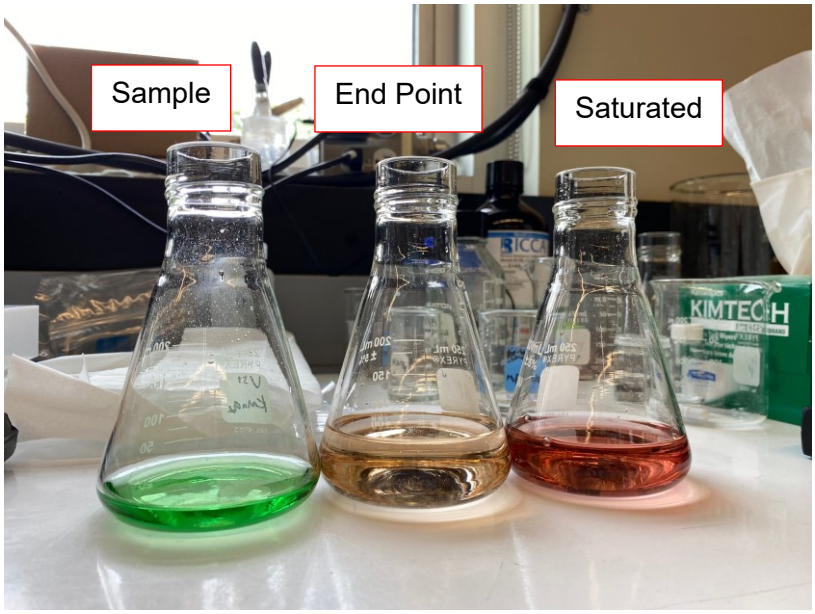

Figure 12. Titration process and its stages.

3.9. Characterization

Selecting proper tools for electrodes assessment is essential to understand enhancement mechanism and suggest better engineering solutions to mitigate electrode limitations. Therefore, a combination of different physical, chemical and electrochemical methods is provided so that different properties can be assessed, and a fair interpretation can be done. The characterization tools used in the *in-situ* and *ex-situ* tests are listed below.

3.9.1. Contact Angle

Keyence VHX digital microscope was used for static contact angle characterization. For that, a water droplet was dropped onto electrode surface and the static contact angle were calculated using measurements tools. Measurements were done right after (~30 s) water droplet was placed onto electrode to avoid the impact of time on

the droplet absorbance. Two measurements were done for each sample for statistical analysis.

3.9.2. Raman Spectroscopy

Thermo-Fisher DXR2 Raman microscope was employed to obtain Raman spectra of the samples. For this tool, I_D/I_G band ratio was calculated in order to determine the introduction of defects during the treatments. D band is associated to nanocrystalline carbon, while G band is associated to amorphous carbon materials. Thus, if I_D/I_G ratio is higher for activated electrodes (compared to pristine), more defects were formed on electrode surface, which can act as active sites for the reactions to take place.

3.9.3. X-ray photoelectron spectroscopy (XPS)

The XPS spectra were taken on a Kratos Axis Ultra DLD with the following parameters: Monochromated Al K-alpha x-rays (1486 eV), 180 W, 160 ev pass energy and 1 eV/step for the surveys, 20 eV pass energy and 0.1 eV/step for the high-resolution spectra and neutralizer on. The main goal of this characterization tool is to understand what functional groups are presented on the different samples and to determine the impact of functional groups on electrodes' performance.

3.9.4. Scanning Electron Microscope (SEM)

SEM/EDAX Vega3 LMH was employed to examine the morphology and roughness of the sample. Morphology of the samples were determine based on the SEM images using a 20kV accelerating voltage and 4,000 magnification.

3.9.5. Brunauer-Emmett-Teller (BET)

BET surface area measurements were performed using a AS 3100 Surface Analyzer. Catalyst materials were loaded in a glass tubing according to minimum load to calculate estimated SSA.

3.9.6. Zeta Potential and Particle Size Distribution Measurements

Malvern zeta potentiostat was used for both zeta potential measurements and particle size distribution. Samples were dispersed in an ethanol solution and information regarding solvents and materials were added in the system so that both measurements could be done.

3.9.7. Cyclic Voltammetry (CV)

In order to investigate electrochemical performance of the treated graphite felt electrodes, CV measurements were done using a VoltaLab potentiostat system and a three-electrodes cell built in-house (Figure 13). This cell is consisted of three electrodes: a working electrode (treated electrodes samples), counter electrode (gold mesh) and an Ag/AgCl reference electrode. To avoid kinetic limitations, counter electrode has an area greater (~10x) than the working electrode. CV tests were performed in both sulfuric acid and vanadium electrolyte.

For sulfuric acid, capacitance and carbolic functional group density were calculated. For capacitance measurements, capacitance current is read from the range 0.6V – 0.8V in the double-layer region (no reactions taking place). Thus, capacitance can be calculated using the following formula:

$$Capacitance = \frac{Charge\ (Q)}{Voltage\ (V)} = \frac{I \cdot time}{V} = \frac{I_{capacitive}}{v} \quad (15)$$

Where $I_{capacitive}$ is the capacitance current and v is the scan rate (mV/s).

Carbolic functional group density was calculated by integrating the carbolic peak (0.4V – 0.6V) using the following formula:

$$Surface\ functional\ density\ group = \frac{Q}{F} \cdot \frac{1000000\ \frac{\mu mol}{mol}}{m} \quad (16)$$

Where Q is the charge, F is the Faraday constant and m is the mass of the sample.

For vanadium electrolyte, peak current ratio (kinetics) and peak potential separation (reversibility) were calculated. CVs were performed at a scan rate of 1 mV/s for a 0 – 1.4V potential range. Tests were performed in room temperature, and for CVs in anolyte, argon was purged to avoid electrolyte oxidation.

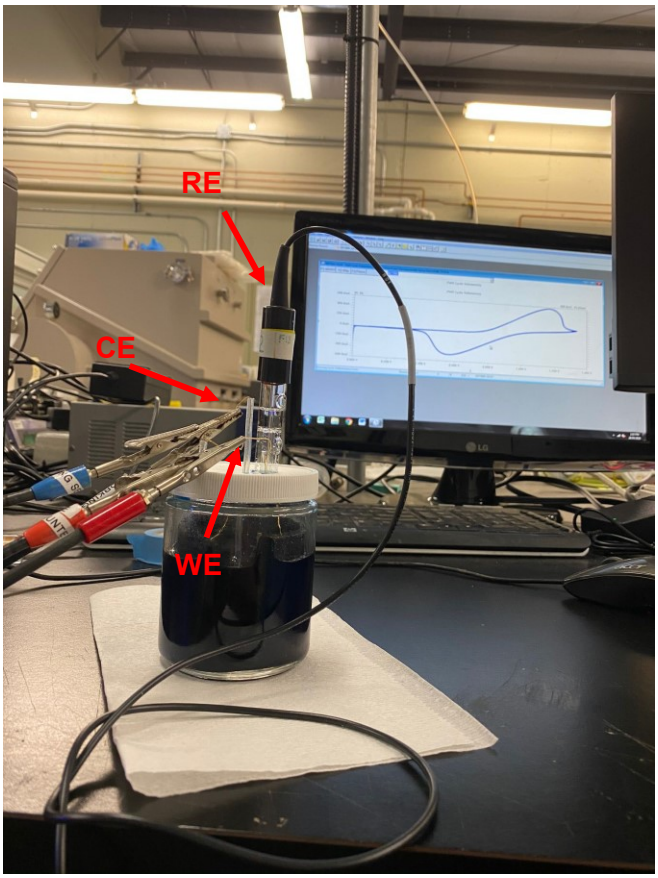

Figure 13. In-house made three-electrode cell set-up.

3.9.8. Electrochemical Impedance Spectroscopy (EIS)

For EIS measurements, the same set-up was used as for CV tests, and EIS measurements were usually done before running CV to avoid changes in electrolyte species. Same electrolytes were used (anolyte and catholyte) and a frequency range from 100 kHz – 10 mHz, 5 mV AC perturbation was applied at OCP potential.

3.9.9. Single Cell Test

A single-cell flow battery (Standard Energy, S.Korea) with 9 cm^2 active electrode area with a serpentine flow field and flow-through structure was used for the performance evaluation (Figure 14). The VRFB charging and discharging was performed using an Arbin battery station. The single cell was assembled using gold current collectors, graphite bipolar plates, gasket materials and frames. Activated electrodes were used as positive or negative electrodes, and a Nafion^{TM} 212 membrane was used in order to minimize crossover. After assembly, the test cell was compressed, and tubings were connected to the electrolyte tanks. For performance testing, a flow rate of 25 mL/min was used with a peristaltic pump. Two compartments with 30 mL of commercial electrolyte were employed for the anolyte and catholyte, being the negative electrolyte tank purged with argon to avoid air oxidation. All tests were performed at room-temperature and at i = 80 mA/cm^2.

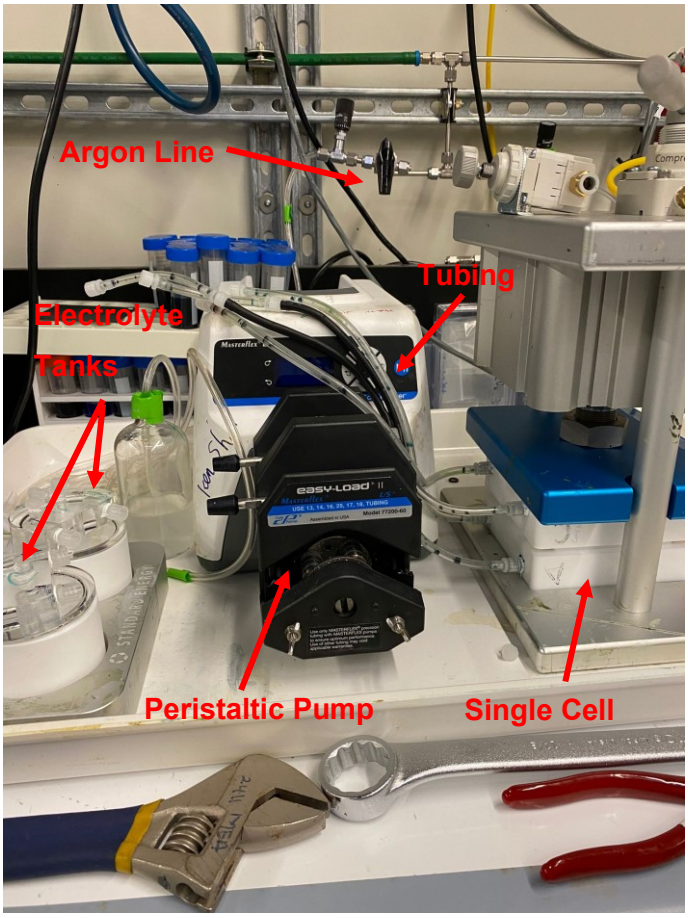

Figure 14. Single cell VRFB test set-up.

Chapter 4.
Results and Discussion

4.1. Thermal Treatment

Thermal treatment is one of the methods often used in literature to introduce desirable functional groups on VRFB carbon electrodes. Different parameters will be analyzed in order to understand the impact of both treatment temperature and time on electrode properties, such as wettability and active surface area. Moreover, activated electrodes aging is evaluated, since functional groups are believed to be not stable.

4.1.1. Temperature Impact

Pristine commercial graphite felts are hydrophobic (Figure 5), which is one of the drawbacks of these materials for liquid flow cells. Since thermal treatment is believed to improve wettability, contact angle measurements were performed to evaluate the impact of temperature on electrode hydrophobicity (Figure 15).

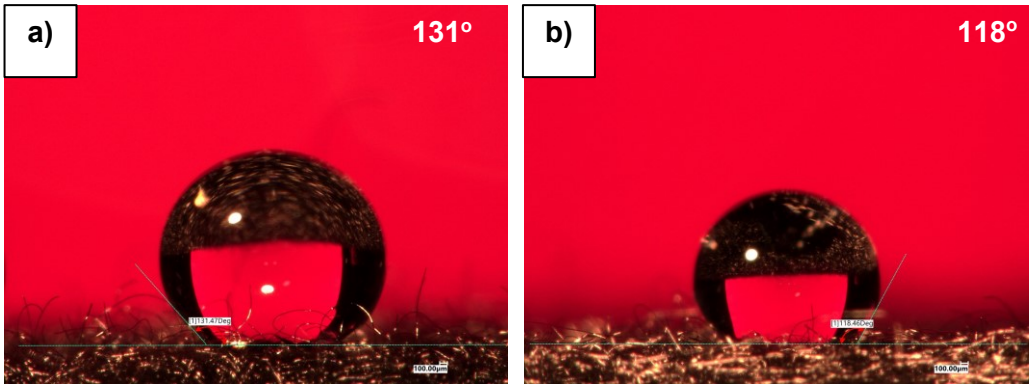

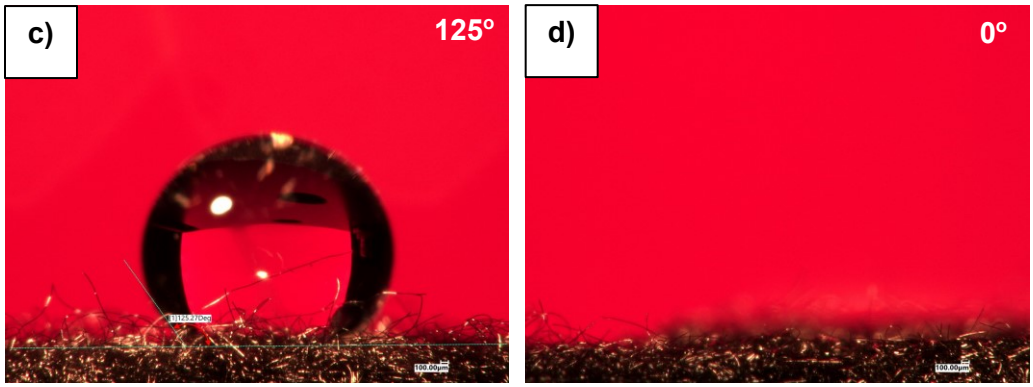

Figure 15. Contact angle measurements for a) GFPristine, b) GF400, c) GF450 and d) GF500.

As it is shown in Figure 15, temperature has a great influence on samples wettability. While pristine sample showed a hydrophobic behavior, hydrophilicity was drastically improved for electrodes treated at higher temperature. Lower temperatures (GF400) seem to not fully activate GFEs, and changes in hydrophobicity were minor, while higher temperatures (500°C) showed completely hydrophilic behavior, where water droplet gets completely absorbed, compared to GFPristine, where water droplets stick to the electrode surface (see Appendix).

Morphology of activated GFEs was evaluated using SEM. As it can be seen from Figure 16, GFPristine and GF400 have a relatively smooth surface, which indicates that treatment lower temperature has little effect on roughness. However, GF500 showed slightly rougher fibers, suggesting that some defects may be introduced during thermal treatment process, which can be act as active sites for the reactions to take place.

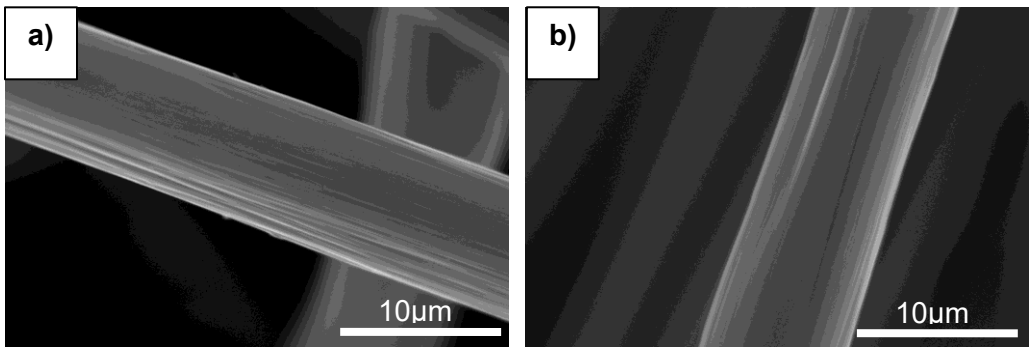

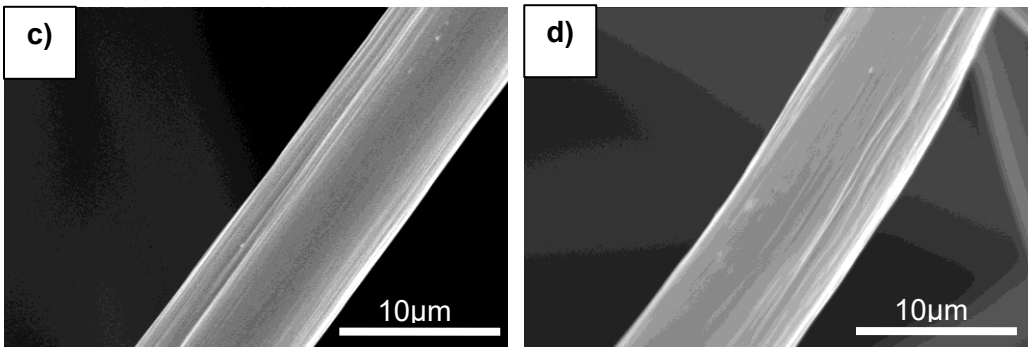

Figure 16. SEM images of a) GFPristine, b) GF400, c) GF450 and d) GF500.

Since samples roughness and morphologies seemed affected for few samples, Raman spectroscopy was used as a auxiliary tool to determine how different temperature can impact material roughness and defect formation. For that, I_D/I_G ratio was calculated, which can be useful to estimate the defects in the sample.

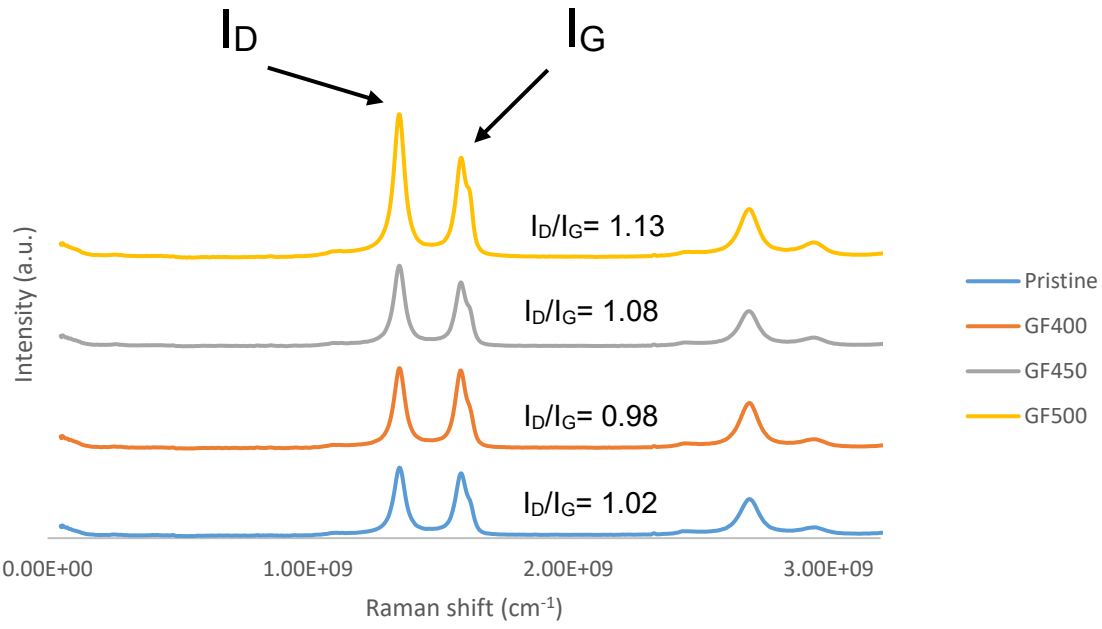

Figure 17. Raman I_G/I_D ratio for different thermally treated electrodes.

As shown in Figure 17, most of the samples showed an I_D/I_G ratio close to one, though temperature seems to increase the number of defects. Both GFPristine and GF400 had a ratio close to 1, suggesting a smooth and little or no defects on electrode surface as shown in SEM images, while higher temperature samples showed higher ratio. Among activated samples, GF500 showed the highest I_D/I_G ratio, which means that more defects were introduced onto sample surface during thermal treatment. More defects on electrode surface can provide more active surface area for electrochemical reactions, which can be translated into improved kinetics.

Physical characterization itself isn't enough to fully assess the electrode performance, hence chemical characterization was also performed to better understand physical and chemical properties correlation. For chemical analysis, XPS measurements (Figure 18) were done to determine the surface elemental composition.

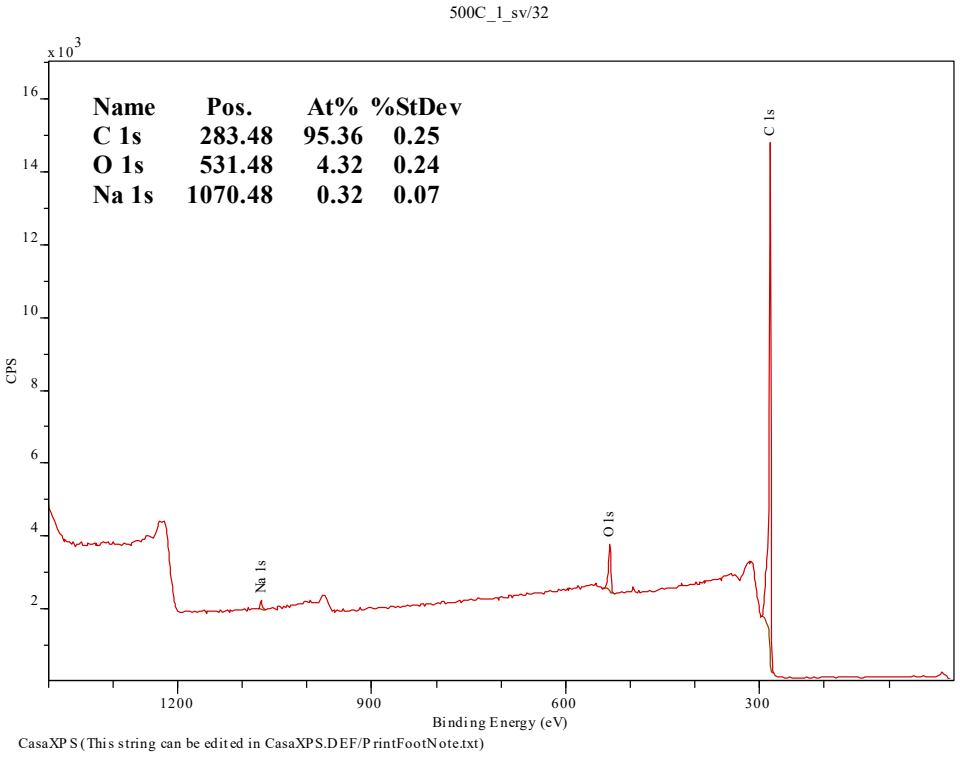

Figure 18. XPS Analysis – Surface composition for GF500.

After analyzing XPS data, it was noted that samples treated at higher temperatures showed higher oxygen peaks, which indicates that more oxygen is being introduced to materials surface during thermal treatment and organic species are being burned off, since carbon content in the surface is decreasing. Table 13 shows the composition for GFEs thermally treated at different temperatures

Table 13. XPS surface elemental composition for different thermally treated electrodes.

Sample	C [%]	O [%]	N [%]	Na [%]
GF400	97.63	1.6	0.77	-
GF450	96.7	2.22	0.86	0.22
GF500	95.36	4.32	-	0.32

As can be seen in Table 13, an increase of oxygen content is noticeable after each thermal treatment. For instance, sample treated at 500°C shows an oxygen content amount almost 3x higher than the one treated at 400°C. It's also important to notice that besides C, O and N, some other elements can be seen in the samples. Although these contaminants are present, it is believed that due their small quantity, they shouldn't have any impact on electrode performance.

Besides elemental composition analysis, O_{1s} deconvolution oxygen peaks analysis was also done so that different oxygen functional groups could be evaluated (Figure 19). For that C=O, C-O and adsorbed O (mostly adsorbed water or chemicals on the surface).

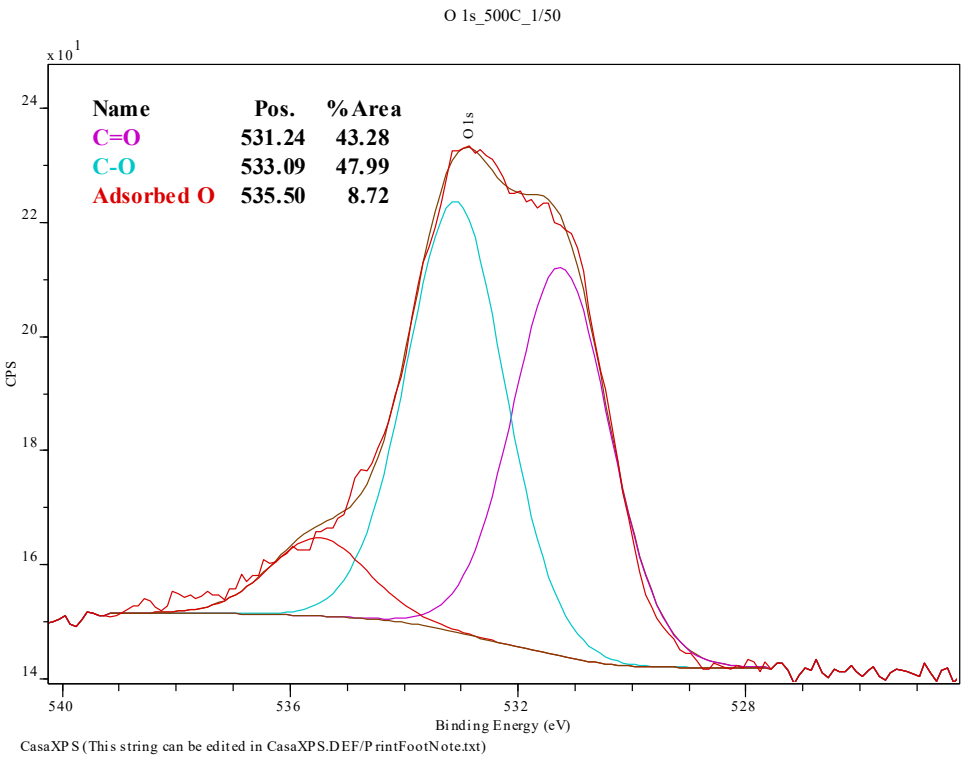

Figure 19. XPS Analysis - O1s Deconvolution for GF500.

As shown in O_{1s} deconvolution in Table 14, oxygen functional groups in different amounts can be introduced by varying the thermal treatment temperature. Activated samples at heat treatment 400 and 450°C for 6h in air showed similar C=O and C-O amounts, while GF500 showed significant increase of all functional groups.

Table 14. XPS functional groups analysis for different thermally treated electrodes.

Sample	C=O	C-O	Adsorbed O
GFPristine	1.54	1.11	-
GF400	1.07	0.49	0.04

Sample	C=O	C-O	Adsorbed O
GF450	1.37	0.72	0.13
GF500	1.86	2.16	0.30

As Skyllas-Kazacos discussed [11], C-O groups are believed to be associated with phenolic groups, and C=O groups are believed to be associated with both carboxylic and carbonyl groups. C-O groups are desirable because they behave as active site and have catalytic effects. Skyllas-Kazacos also argued that improvements in hydrophobicity are due to the increase of C-O groups, which align with contact angle measurements and surface tension calculations.

Since temperature seems to improve electrode wettability, capacitance measurements were performed during cyclic voltammetry tests so that electrochemical surface area could be evaluated for thermally treated electrodes. From these measurement, electrochemical active surface area and carbolic functional groups can be evaluated, as it is shown in Figure 20.

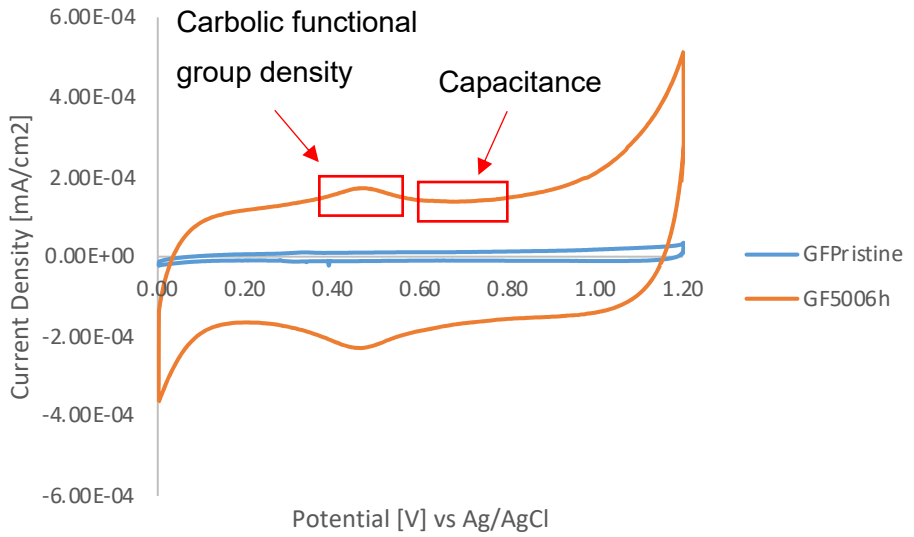

Figure 20. CV measurements in H_2SO_4 for thermally treated sample (GF500) and pristine.

As shown in Figure 20, capacitance was drastically improved after thermal treatment. Carbolic functional group density was calculated between 0.4V – 0.6 V, while capacitance values were calculated from double layer capacitance region (0.6 V – 0.8V), where no reactions take place. Carbolic group density and capacitance values for thermally treated samples can be seen below in Table 15.

Table 15. Capacitance and carbolic functional group density results for different thermally treated electrodes.

Sample	**Carbolic functional group density** [µmol]	**Capacitance** [µF]
GFPristine	0.000	1.06
GF400	0.001	2.31
GF450	0.003	3.74
GF500	0.009	13.43

As it can be seen in Table 15, although GF400 and GF450 showed slight improvements in capacitance, GF500 showed the highest capacitance, which was 10x higher than pristine GF. Enhanced capacitance can be explained by improved wettability, which was observed in CA measurements, where electrodes that showed similar CA also showed similar capacitance, while GF500 showed the highest capacitance and lowest contact angle. Thus, higher capacitance can be translated into more electrochemical active surface area and improvements can be seen in other electrochemical properties that will be discussed later.

Carbolic functional group density was also increased for thermally treated samples, aligning to XPS data, which showed higher oxygen content. Although pristine GFE showed no carbolic group density and GF400 had not a significant increase, sample treated at higher temperature (GF500), showed the highest carbolic content, confirming that higher temperature can introduce more oxygen functional groups, which is desirable for this application.

For electrochemical characterization, CV measurements were carried out in the positive electrolyte. For these measurements, anodic and cathodic peak potential separation and peak current ratio were calculated, for the evaluation of the electrochemical activity and reversibility for V^{2+}/V^{3+} and V^{4+}/V^{5+} redox reactions. As it can be seen from Figure 21, after thermal treatment, samples showed closer peak potential separation ΔE (improved reversibility) and higher peaks current ratio J_{pa}/J_{pc} with ratio closer to one (improved kinetics)

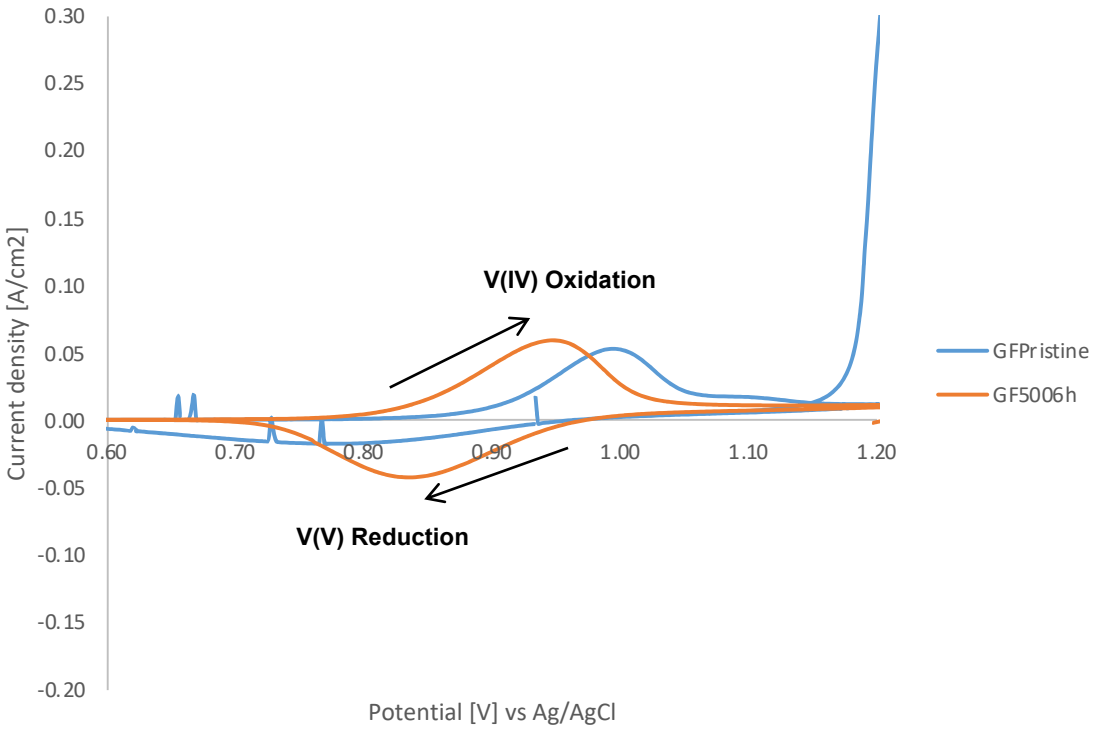

Figure 21. CV curves comparison for thermally treated electrode (GF500) and pristine.

Table 16. CV results for electrochemical properties for thermally treated electrodes.

Sample	J_{pa}/J_{pc}	ΔV [V]
GFPristine	3.01	0.210
GF400	2.10	0.160
GF450	1.82	0.150
GF500	1.38	0.110

As shown in Table 16, thermally treated GFs showed lower peak current ratio and potential separation, compared to the pristine. While GF400 and GF450 had similar results but, GF500 showed the lowest peak potential separation and a J_{pa}/J_{pc} ratio closer to 1, showing improvements in both electrochemical activity and reversibility for V^{4+}/V^{5+} redox reaction

Electrochemical impedance spectroscopy in the combination with measurements of CVs allows to carry out further analysis of electrode ohmic and charge transfer (interface electrolyte/electrode) resistance and double layer capacitance, which can give us an insight on kinetics and electrochemical active surface area properties. Two different parameters from Nyquist plots were analyzed: R_S (solution resistance) and R_{ct} (charge transfer resistance). R_S is the intersection with the X-axis at high frequencies, and R_{ct} is the diameter of the semi-circle at low frequencies. EIS measurements were also performed as part of the electrochemical characterization, so improvements in charge transfer resistance can be evaluated and correlated to kinetics improvements.

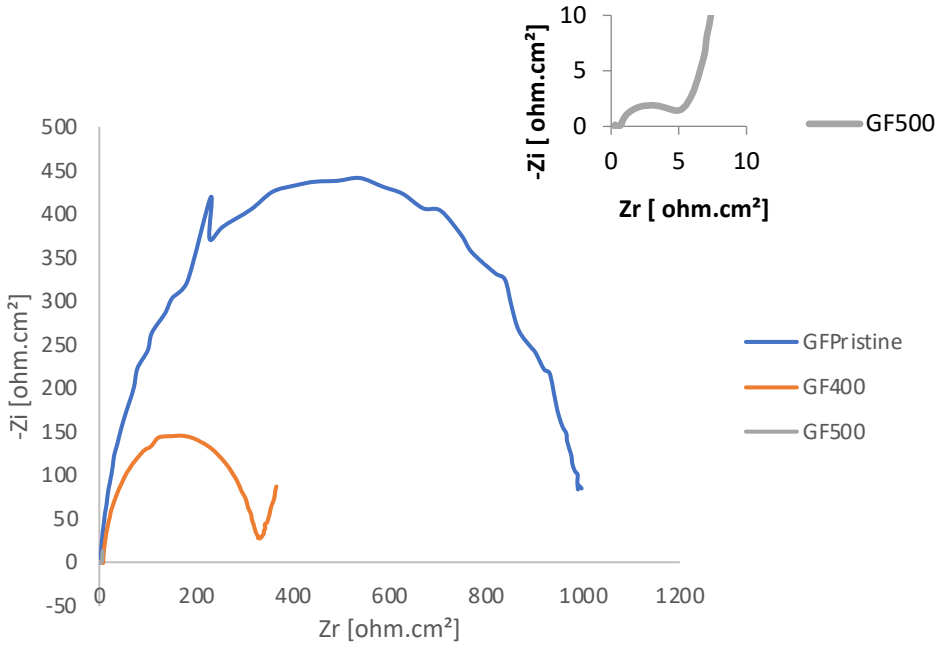

Figure 22. Nyquist plots for thermally treated electrodes.

As it can be seen in Figure 22, resistance was drastically improved for both samples (higher and lower temperatures). However, while GF400 showed only 3x improvement, GF500 showed a R_{ct} value 200x lower compared to pristine GFE. As shown in Table 17. Improvements in charge transfer resistance can be explained by enhanced wettability and active surface area, which have an impact on electrode kinetics and charge transfer resistance.

Table 17. EIS results for thermally treated electrodes.

Sample	R_s [ohm.cm²]	R_{ct} [ohm.cm²]
GFPristine	0.36	997.15
GF400	0.55	326.89
GF500	0.11	4.98

In-situ VRFB cycling tests were also performed to evaluate electrodes performance (Figure 23). For that, a single cell was assembled using thermally treated electrodes both as positive and negative electrode. VRFB cycling tests can be used to understand the correlation between *ex-situ* and *in-situ* performance so that improvements mechanism can be evaluated.

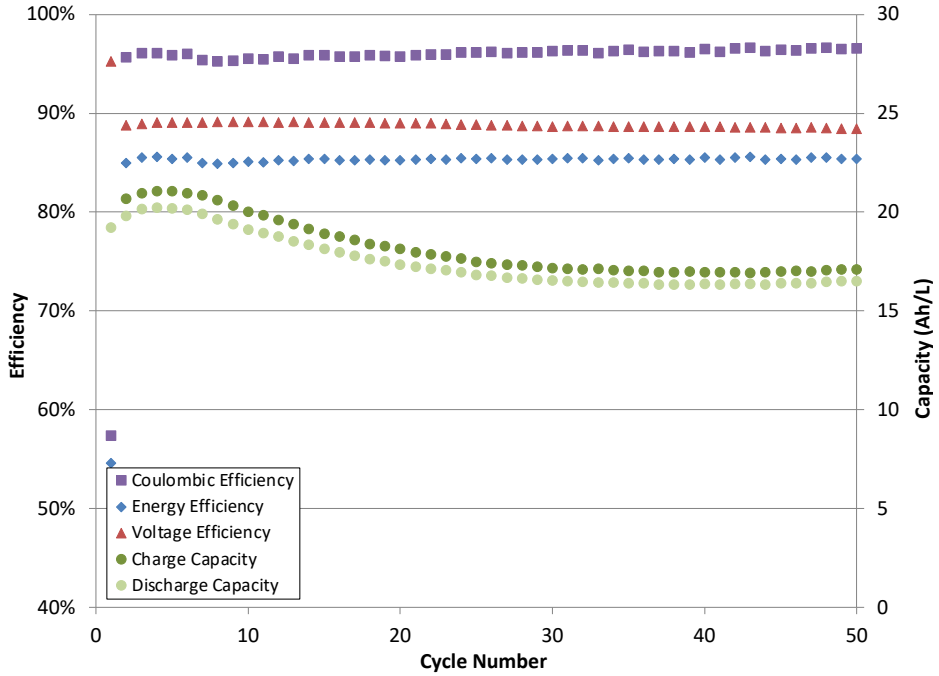

Figure 23. *In-situ* VRFB cycling test for thermally treated electrode GF500.

Cycling VRFB tests were important to evaluate both electrode performance and stability. Parameters such as EE, VE and CE are calculated, and performance comparison can be done (Table 18).

Table 18. Performance of VRFB system using different thermally treated electrodes.

Sample	EE [%]	VE [%]	CE [%]
GFPristine	73.1	75.8	96.4
GF400	81.3	82.5	98.5
GF450	80.2	82.6	98.1
GF500	85.2	88.5	96.2

As expected, GF500 showed the best performance overall among different thermally treated samples, showing a ~12% enhancement in energy efficiency. GF400 and GF450 showed similar results, which can be explained by similar physical and chemical properties. Though there is not a significant difference between GF400 and GF450 efficiencies, both samples also showed better EE% values than baseline, showing a ~8% improvement.

Improvements in electrode performance can be explained by enhancements in both wettability and active electrochemical surface area. Although functional groups introduced via thermal treament can improve wettability and seem to have impact on reversibility, as it was shown in CVs results, capacitance and electrochemical active surface area are the main parameter that correlates to *in-situ* performance, since improved performance are related to kinetics improvements. In summary, thermal treatment can lead to the formation of functional groups on electrode surface, which can improve physical and chemical properties, though improvements in active electrochemical surface area is the main mechanism behind electrode performance improvements.

4.1.2. Time Impact

As it has been discussed in literature, both temperature and time influence electrode performance since they can impact different properties. Hence, since GF500 showed the best performance among treated samples, different times were tested to understand the impact of time on physical and chemical properties. For that, electrodes were thermally treated during 3h, 6h and 12h at 500ºC, and they were denoted as GF5003h, GF5006h and GF50012h, respectively.

Wettability was evaluated during CA measurements, and as it can be seen in Figure 24, time has less influence during thermal treatment compared to temperature. All samples showed a hydrophilicity behavior, though GF5003h was the only sample that did not showed a total hydrophilic behavior, suggesting that samples need a longer time to fully activate electrode surface.

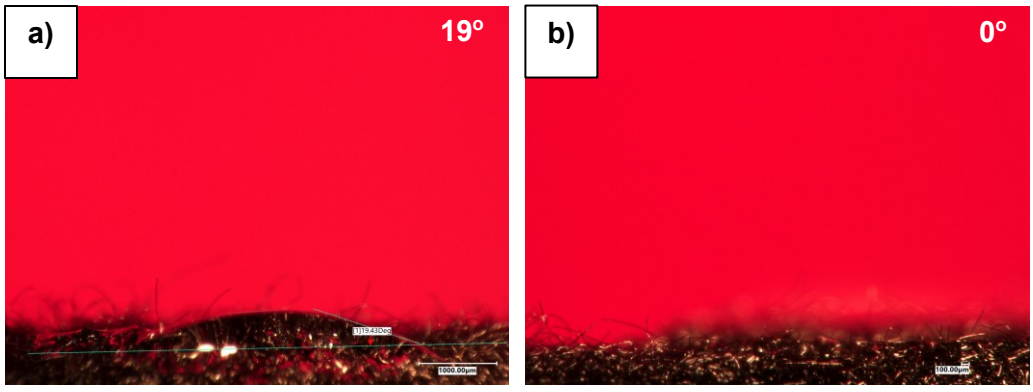

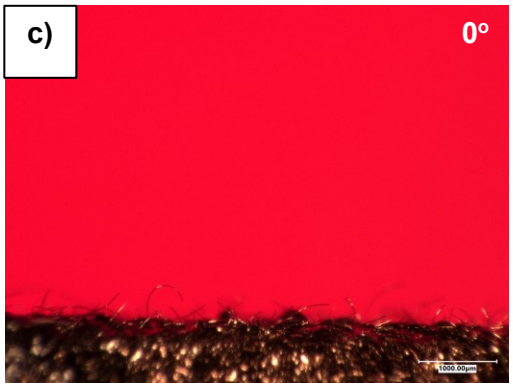

Figure 24. Contact angle measurements for a) GF5003h, b) GF5006h and c) GF50012h.

SEM was also used to evaluate electrode morphology, which showed that electrodes roughness wasn't affected by treatment time, suggesting that temperature is the main parameter that has a major impact on electrode roughness.

Since all samples are hydrophilic, CA measurements alone cannot be used to assess wettability and enhancement of the electrochemical surface area. Thus, capacitance measurements were also performed.

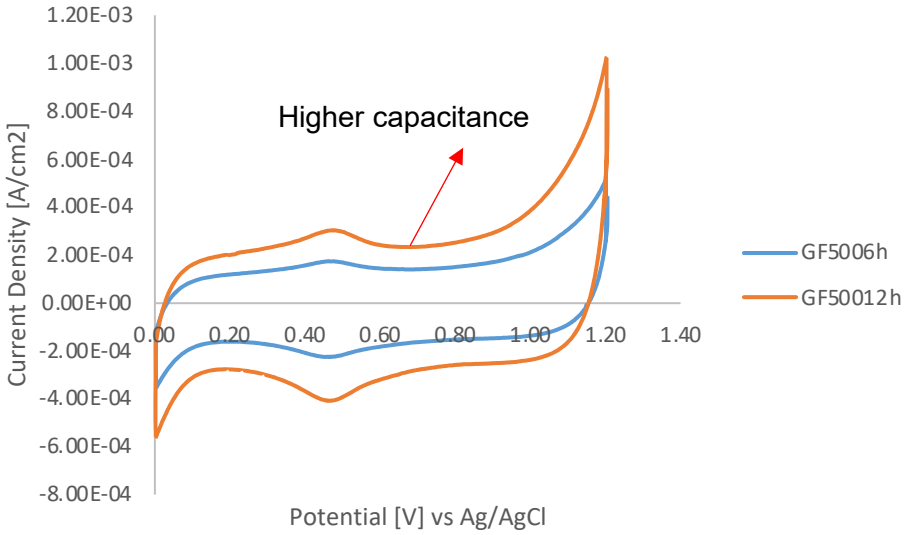

Figure 25. CV measurements in H_2SO_4 for thermally treated electrodes – time effect.

As it can be seen from Figure 25, time has also great influence on capacitance and active electrochemical area. Values for carbolic functional group density and capacitance for activated samples are listed below in Table 19.

Table 19. Capacitance and Functional group density values for thermally treated electrodes – time impact.

Sample	**Carbolic functional group density** [µmol]	**Capacitance** [µF]
GFPristine	0.000	1.06
GF5003h	0.011	10.74
GF5006h	0.010	13.43
GF50012h	0.017	22.79

As it is shown in Table 19, samples treated at longer times showed higher capacitance. Although GF5003h showed similar results compared to GF5006h, GF50012 showed a significant improvement (~20x) compared to pristine GF. Carbolic functional group density was also improved, suggesting that more functional groups were introduced during longer treatment times.

Another tool used to access electrochemical properties was CV. As it can be seen from Figure 26, samples treated at longer times showed similar performance. Both peak potential separation and peak current ratio was calculated and presented in Table 20.

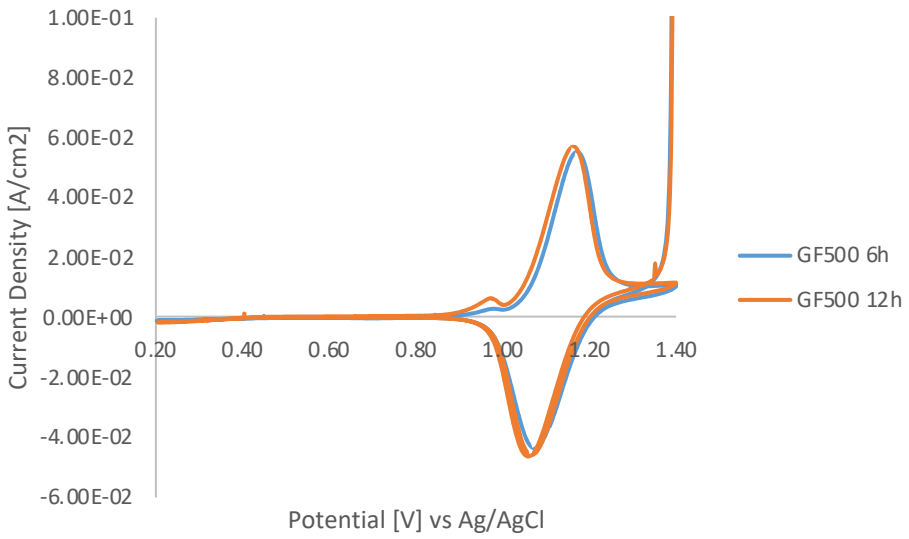

Figure 26. CV curves for different thermally treated electrodes – time impact.

As it can be seen in Table 20, both samples showed similar results for peak potential separation, while peak current ratio showed better improvement. Hence, longer treatment time may affect peak current ratio the most, which is related to kinetics and enhanced electrochemical surface area, while reversibility impact was minor.

Table 20. CV results for different thermally treated electrodes – time impact.

Sample	J_{pa}/J_{pc}	ΔV [V]
GFPristine	3.01	0.210
GF5003h	1.58	0.150
GF5006h	1.38	0.110
GF50012h	1.22	0.100

As it was shown in the *ex-situ* characterization analysis, longer activation process can lead the formation of higher content of oxygen functional groups, which can improve wettability and electrochemical surface area, key parameters for kinetics improvements. Although further *in-situ* performance needs to be done in order to evaluate the impact of thermal treatment time, results showed that GF50012h would likely have a higher performance compared to GF5006h. Even though GF50012h showed improvements for all *ex-situ* characterization tests, GF5006h was selected as activated baseline for later catalyst deposition samples for process simplification, since it requires less time to be prepared. However, to achieve higher efficiencies, GF50012h should be used instead of GF5006h.

4.1.3. Storage Time Impact

Commercial graphite felt electrodes can be purchased either as pristine (non-activated) or activated, though functional group stability is still not quite understood. Thus, an investigation of aging effect (storage time) of different thermally treated samples was carried out. For that, activated samples were stored for 2 years and then submitted to the same set of characterization tools in order to understand the effect of aging on different properties, especially on wettability and electrochemical activity. Though 2 years may seem exaggerated, companies may purchase felts rolls and store them for longer times, which is the main motivation of this investigation.

Contact angle measurements were performed to understand the impact of aging on activated electrodes. At it can be seen in Figure 27, aged samples showed hydrophobic behavior like pristine GF, suggesting that functional groups in the surface got degraded and oxidized during time in exposure with air.

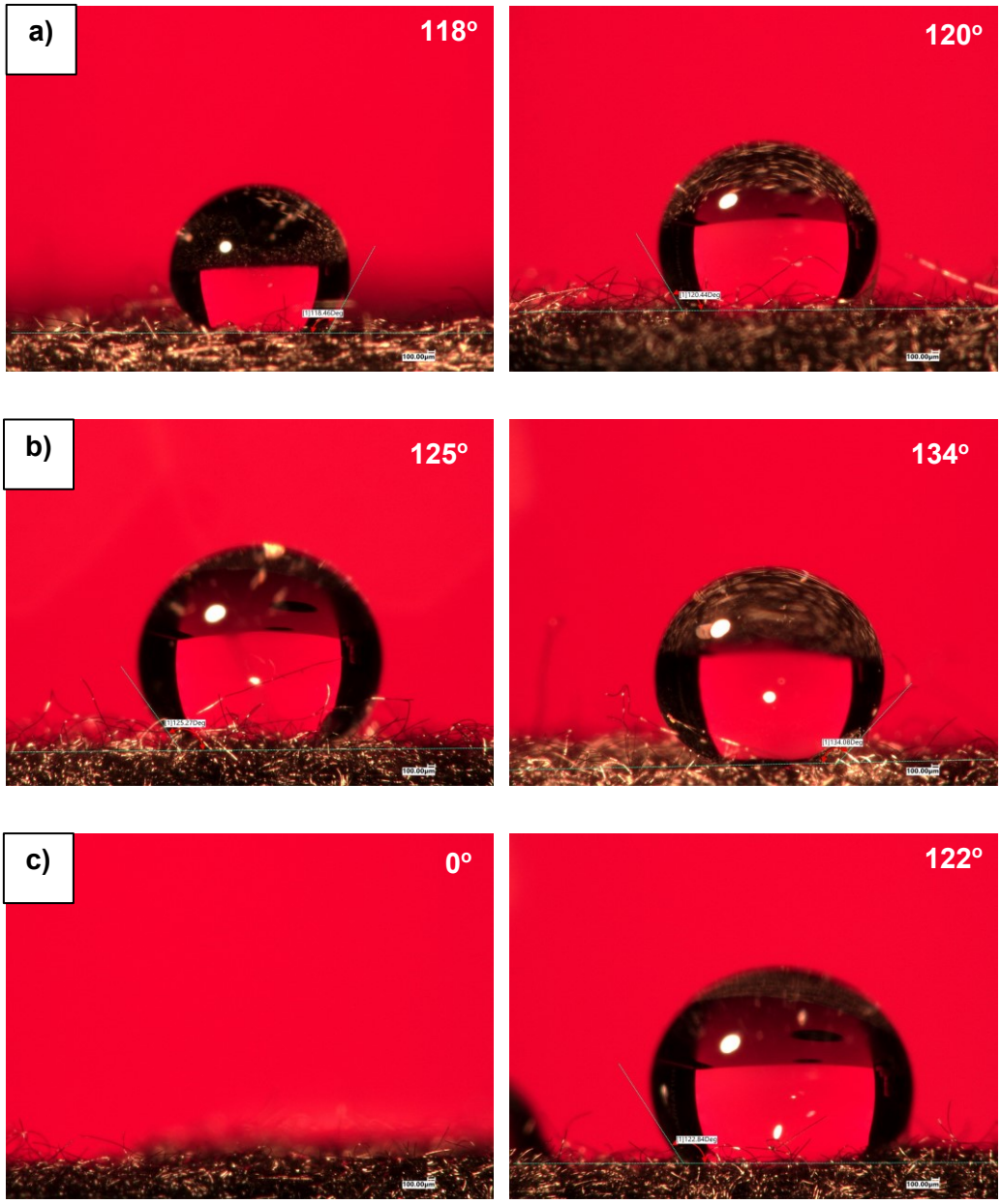

Figure 27. Contact angle measurements for freshly treated (left) and aged (right) electrodes for a) GF400, b) GF450 and c) GF500.

SEM analysis was also done in order to understand changes on surface roughness. As it was expected, no changes in roughness were seen. Hence, any electrochemical activity change can be explained due to surface chemistry rather than surface roughness.

Since samples showed a hydrophobic behavior, capacitance measurements were performed to understand the impact of aging in electrochemical active area (Figure 28).

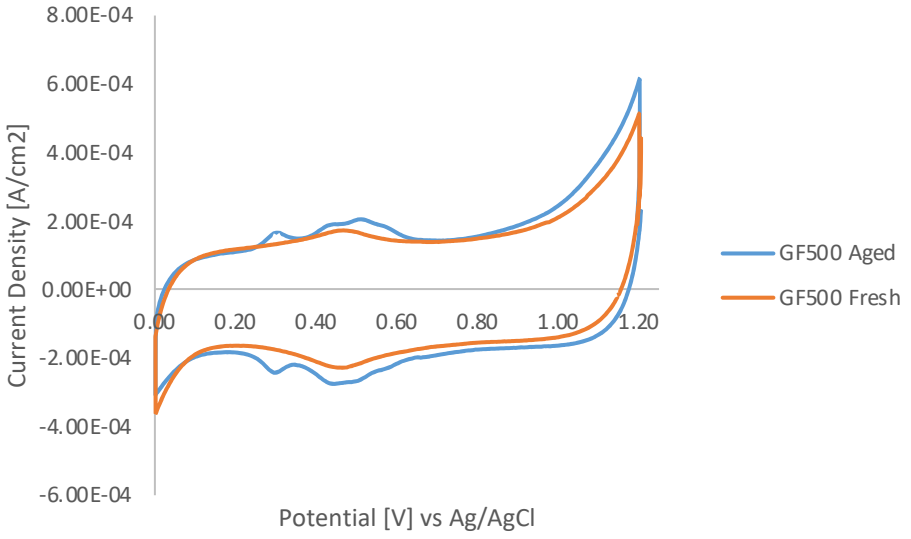

Figure 28. CV measurements in H_2SO_4 for thermally treated electrodes – aging effect.

Capacitance seems to be unaffected, though contact angle measurements showed similar results compared to GFPristine. Results for capacitance and functional group density for different aged samples are shown below in Table 21.

Table 21. Capacitance and carbolic functional group density results for thermally treated electrodes – aging effect.

Sample	Fresh		Aged	
	Carbolic functional group density [µmol]	**Capacitance** [µF]	**Carbolic functional group density** [µmol]	**Capacitance** [µF]
GFPristine	0.000	1.06	-	-
GF400	0.001	2.31	0.001	1.43
GF450	0.003	3.74	0.002	3.25
GF500	0.009	13.43	0.024	14.02

As it can be seen in Table 21, capacitance showed minor degradation signs and it was slightly decreased compared to freshly treated samples. GF400 showed the highest degradation, where capacitance value was similar GFPristine, probably because GF400 was not fully activated, as it was shown before. However, both GF450 and GF500 showed similar results compared to freshly treated samples. Hence, wettability seems to be affected only on the surface, rather than electrode's bulk.

CVs were also performed to understand the impact of aging on other electrochemical properties (Figure 29). Peak potential separation and peak current ratio were calculated for aged samples and then compared to fresh ones (Table 22).

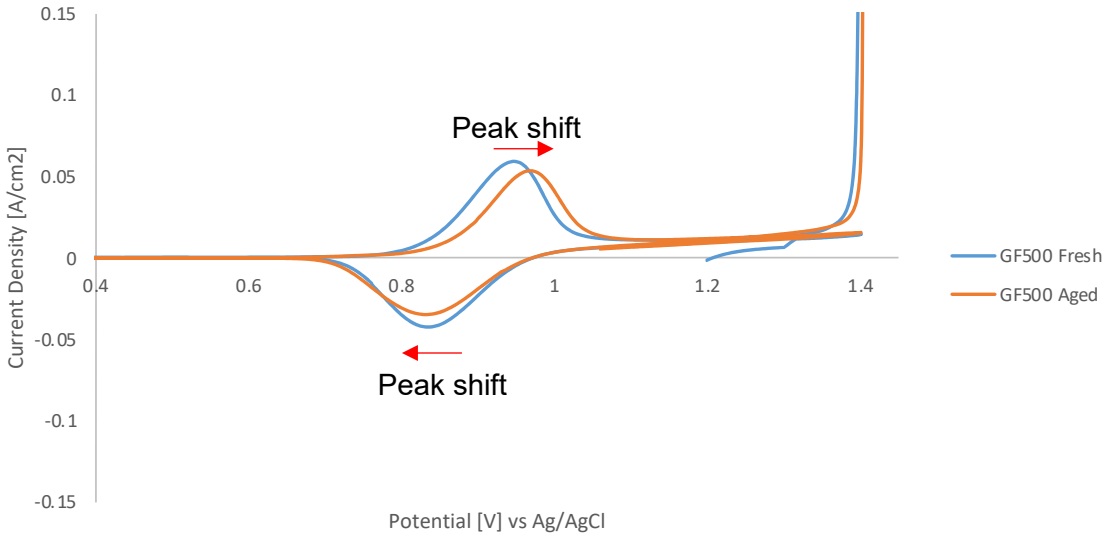

Figure 29. CV curves comparison between aged and pristine thermally treated GF500 electrodes.

As it can be seen in the Figure 29, both peak current ratio and potential separation were impacted and showed lower electrochemical performance compared to freshly treated samples. Results for both fresh and aged samples are listed below in Table 22.

Table 22. CV results for thermally treated GF500 electrodes – aging impact.

Sample	Fresh		Aged	
	J_{pa}/J_{pc}	ΔV [V]	J_{pa}/J_{pc}	ΔV [V]
GFPristine	3.01	0.210	-	-
GF400	2.10	0.160	1.85	0.180
GF450	1.82	0.150	2.07	0.180
GF500	1.38	0.110	1.55	0.140

As it is shown in Table 22, both activity and reversibility were slightly decreased after aging. Although capacitance for fully activated samples stayed unchanged, other electrochemical properties are degraded over time and may pose a concern for electrode performance in VRFB cycling tests.

Hence*, in-situ* VRFB cycling tests were also performed to evaluate the aging effect on electrodes performance. For that, a single cell was assembled using aged GF500 electrodes both as positive and negative electrode. VRFB cycling tests can be used to compared fresh and aged electrodes and understand the impact of aging on electrode performance and determine the feasibility of storing activated electrodes for later use. Results are shown in Table 23.

Table 23. Performance of VRFB system with pristine and aged thermally treated GF500 electrodes.

Sample	EE [%]	VE [%]	CE [%]
GF500 (Fresh)	85.2	88.5	96.2
GF500 (Aged)	86.8	89.5	97.0

As it can be seen in Table 23, aged GF500 electrodes showed higher performance compared to freshly treated ones. Ex-situ characterization for electrochemical performance was only done in the positive electrolyte. Hence, it may be possible that aging had a favorable effect on the negative electrode performance, which was translated into a higher VRFB performance. samples size. The main conclusion from these results appears to be that aging for 2 years does not actually reduce VRFB performance. Yet, this does not consider degradation that may occur over time when the electrodes are assembled and operated in the VRFB. Hence, it is reasonable to either procure activated felt electrodes or treat pristine electrodes in a single batch and store activated samples, though freshly treated electrodes are always preferable.

4.1.4. Re-treatment Impact

Re-treatment was also investigated since aging may pose a concern and electrochemical properties may degrade over time. Hence, to retain the same properties as freshly treated electrodes, re-treatment may be an option.

Analysis of treated morphology of GFEs using SEM was done to understand the impact of re-treatment on the surface roughness. Though samples were re-treated, no changes could be seen in electrode roughness. Thus, changes and improvements are probably due to electrochemical active surface area (due to hydrophilicity) and surface chemistry, rather than active surface area for physical properties.

To evaluate samples' wettability, CA measurements for re-treated samples were performed and then compared to freshly treated samples (Figure 30).

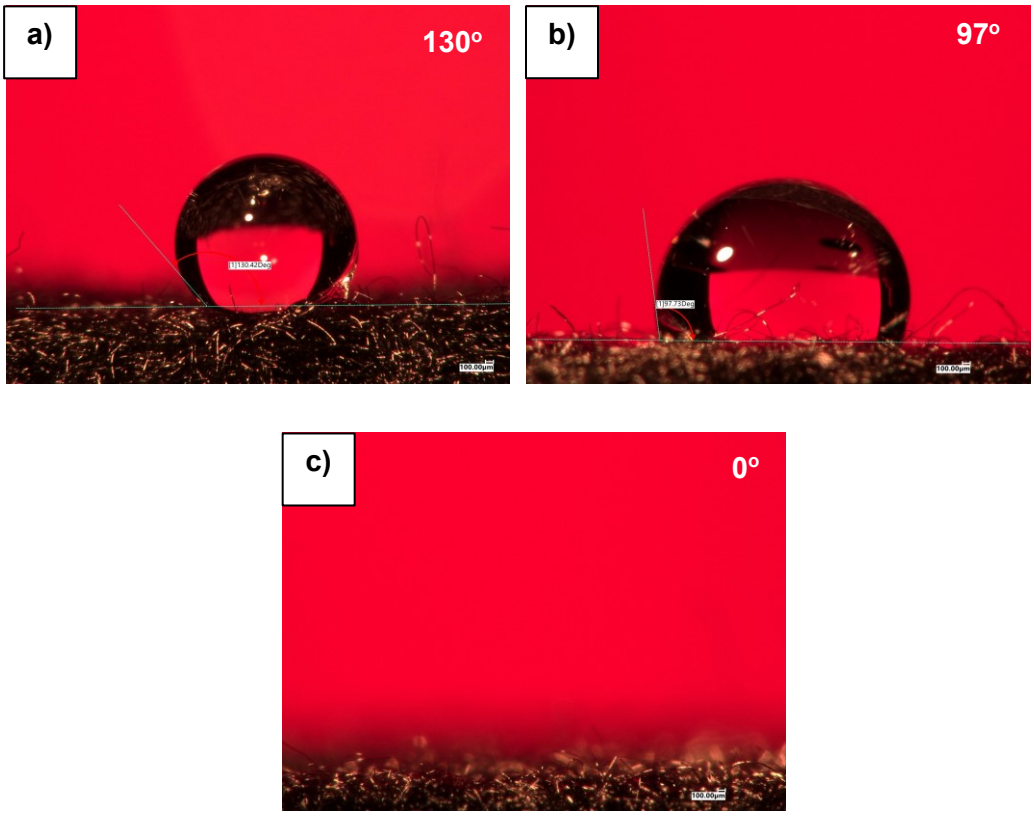

Figure 30. Contact angle measurements for re-treated electrodes a) GF400, b) GF450 and c) GF500.

As shown in Figure 30, re-treatment of aged electrodes seems to have improvements in CA compared to freshly treated ones. Although both GF400 and GF450 still show hydrophobic behavior, CA were lower for both electrodes, which may be translated into higher capacitance and electrochemical surface area. As expected, GF500 showed the same hydrophilic behavior, and improvements in electrochemical surface area can be only evaluated using capacitance measurements.

In order to understand the impact of re-treatment of GFE, capacitance and functional group density values were calculated from CV measurements (Figure 31).

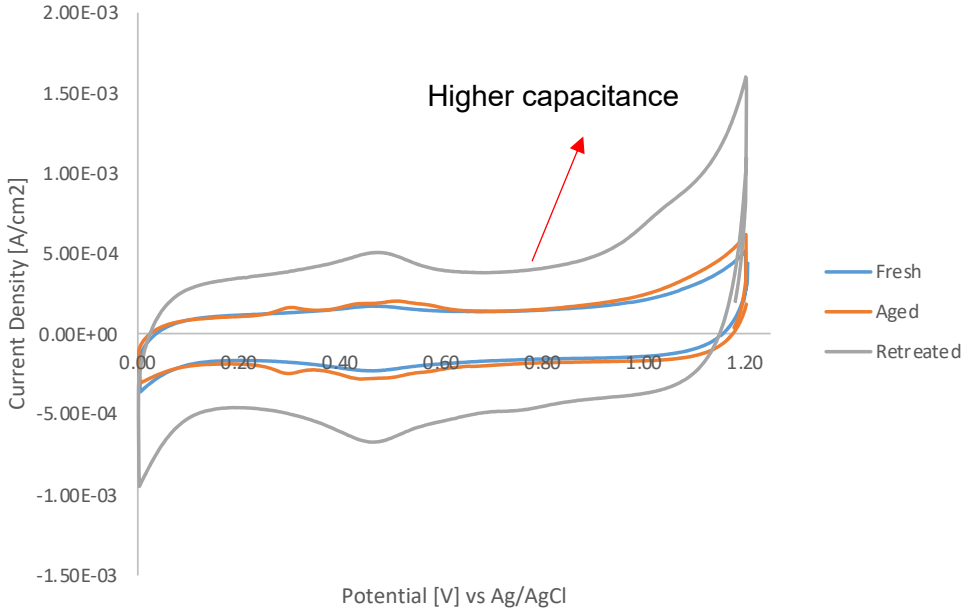

Figure 31. CV measurements in H_2SO_4 for thermally treated electrodes – re-treatment impact.

As it can be seen from Figure 31, capacitance was further improved after re-treatment compared to fresh samples. Values for both group density and capacitance for re-treated samples are shown below in Table 24.

Table 24. Capacitance and carbolic functional group density results for different thermally treated electrodes – re-treatment impact.

Sample	Fresh		Re-treated	
	Carbolic functional group density [µmol]	**Capacitance** [µF]	**Carbolic functional group density** [µmol]	**Capacitance** [µF]
GFPristine	0.000	1.06	-	-
GF400	0.001	2.31	0.003	3.03
GF450	0.003	3.74	0.007	10.18
GF500	0.009	13.43	0.028	37.91

Compared to freshly treated electrodes, all re-treated samples showed improvements in capacitance. GF400 showed similar capacitance to freshly treated electrode, showing that improvements for not fully activated electrodes are temporary and can be reached again when retreated. Activated samples such as GF450 and GF500, which kept their capacitance improvements from previous treatment, showed further improvements after re-treatments. Both samples showed 3x higher capacitance compared to freshly treated electrodes.

CVs were also performed using in vanadium electrolyte in order to understand potentially further improvements in other electrochemical parameters such as activity (kinetics) and reversibility (Figure 32).

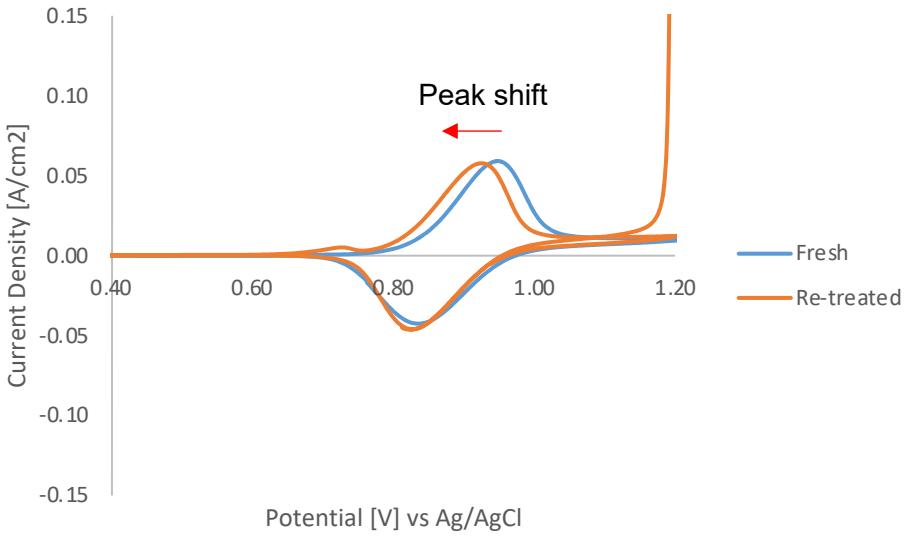

Figure 32. CV curves comparison for re-treated electrode (GF500) and pristine.

Through analysis of CV results, it was noticed that mainly peak current ratio was drastically improved for all samples, while peak potential separation was slightly improved. Values for both peak potential separation and peak current ratio for re-treated electrodes are listed below in Table 25.

Table 25. CV results for different thermally treated electrodes – re-treatment impact.

Sample	Fresh		Re-treated	
	J_{pa}/J_{pc}	ΔV [V]	J_{pa}/J_{pc}	ΔV [V]
GFPristine	3.01	0.21	-	-
GF400	2.10	0.16	1.89	0.16
GF450	1.82	0.15	1.39	0.12
GF500	1.38	0.11	1.25	0.10

As it can be seen in Table 24, both parameters were further enhanced after re-treatment. GF400, which is not fully activated, showed similar results to freshly treated electrode, showing that improvements can be achieved again when retreated. Other samples also showed improvements after re-treatment, which can be explained both for recovering functional groups that were degraded overtime and further improving active surface area.

As it was shown, aging can pose a concern for electrode performance, since functional groups seem to be oxidized from the surface and some properties such as wettability and reversibility can be degraded. Thus, in order to recover high performances, re-treatments can be done. Submitting the electrodes for additional thermal treatment can make the samples recover oxygen functional groups and enhance other physico-chemical properties that can be translated into improved electrochemical properties such as kinetics and reversibility. Results have shown that re-treated samples can achieve higher performance compared to freshly treated ones, which can be useful not only to enhance system performance, but also to recycle aged samples.

4.2. Thermo-Chemical Treatments

Besides thermal treatment, other chemical treatments were proposed so that more functional groups can be introduced to thermally treated samples and potentially improve other properties. For that, different oxidizing agents were used and GF400 was selected as baseline.

Contact angle measurements were also performed to understand if chemical treatments have any further improvements, especially for not fully activated electrodes (Figure 33).

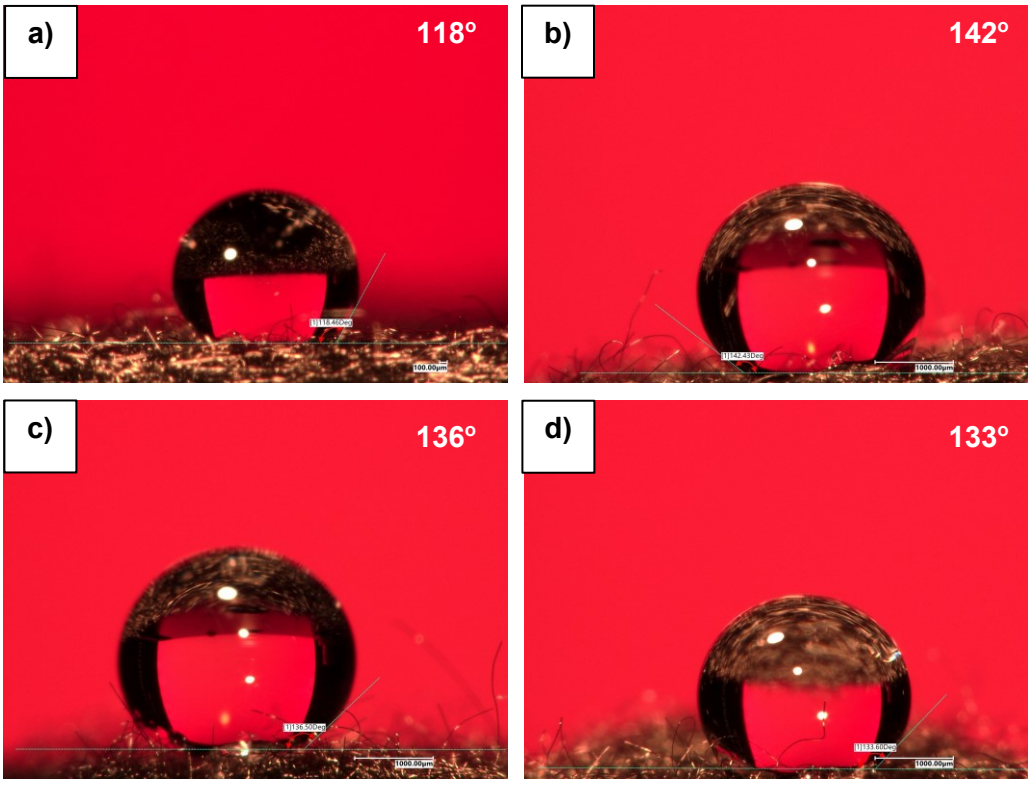

Figure 33. Contact angle measurements for a) GF400 (baseline), b) GF400 - 10H_2O_2, c) GF400 - 30H_2O_2 and d) GF400 - HNO_3.

As shown in Figure 33, all thermo-chemical treated samples showed similar hydrophobic behavior and CA values, suggesting that functional groups introduced via chemical treatments may have an impact on electrochemical properties, but not on wetting properties,

Since some chemical treatments can both introduce functional groups and impact electrode' roughness, SEM was also used to assess surface roughness for chemically treated samples, but no changes were seen after chemical treatments, suggesting that oxidizing agents used have impact only on surface chemistry, but no etching effect.

Raman was used to understand the impact of chemical treatment on material defect. I_D/I_G band ratio was calculated for every electrode (Figure 34).

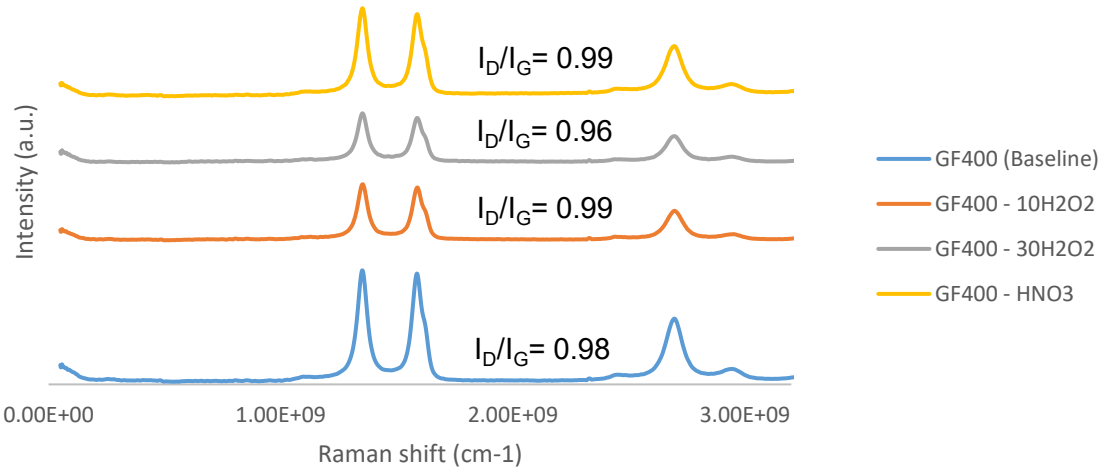

Figure 34. Raman I_G/I_D ratio for different thermo-chemically treated electrodes.

As it is shown in Figure 34, thermo-chemically treated electrodes showed little or no change to I_D/I_G ratio as it was expected from SEM images, suggesting that no defects were introduced during chemical treatments and that any change in performance is mostly due to chemical changes in the surface, rather than physical improvements.

For chemical analysis, XPS was used to understand the impact of chemical treatment on chemical surface. Analysing oxygen peaks for XPS results, H_2O_2 electrodes showed similar results, while HNO_3 showed higher oxygen peaks. Electrodes results can be seen in Table 26

Table 26. XPS surface elemental composition for different thermo-chemically treated electrodes.

Sample	C [%]	O [%]	N [%]	Na [%]	S [%]	Si [%]
GF400	97.63	1.6	0.77	-	-	-

Sample	C [%]	O [%]	N [%]	Na [%]	S [%]	Si [%]
GF400 - 10H_2O_2	96.43	2.65	0.66	-	0.26	-
GF400 - 30H_2O_2	97.08	2.20	0.46	-	0.19	-
GF400 - HNO_3	93.81	4.25	0.83	0.40	0.11	0.44

As it can be seen in the Table 27, oxygen content was slightly increased hydrogen peroxide samples, while nitric acid electrode showed almost 3x oxygen content compared to baseline. Hence, combining chemical treatment to thermally treated samples can further increase oxygen content onto electrodes surface. However, functional groups introduced during chemical treatments may have different impact on electrode performance compared than the ones introduced via thermal treatment. Thus, O_{1s} analysis was done in order to investigate the amount of different functional groups (Table 27).

Table 27. XPS functional groups analysis for different thermo-chemically treated electrodes.

Sample	C=O	C-O	Adsorbed O
GF400	1.07	0.49	0.04
GF400 - 10H_2O_2	1.44	0.99	0.02
GF400 - 30H_2O_2	1.38	0.72	0.10
GF400 - HNO_3	2.79	1.28	0.18

As it can be seen in Table 27, although H_2O_2 samples showed more adsorbed oxygen, C-O and C=O amount were lower compared to nitric acid sample. However,

values were not significantly enhanced compared to baseline, which may explain the similar wettability results.

Since the introduction of functional groups via chemical treatments, didn't show any visible difference in CA measurements, CVs were also performed in sulfuric acid to measure capacitance and understand the correlation between functional groups and capacitance related to active electrochemical surface area (Figure 35).

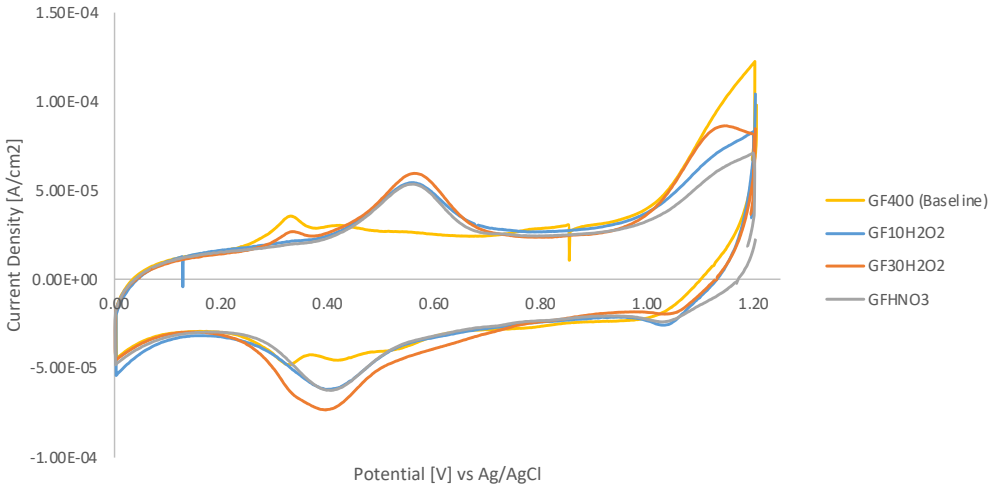

Figure 35. CV measurements in H_2SO_4 for thermo-chemically treated electrodes.

As shown in Figure 35, capacitance values were similar for all thermo-chemically treated electrodes and baseline, though functional groups were drastically improved, as higher and more evident peaks appeared. Values for both functional group density and capacitance are shown in Table 27.

Table 28. Capacitance and Functional group density results for different thermo-chemically treated electrodes.

Sample	**Carbolic functional group density** [µmol]	**Capacitance** [µF]

GF400	0.001	2.31
GF400 - 10H_2O_2	0.005	2.47
GF400 - 30H_2O_2	0.006	2.19
GF400 - HNO_3	0.005	2.31

As it can be seen above, capacitance values were unchanged after chemical treatments, which aligns with CA measurements. Although capacitance was unchanged, functional groups density were enhanced, which aligns with XPS results. Results indicate that wettability isn't determined by only functional groups, but also their concentration, which didn't further improve samples hydrophilicity for thermo-chemical activated samples.

Since little or no change were seen for physical and electrochemical properties, electrochemical characterization was done to investigate the impact of chemically treated samples on different electrochemical parameters (Figure 36).

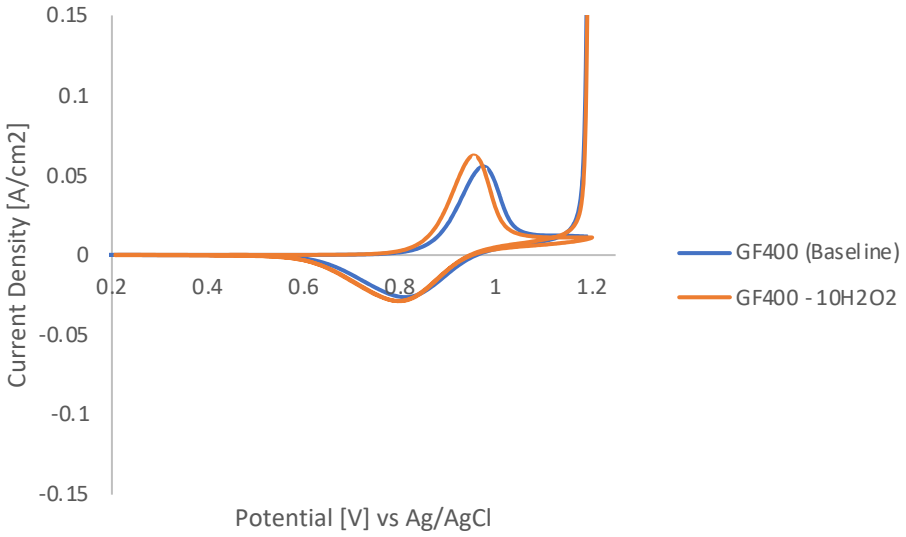

Figure 36. CV curves comparison for thermo-chemically treated electrode (GF400 – 10H_2O_2) and baseline (GF400).

As it can be seen above, samples showed similar performances among them and compared to baseline, though peaks were shifted. Peak potential separation and current ratio were calculated and can be seen in Table 29.

Table 29. CV results for different thermo-chemically treated electrodes.

Sample	J_{pa}/J_{pc}	ΔV [V]
GF400	2.10	0.160
GF400 - $10H_2O_2$	2.15	0.150
GF400 - $30H_2O_2$	2.22	0.120
GF400 - HNO_3	2.19	0.170

As shown in Table 29, potential peak separation was not affected, as it was expected, since it is related to wettability, while current peak separation was improved, only GF400-HNO_3 showed increased in potential peak separation value.

Lastly, *in-situ* VRFB tests were performed to evaluate the performance of chemically treated samples. Results for different thermo-chemical samples are listed below in Table 30.

Table 30. Performance of VRFB system using different thermo-chemically treated electrodes.

SAMPLE	EE [%]	VE [%]	CE [%]
GF400	81.3	82.5	98.5
GF400 - $10H_2O_2$	78.0	79.4	98.2
GF400 - $30H_2O_2$	73.8	73.9	99.9

GF400 - HNO_3	67.0	68.3	98.1

As it can be seen above, all thermo-chemically treated samples showed worst performance compared to baseline. Since wettability and active electrochemical active surface area were unchanged, performance may be mainly impacted by different functional groups introduced by chemical treatments, which are increasing charge transfer resistance, as it was discussed in literature. GF400-10H_2O_2 showed closer performance results compared to baseline (GF400), and a slightly higher charge transfer resistance (~387 ohm.cm^2) compared to baseline (~327 ohm.cm^2), confirming literature statement that chemical treatments can increase charge transfer resistance and lower electrode performance. It was also seen for GF400 – HNO_3, which showed the highest functional groups content in XPS data, and lowest energy efficiency performance during VRFB cycling tests. Hence, another way of combining thermal and chemical activation would be having the chemical treatment before thermal treatment, so that it could not only clean electrodes surface prior thermal treatment, but also introduce functional groups that could be transformed and improved after thermal treatment.

4.3. Catalyst Materials for positive electrode

Different catalyst materials have been proposed for positive electrode application, though there is still room for improvements and gaps that need to be filled, especially for noble metals, which improvements have not been fully explained. Thus, for this part of the work, noble metals, such as iridium and ruthenium have been tested in the combination with other materials to evaluate its impact of electrode performance. Since noble metals are expensive, different non-noble materials were also tested as alternative materials for cathode applications.

4.3.1. Material Selection

For positive electrodes, GF electrode treated at 500ºC for 6h in air (further GF500) was chosen as baseline electrode, since it showed the best performance among thermally treated samples as positive electrode, and it also showed improvements for the negative reactions. Moreover, it was the only sample with a completely hydrophilic behaviour, which is desirable for coating process, so the catalyst ink can penetrate and impregnate the bulk of the electrode. Samples were cut in the desired shape (3x3 cm), and then coated using vacuum dip coating method using a vacuum oven for the complete impregnation of diluted catalyst inks at 30Hg. For this section, electrodes were divided into two categories: noble metals and non-precious metals. The positive electrodes description is listed below in Table 31.

Table 31. Summary of coated electrodes and catalysts used – positive electrode materials.

Catalyst	Sample
Baseline	GF500
Noble Metals	Ir_7Ru / GF500 [40%(50%Ir40%Ru10%Se)/rGO]/GF500 [40%(50%Ir40%Ru10%Se)/5% Sb-SnO_2]/GF500
Non precious Metals	[40%WO_3/rGO]/GF500 [40%Mn_3O_4/XC72]/GF500 [75%($Ta_{0.4}Nb_{0.6}Ti_{0.9}O_2$)/XC72]/GF500

4.3.2. Catalyst Ink Formulation – Solvent Selection

Different solvents for catalyst ink formulation were tested to achieve a homogeneous catalyst distribution on the surface of GF fibers Ir/C was used as a baseline, but if needed, catalyst ink formulation could be changed in case different support or catalyst materials didn't show a good distribution. Catalyst coating results are shown in Figure 37.

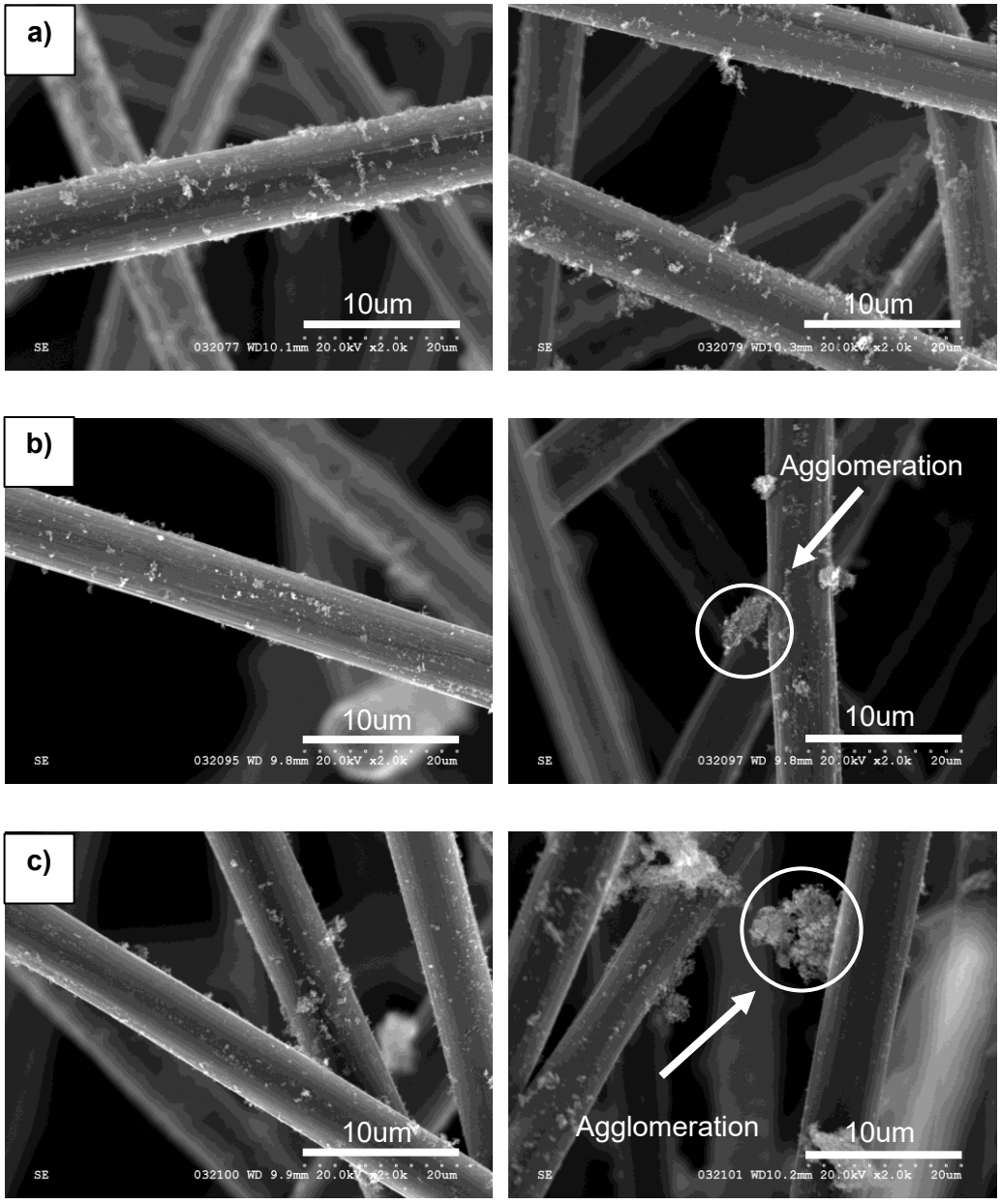

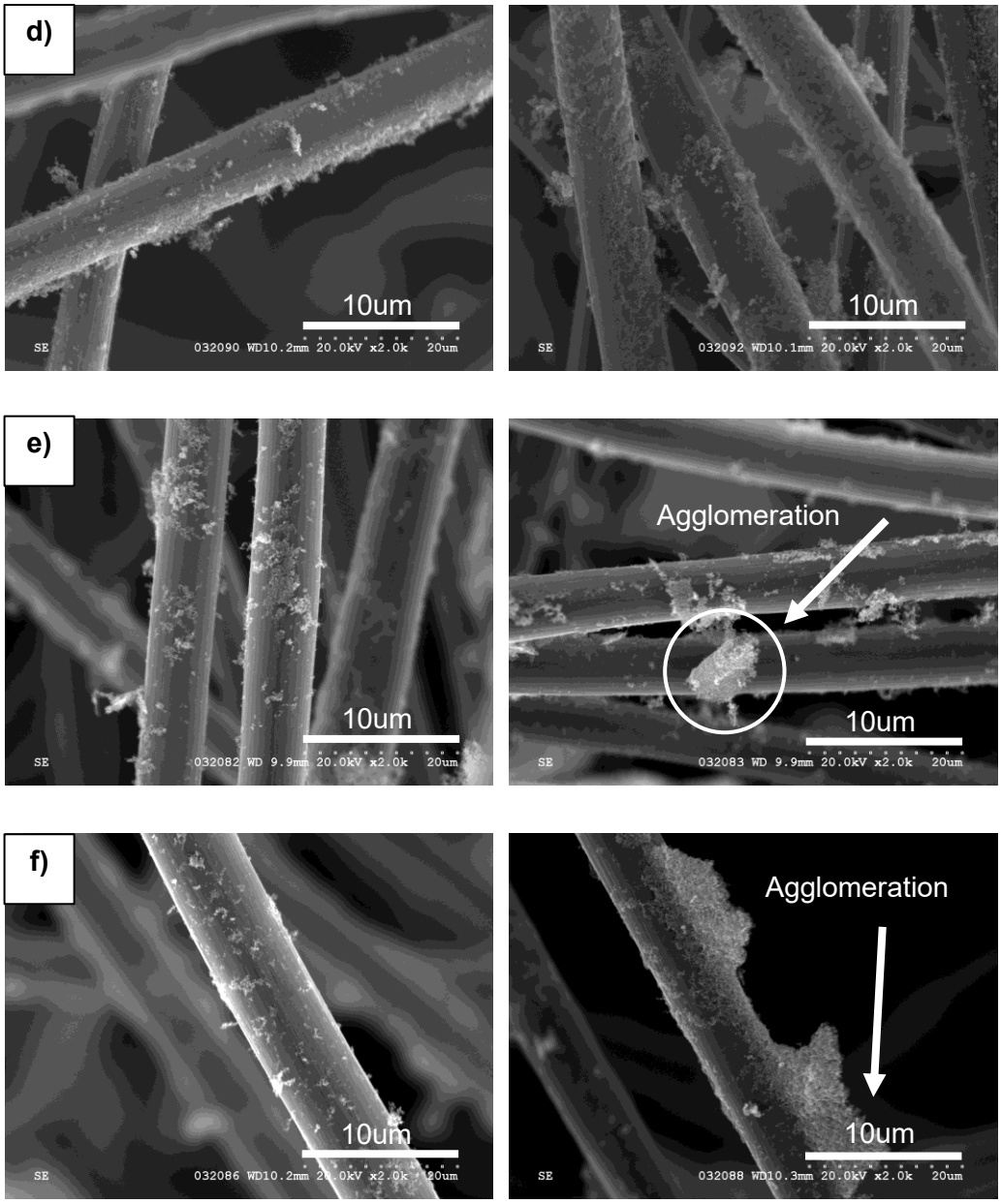

Figure 37. SEM images of Ir/C catalyst coating using different solvents a) Pure Ethanol, b) Pure Isopropanol, c) Pure Methanol, d) Water / Ethanol, d) Water / Isopropanol and e) Water / Methanol.

Based on SEM images, ethanol showed the best catalyst deposition pattern among different solvents. While methanol and isopropanol showed particles agglomeration and randomly distribution, ethanol (both pure and 50% ethanol solution) showed little or no agglomeration and an even distribution, hence being selected as

solvent for catalyst ink formulation. Ethanol solutions were chosen over pure ethanol because it showed better fibers coverage and distribution. For every sample, baseline ink formulation was tested, and SEM analysis was done prior *in-situ* tests to make sure catalyst distribution was efficient.

4.3.3. Noble Metals

The first samples studied in this chapter are related to noble metals such as Ir and Ru, which performance has not been fully investigated in literature and their advantages are still unclear. Thus, different electrodes using Ir and Ru as main catalyst materials were fabricated and tested,using rGO and Sb-SnO_2 as support to further improve active surface area. SEM analyses were done for coated electrodes, which is shown in Figure 38.

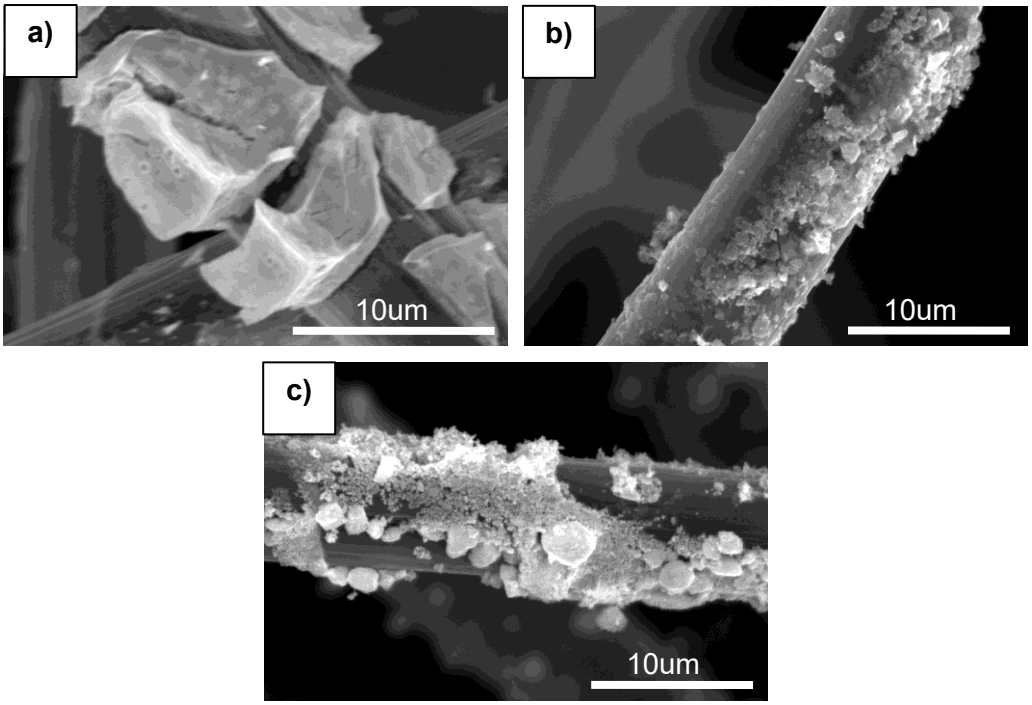

Figure 38. SEM figures for different noble metal coated samples a) Ir_7Ru/GF500, b) 40%(50%Ir40%Ru10%Se)/rGO and c) 40%(50%Ir40%Ru10%Se)/5% Sb-SnO_2.

As it can be seen in Figure 38, catalyst coating for all electrodes showed good coverage, evenly distribution and little or no particles agglomeration, which are desirable features for coated electrodes. While supported catalysts showed a thicker catalyst layer for both support materials, Ir_7Ru/GF500 showed catalyst blocks that may be easily washed off during electrolyte flow.

Initially, GF500 (baseline) showed total hydrophilic behaviour, which may be affected after catalyst coating, depending on catalyst hydrophilicity nature. Hence, to evaluate the impact of different catalyst materials on electrode hydrophilicity, CA measurements were performed. Results are shown in Figure 39.

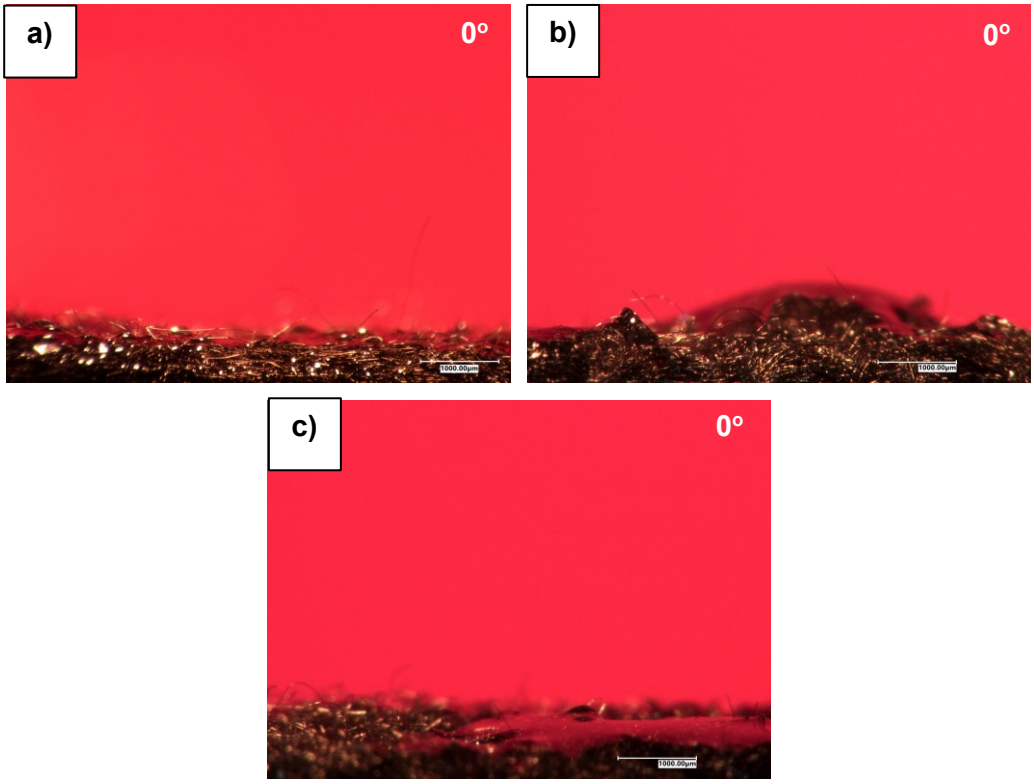

Figure 39. Contact angle measurements for a) GFIr7Ru, b) 40%(50%Ir40%Ru10%Se)/rGO and c) 40%(50%Ir40%Ru10%Se)/5% Sb-SnO_2.

As it can be seen in Figure 39, all samples showed the same hydrophilicity as the baseline electrodes, suggesting that selected catalyst materials had no impact on sample wettability. Hence, further analysis was done to evaluate catalyst materials impact on surface area. For that, CV measurements in sulfuric acid were performed (Figure 40) and capacitance values were calculated (Table 32).

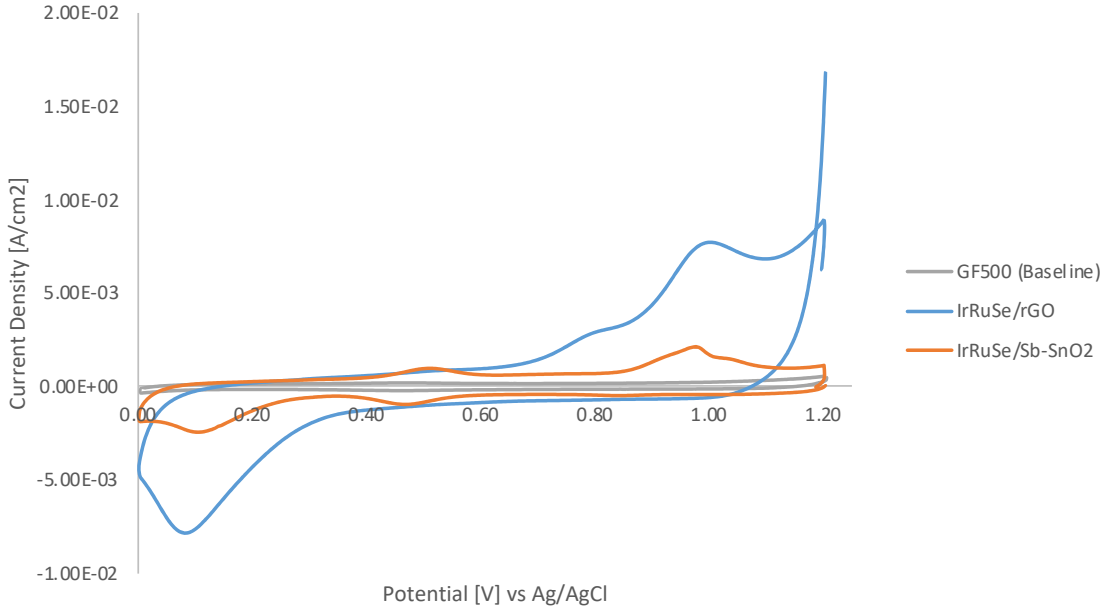

Figure 40. CV measurements in H_2SO_4 for different noble metal coated electrodes.

Table 32. Capacitance and functional group density results for different noble metal coated electrodes.

Sample	**Carbolic functional group density** [µmol]	**Capacitance** [µF]
GF500 (Baseline)	0.009	13.43
Ir_7Ru/GF500	0.026	43.09
40%(50%Ir40%Ru10%Se)/rGO	0.026	90.91
40%(50%Ir40%Ru10%Se)/5% Sb-SnO_2	0.056	61.30

As expected, supported samples showed the higher capacitance (electrochemical surface area) compared to non-supported sample. Also, rGO supported catalysts showed 3x higher capacitance compared to ceramic support, which was also expected, since rGO has a higher SSA compared to Sb-SnO_2. Hence, support materials selection is also important when proposing new catalyst materials since kinetics can be improved based on catalyst surface area.

Lastly, the electrochemical characterization was done to understand the impact of catalyst materials on electrochemical reversibility and activity for V^{4+}/V^{+5} redox reactions. First, CV in vanadium electrolyte were performed (Figure 41) and two different parameters were calculated: peak potential separation and peak current ratio were calculated. Results for both parameters are show in Table 33.

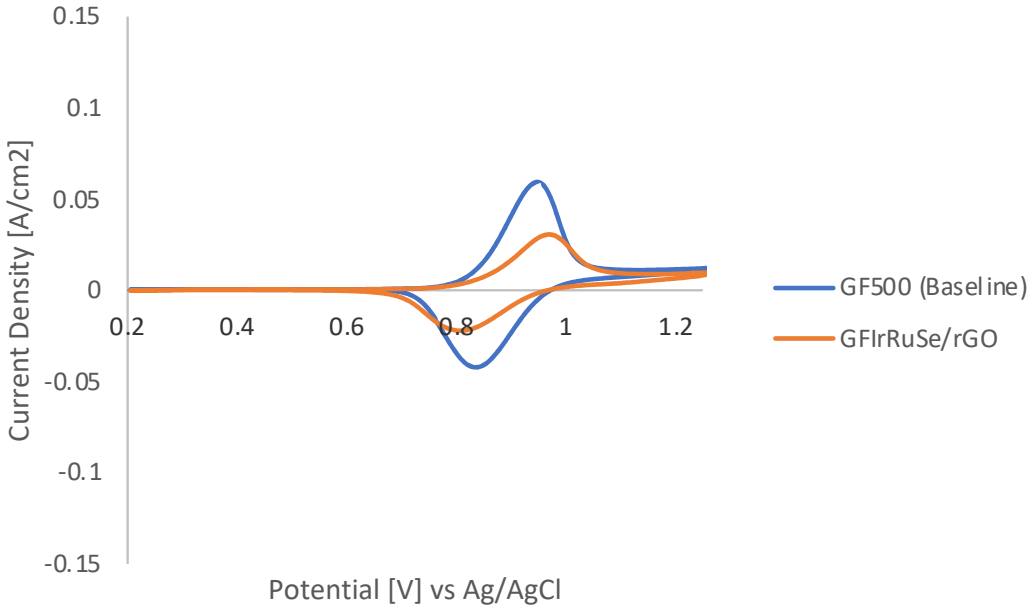

Figure 41. CV curves comparison for t noble metal coated electrode (40%(50%Ir40%Ru10%Se)/rGO) and baseline (GF500).

Table 33. CV results for different noble metal coated electrodes.

Sample	J_{pa}/J_{pc}	ΔV [V]
GF500 (Baseline)	1.38	0.11
Ir_7Ru/GF500	1.23	0.12
40%(50%Ir40%Ru10%Se)/rGO	1.35	0.16
40%(50%Ir40%Ru10%Se)/5% Sb-SnO_2	1.24	0.16

As shown in Table 33, changes for both parameters were minor as reversibility (peak potential separation) and activity (peak current ratio) have similar values compared to baseline.

EIS measurements were also performed to evaluate the performance difference between different supports. Results for the charge transfer resistance can be seen in Table 34.

Table 34. EIS results for different noble metal coated electrodes.

Sample	R_s [ohm.cm²]	R_{ct} [ohm.cm²]
GF500 (Baseline)	0.11	4.98
Ir_7Ru/GF500	0.76	0.25
40%(50%Ir40%Ru10%Se)/rGO	0.12	0.10
40%(50%Ir40%Ru10%Se)/5% Sb-SnO_2	0.42	0.46

While both samples significantly showed improvements in R_{ct}, 40%(50%Ir40%Ru10%Se)/rGO showed lower R_{ct} valued compared to 40%(50%Ir40%Ru10%Se)/5% Sb-SnO_2, most likely due improvements in capacitance and then kinetics. Thus, for *in-situ* VRFB tests, 40%(50%Ir40%Ru10%Se)/rGO will likely show better performance.

After *ex-situ* characterization was completed, *in-situ* VRFB single tests were performed, and electrode's performance was evaluated. Results for efficiencies are listed below in Table 35.

Table 35. VRFB Cycling Test for different noble metals coated electrodes.

Composition	Electrode	EE [%]	CE [%]	VE [%]
GF500 (Baseline)	Positive and Negative	85.2	96.2	88.5
Ir_7Ru/GF500	Positive	86.3	95.0	90.9
40%(50%Ir40%Ru10%Se)/rGO	Positive	87.3	97.2	89.8
40%(50%Ir40%Ru10%Se)/5% Sb-SnO_2	Positive	87.0	96.6	90.0

As expected, 40%(50%Ir40%Ru10%Se)/rGO showed the best performance among activated GFEs, though the EE was similar for the 40%(50%Ir40%Ru10%Se)/5% Sb-SnO_2 sample. For those samples, ~2% improvement can be seen in energy efficiency. Improvements were mostly due to enhancements in surface area and charge transfer resistance. Performance may be further improved if loading is increased so active surface area is also enhanced. However, there is a trade-off between higher loading and capacitance, since agglomeration can also occur, and pores may be blocked.

Noble metals such as Ir and Ru showed catalytic activity towards the positive couple, which can be used as catalyst materials for positive electrodes. Those metals, when combined with support materials, can improve key parameters such as active electrochemical surface area, which can improve electrochemical properties such as kinetics. However, stability seems to be a problem for those catalysts, which explain performance degradation. Hence, better catalyst coating methods should be designed to minimize catalyst dissolution.

4.3.4. Non-precious metals

According to literature and patent analysis, non-noble metal oxides as catalysts for positive electrodes were studied in this section their higher cost efficiency, stability, and electronic conductivity. SEM was used to understand catalyst deposition and evaluate coating quality regarding a distribution, coverage and potentially particle agglomeration (see Figure 42).

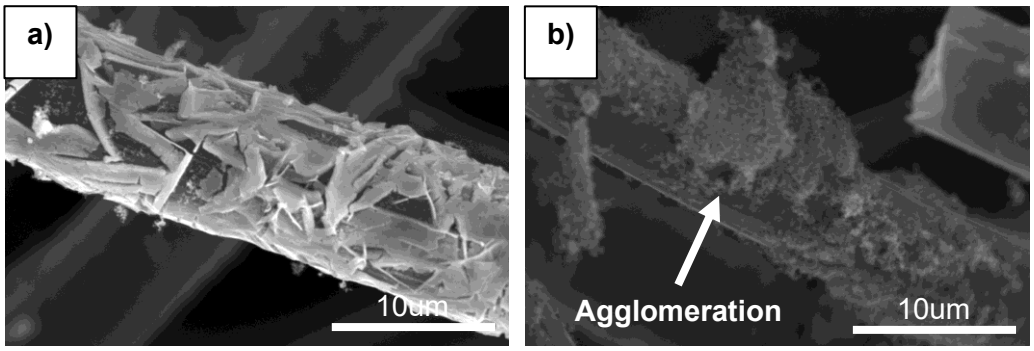

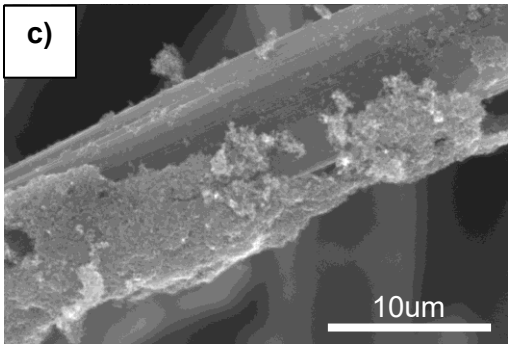

Figure 42. SEM figures for different non-noble metal oxides coated electrodes a) GFWO_3/rGO, b) Mn_3O_4/XC72 and c) TaNbTiO_2/XC72.

As it can be seen in Figure 42, all coated samples showed good deposition. WO_3/rGO showed complete coverage, while TaNbTiO_2/XC72 showed thicker layer that didn't completely cover electrode's fibers. Mn_3O_4 showed reasonable coverage, but agglomeration can be seen. Perhaps, ratio between catalyst and support could be increased for Mn_3O_4 samples and loading for TaNbTiO_2 could be also increased to improve catalyst coverage.

Metal oxides are hydrophilic and theoretically should not pose any concerns for samples wettability. However, different carbon supports were used, which can impact sample hydrophilicity, since carbon is hydrophobic. Hence, CA measurements were performed to evaluate the impact of the different catalyst materials (see Figure 43)

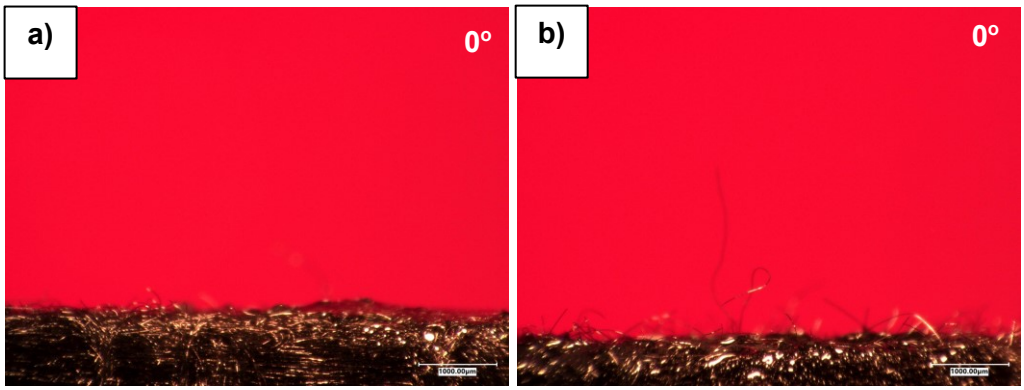

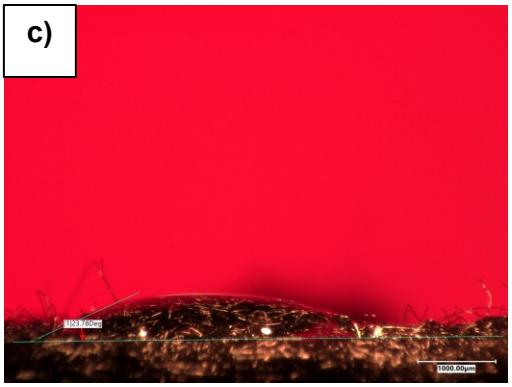

Figure 43. CA measurements for different non-noble metal oxides coated electrodes a) GFWO_3/rGO, b) Mn_3O_4/XC72 and c) TaNbTiO_2/XC72.

As shown in Figure 43, all samples showed hydrophilic behaviors. While WO_3/rGO and Mn_3O_4 showed completely hydrophilic behavior, Ta$NbTiO_2$ showed a 23º CA value, though water droplet could've been absorbed after few minutes in measurements were taken after longer times. Hence, selected catalyst should also not interfere on electrode wettability and not pose a concern.

For electrochemical analysis, cyclic voltammetry was the first tool used in order to understand how different catalyst impact electrode' electrochemical active surface area. For that, CV measurements in sulfuric acid were performed so capacitance and carbolic functional group density can be evaluated (see Figure 44).

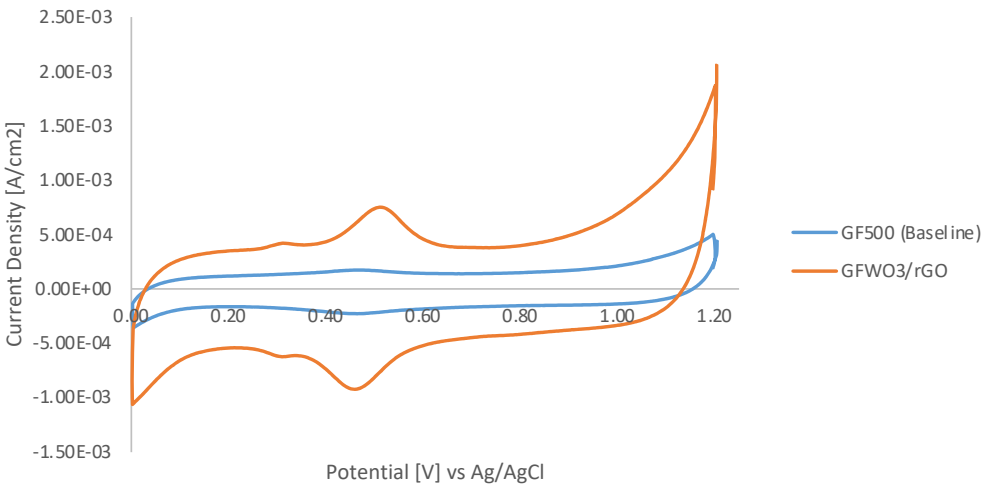

Figure 44. CV measurements in H_2SO_4 for non-noble metal oxide coated electrode (40%WO_3/rGO) and baseline (GF500).

As expected, supported samples showed higher capacitance, which is the main advantage of using different carbon supports combined with metal oxides. Results for both functional group density and capacitance are shown in Table 36.

Table 36. Capacitance and functional group density results for different non-noble metal oxides coated electrodes.

Sample	**Carbolic functional group density** [µmol]	**Capacitance** [µF]
GF500 (Baseline)	0.009	13.43
40%WO_3/rGO	0.055	38.07
40%Mn_3O_4/XC72	0.108	30.16
75%($Ta_{0.4}Nb_{0.6}Ti_{0.9}O_2$)/XC72	0.290	45.73

As it can be seen in Table 36, all coated GFEs showed improvements in capacitance. Although Mn_3O_4 showed a good distribution, lower capacitance value may reflect in particles agglomeration.75%($Ta_{0.4}Nb_{0.6}Ti_{0.9}O_2$)/XC72 showed the highest capacitance, which may be explained by its core-shell design and high electronic conductivity related to the Ketjen carbon black (XC72) core and durable, hydrophilic shell $TaNbTiO_2$. Electrochemical properties of the developed activated GFE such as electrochemical reversibility and kinetics were evaluated.

Other than sulfuric acid, CV were also performed in vanadium electrolyte to evaluate changes in electrochemical properties such as reversibility and kinetics (Figure 45).

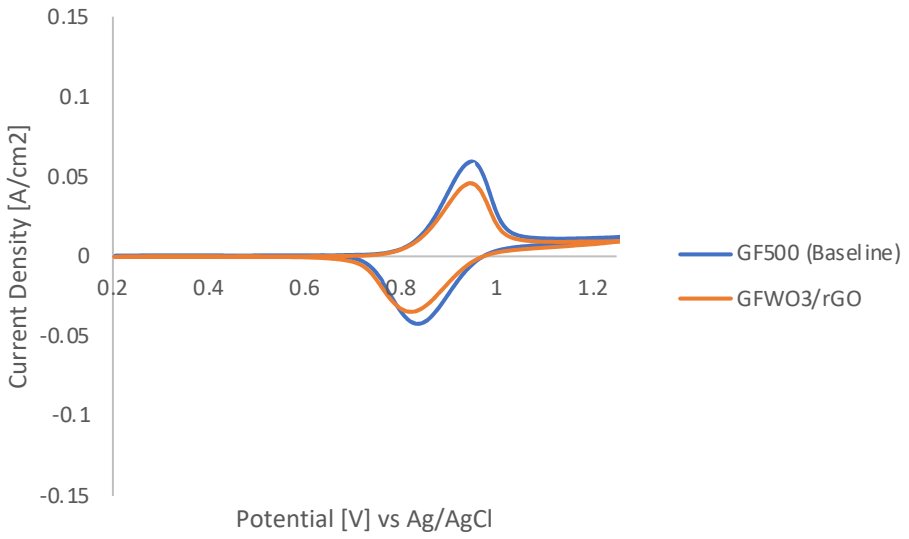

Figure 45. CV curves comparison for non-noble metal oxides coated electrode (40%WO_3/rGO) and baseline (GF500).

As it can be seen from Table 37, changes for both parameters were minor as reversibility (peak potential separation) and activity (peak current ratio) have similar values compared to baseline, as it was also shown for noble metals.

Table 37. CV results for different non-noble metal oxides coated electrodes

Sample	J_{pa}/J_{pc}	ΔV [V]
GF500 (Baseline)	1.38	0.11
40%WO_3/rGO	1.32	0.12
40%Mn_3O_4/XC72	1.38	0.13
75%($Ta_{0.4}Nb_{0.6}Ti_{0.9}O_2$)/XC72	1.40	0.11

EIS measurements were also performed in order to evaluate charge transfer resistance changes caused by different catalysts. Results for charge transfer resistance are listed below in Table 38.

Table 38. EIS results for different non-noble metal oxides coated electrodes.

Sample	R_s [ohm.cm²]	R_{ct} [ohm.cm²]
GF500 (Baseline)	0.11	4.98
40%WO_3/rGO	0.22	0.10
40%Mn_3O_4/XC72	0.91	0.17
75%($Ta_{0.4}Nb_{0.6}Ti_{0.9}O_2$)/C	0.17	0.63

As it can be seen in Table 38, all samples showed improved charge transfer resistance. WO_3/rGO showed the lowest R_{ct}, which was expected, since rGO has higher

surface area and electronic conductivity compared to other carbon supports. Also, it's discussed in literature that there is a W-C synergy, which can explain the lower R_{ct}.

After applying all characterization tools, *in-situ* cycling tests were done to determine the electrode's performance in a VRFB system. Based on the data obtained from these measurements, parameters such as energy, voltage and coulombic efficiency were analyzed and samples with the most improved performance can be determined (See Table 39).

Table 39. VRFB Cycling Test for different non-noble metal oxides coated electrodes.

Composition	Electrode	EE [%]	CE [%]	VE [%]
GFPristine	Positive and Negative	73.1	96.4	75.8
GF500 (Baseline)	Positive and Negative	85.2	96.2	88.5
40%WO_3/rGO	Positive	87.8	97.2	90.3
40%Mn_3O_4/XC72	Positive	85.2	96.0	88.8
75%($Ta_{0.4}Nb_{0.6}Ti_{0.9}O_2$)/XC72	Positive	86.0	95.6	89.9

Based on *in-situ* VRFB tests, the two samples that showed best performance as positive electrode were GF 40%WO_3/rGO and 75%($Ta_{0.4}Nb_{0.6}Ti_{0.9}O_2$)/XC72. Although 40%(50%Ir40%Ru10%Se)/rGO showed a slightly difference in energy efficiency after 50th cycle compared to WO_3 samples (EE around 88%), it degraded faster than WO_3/rGO.

Thus, WO_3/rGO would be a good candidate to replace noble metals catalyst, since it is cheaper and more durable compared to Ir catalyst samples.

Results showed that non-noble metal oxides can also be good candidates for catalyst materials for positive electrodes. Non-noble catalyst samples showed the same improvements in both physical and chemical properties (mostly wettability) that were translated into improvements in electrochemical performance (kinetics). In fact, WO_3 catalyst showed not only higher performance compared to noble metal ones, but also better catalyst stability. Besides enhance active surface area and kinetics, W-C bond is also believed to be the reason for electrode performance, which was discussed in literature [104]. In short, inexpensive catalyst materials such as WO_3 can be used as alternative solutions for positive electrodes, which can show as high performance as noble metals and maintain performance stability after longer cycles.

4.4. Catalyst Materials for negative electrode

Negative electrodes require different additional efforts both due to V^{2+}/V^{3+} reactions being the most sluggish reactions and side reactions such as hydrogen evolution. Hence, catalyst materials were selected based on literature review analysis based on materials that can reduce hydrogen evolution, such as Bi, Ti, and In. Mitigating HER is one of the most important features for negative catalyst selection, other than SSA electronic conductivity.

For negative electrodes, GF500 was also chosen for baseline since it also showed improvements in electrochemical performance as negative electrode. Also, since the slushiness of the negative couple reactions are associated to wetting properties [80], GF500 was selected since it showed most hydrophilic behavior. Samples were cut in the desired shape (3x3 cm), and then coated using same dip coating method used for the positive electrodes. For this section, samples were divided into two categories: Metals and ceramics. The anode samples description is shown below in Table 40.

Table 40. Summary of coated samples and catalysts used – negative electrode materials.

Catalyst	Sample
Baseline	GF500
Metals	Bi/GF500
Ceramics	[75%($Ta_{0.4}Nb_{0.6}Ti_{0.9}O_2$)/XC72]/GF500
	5% In-SnO_2/GF500

4.4.1. Metal and Metal Oxides

SEM analyses were done in order to evaluate catalyst deposition (Figure 45). While ceramic catalyst showed good catalyst coverage and distribution, metal sample showed random bigger particles distribution, which may pose a concern for catalyst stability and active surface area.

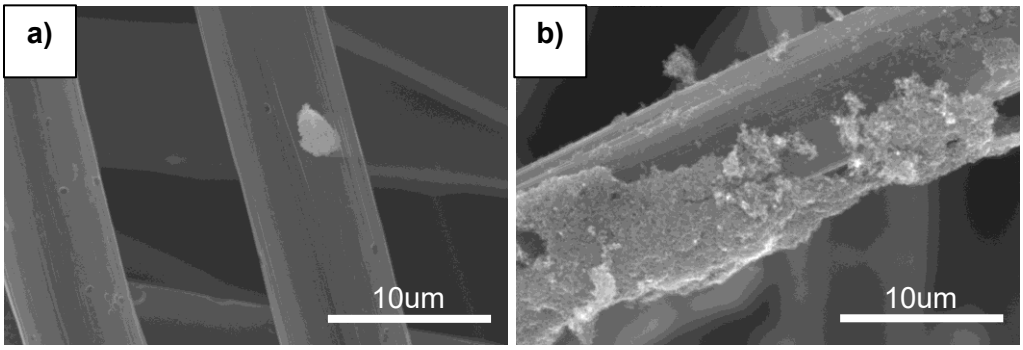

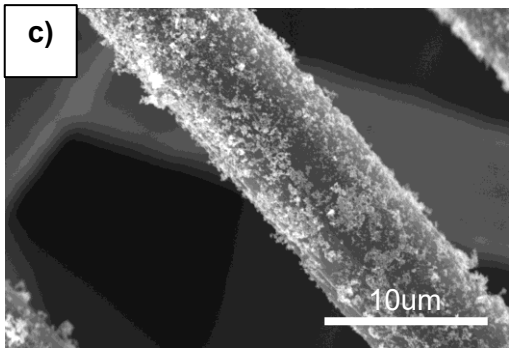

Figure 46. SEM figures for different anode coated electrodes a) Bi/GF500, b) GFTaNbTiO$_2$/XC72 and c) GFIn-SnO$_2$/GF500.

As mentioned before, metal oxides are hydrophilic, hence they shouldn't pose a concern for wettability. CA measurements were done in order to confirm sample hydrophilicity, and as it was expected, all samples showed completely hydrophilic behavior. Thus, capacitance measurements should be done in order to assess samples wettability and then electrochemical active surface area. For that, CV measurements were performed in sulfuric acid (Figure 47) and results for both functional group density and capacitance are shown in Table 41.

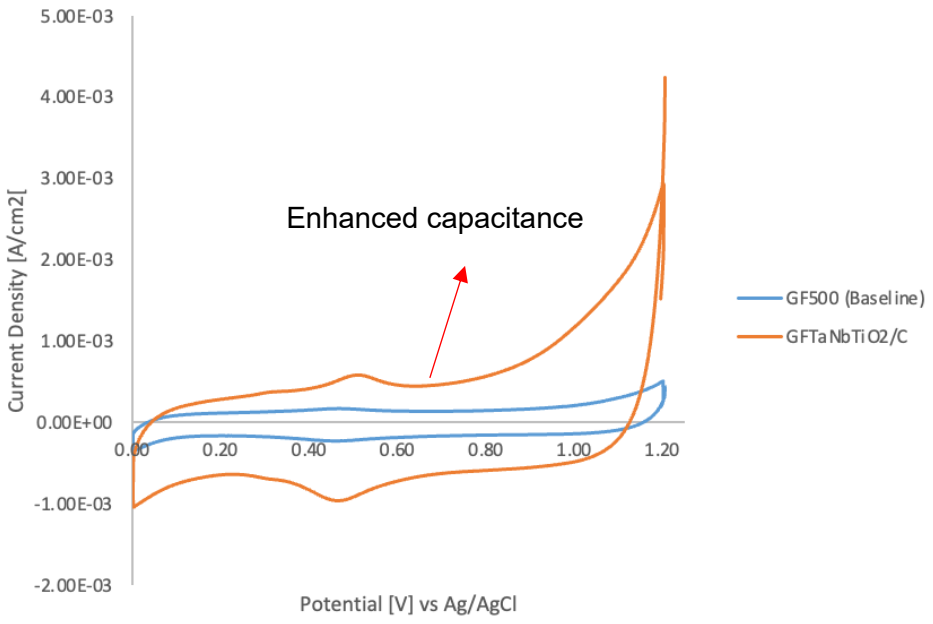

Figure 47. **CV measurements in H_2SO_4 for coated electrode ([75%($Ta_{0.4}Nb_{0.6}Ti_{0.9}O_2$)/XC72]/GF500) and baseline (GF500).**

Table 41. **Capacitance and functional group density results for different coated electrodes.**

Sample	**Carbolic functional group density** [µmol]	**Capacitance** [µF]
GF500 (Baseline)	0.009	13.43
Bi/GF500	0.023	14.73
[75%($Ta_{0.4}Nb_{0.6}Ti_{0.9}O_2$)/XC72]/ GF500	0.290	45.73
In-SnO_2 / GF500	0.016	18.11

Although all samples showed increased capacitance values, only 75%($Ta_{0.4}Nb_{0.6}Ti_{0.9}O_2$)/XC72 showed significantly high capacitance and functional group

density. Bi/GF500 was expected to have not significant improved due to randomly particles distribution. Low capacitance for In-SnO_2 sample may be explained due to low catalyst SSA and/or small loading.

CV measurements were also performed using vanadium electrolyte (anolyte) so that electrochemical properties can be evaluated (Figure 48). Results for both peak potential separation and current ratio are listed below in Table 42.

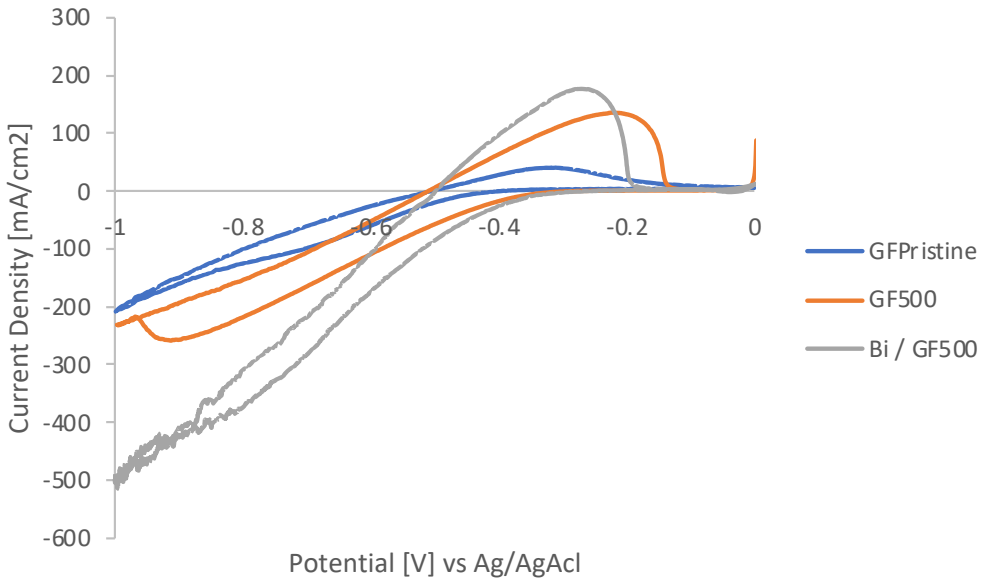

Figure 48. CV curves for different activated electrodes in anolyte.

Table 42. CV results for different coated electrodes.

Sample	J_{pa}/J_{pc}	ΔV [V]
GFPristine*	-	-
GF500 (Baseline)	0.55	0.50
Bi/GF500	0.64	0.55
[75%($Ta_{0.4}Nb_{0.6}Ti_{0.9}O_2$)/XC72]/ GF500	0.60	0.47
In-SnO_2 / GF500	0.46	0.54

***Note**: GFPristine showed no cathodic peak, thus no peak potential separation and peak current density were calculated.

As it can be seen in Table 42, all samples showed similar peak potential separation (reversibility) values, though 75%($Ta_{0.4}Nb_{0.6}Ti_{0.9}O_2$)/XC72 showed the lowest peak potential separation value. For kinetics analysis, only In-SnO_2 / GF500 showed worsen peak current ratio, which aligns with capacitance measurements. While most of the samples showed improvements in only one of the parameters, 75%($Ta_{0.4}Nb_{0.6}Ti_{0.9}O_2$)/XC72 showed improvements in both, being a potential candidate for higher performance in *in-situ* VRFB tests.

EIS were also performed to evaluate changes in R_{ct}. Results for charge transfer resistance are shown below in Table 43.

Table 43. EIS results for different coated electrodes.

Sample	R_s [ohm.cm²]	R_{ct} [ohm.cm²]
GFPristine	0.68	20.04
GF500 (Baseline)	1.35	0.18
Bi/GF500	1.56	0.19
[75%($Ta_{0.4}Nb_{0.6}Ti_{0.9}O_2$)/XC72]/ GF500	1.39	0.19
In-SnO_2 / GF500	1.31	0.17

As shown in Table 43, Bi/GF500 showed higher resistance values (both R_s and R_{ct}), while R_{ct} for other samples were close baseline. R_{ct} for baseline sample is already low, hence catalyst materials may have not further improved charge transfer resistance.

Lastly, cycling VRFB tests were performed to evaluate activated samples performance and stability and results for electrodes' efficiencies are listed in Table 44.

Table 44. VRFB results for different coated negative electrodes.

Sample	Electrode	EE [%]	CE [%]	VE [%]
GF500 (Baseline)	Positive and Negative	85.2	96.2	88.5
Bi/GF500	Negative	88.4	97.2	90.9
[75%($Ta_{0.4}Nb_{0.6}Ti_{0.9}O_2$)/XC72] / GF500	Negative	86.8	96.1	90.3
In-SnO_2 / GF500	Negative	84.6	97.0	87.2

As it was expected, 75%($Ta_{0.4}Nb_{0.6}Ti_{0.9}O_2$)/XC72 showed better performance to baseline, while In-SnO_2/GF500 showed worse performance. However, Bi/GF500 showed the highest performance, which may be attributed to the catalyst activity itself, rather than improvements active electrochemical surface area. As it was discussed in literature, Bi is one of the most efficient catalyst materials for the negative electrode. Using macro-sized Bi catalyst materials was enough to achieve higher efficiencies. Hence, nano-sized Bi catalyst material could be used to further improve performance, since it could further improve active surface area. In short, catalyst materials such as Bi, Ti and In were selected since they can prevent or reduce hydrogen evolution. Results shown that both metals and metal oxides can both be potential candidates as catalyst materials for negative electrodes application, being Bi the best catalyst selection among tested samples.

4.5. The importance of pre-cleaning treatment

Pre-treatment cleaning is proposed in literature since it is believed to clean some products left in the GF synthesis [15, 136]. Although some papers recommend it before catalyst coating or thermal treatment, it is still unclear what is the main advantage and mechanism of this treatment. Also, more discussion is needed on what solvents is more efficient and if the improvements are achieved regardless process temperature. Hence, solvents selection and its impact on different temperature will be investigated in this section.

4.5.1. Solvent Impact

Ethanol solution is the main solvent used in literature. However, other solvents such as methanol and acetone were also investigated, which can be more efficient in cleaning some leftovers in the electrode fibers. For this investigation, pristine electrodes were first pre-cleaned using different solvents, such as acetone, ethanol and methanol, and samples were denoted as GF500A, GF500E and GF500M, respectively. After pre-cleaning process, samples were then thermally treated at 500^{o}C for 6h. To assess the

impact of pre-cleaning treatment using different solvents, different characterization tools were used and properties were evaluated.

First, SEM was selected to investigate changes in surface roughness, but no changes were seen for different pre-cleaned samples, suggesting that solvents have no impact on roughness and possible defects, being the thermal process the only mechanism for enhancing roughness.

Another tool to assess electrodes properties was CA, which was used to evaluate changes in wettability. Since solvents may introduce more functional groups to electrode's surface, CA measurements were performed (see Figure 49).

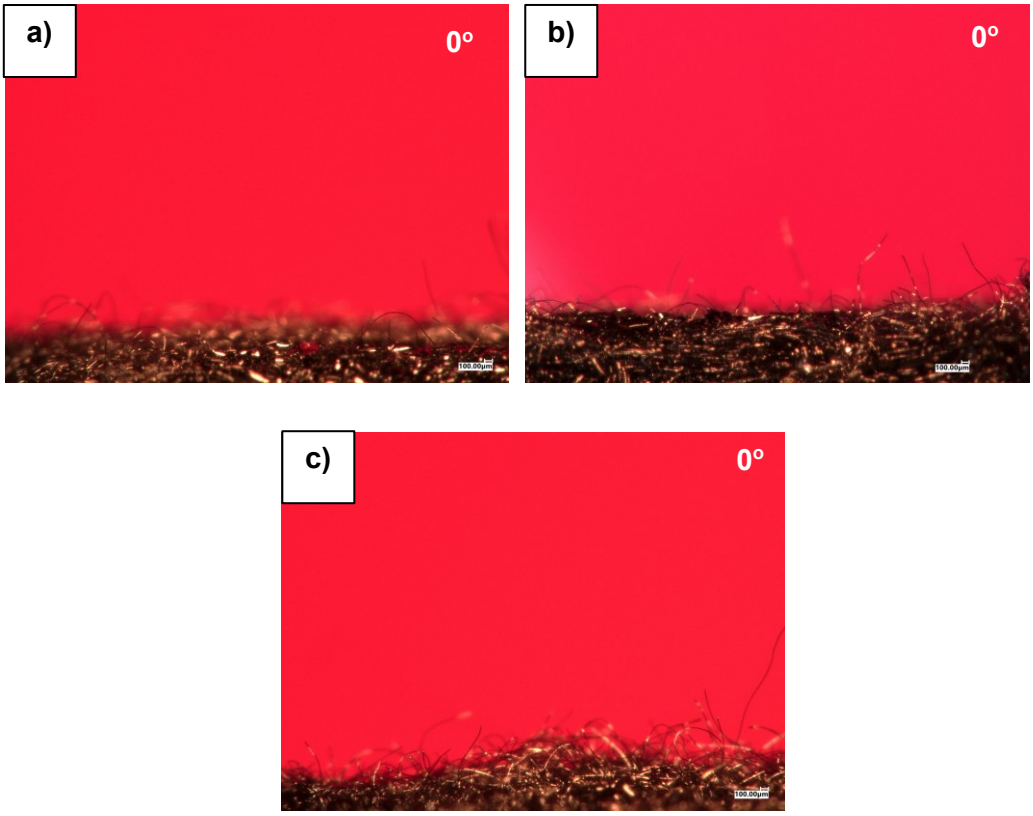

Figure 49. CA measurements for different pre-cleaned electrodes a) GF500A, b) GF500E and c) GF500M.

As shown in Figure 51, pre-cleaned samples showed hydrophilic behavior, similar to baseline (GF500). CA measurements for this sample in specific are not sufficient to evaluate wettability, hence capacitance measurements were also performed (Figure 50).

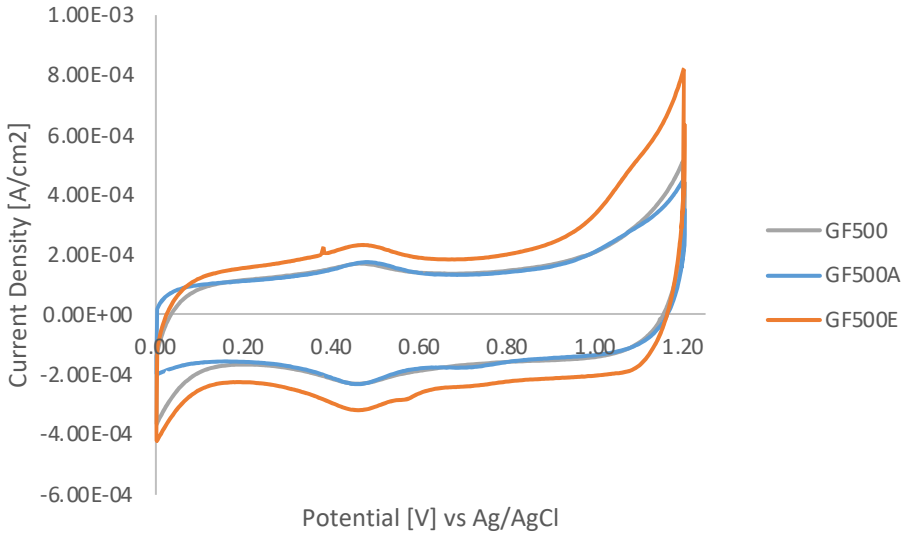

Figure 50. CV measurements in H_2SO_4 for pre-cleaned treated electrodes – solvent impact.

Though methanol and acetone showed little or no effect on electrode capacitance, ethanol was the only solvent that showed improvements in electrochemical active surface area and significantly higher functional group content, as it is shown in Table 45.

Table 45. Capacitance and functional group density results for pre-cleaned treated electrodes – solvent impact.

Sample	Carbolic functional group density [µmol]	Capacitance [µF]
GF500	0.009	13.43
GF500A	0.008	13.24
GF500E	0.151	18.16
GF500M	0.01	12.06

CV measurements were also performed in vanadium electrolyte to evaluate changes in electrochemical properties such as reversibility and kinetics (Figure 51).

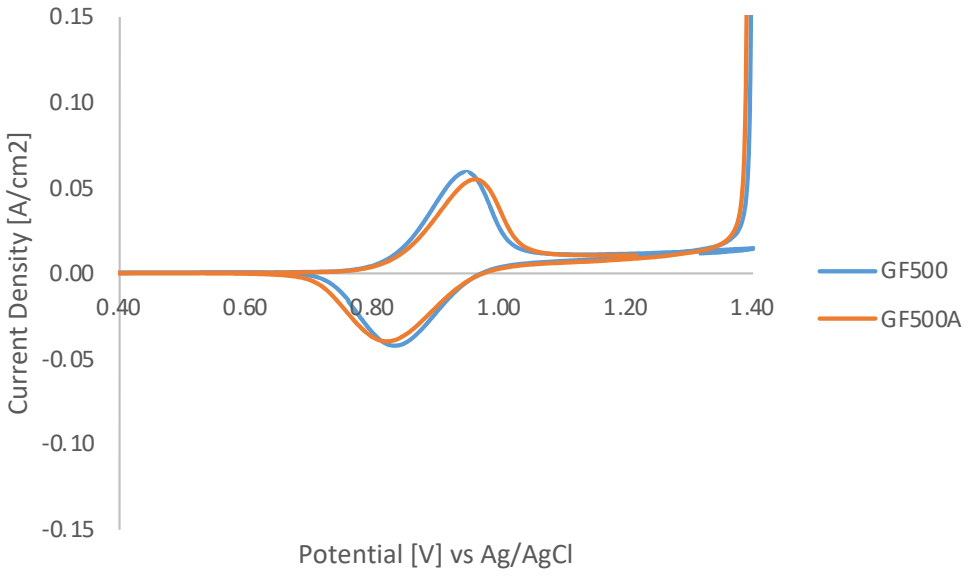

Figure 51. CV curves for pre-cleaned treated electrodes – solvent impact.

After analyzing results for CV measurements, it was noticed that samples showed similar results. Both parameters are shown in Table 46.

Table 46. CV results for pre-cleaned treated electrodes – solvent impact.

Sample	J_{pa}/J_{pc}	ΔV [V]
GF500	1.38	0.11
GF500A	1.37	0.14
GF500E	1.32	0.11
GF500M	1.43	0.12

As it can be seen in Table 46, pre-cleaned samples showed no significant changes in both activity and reversibility, suggesting that the only improvements from solvents come from capacitance improvements, which may be caused by functional groups. Thus, XPS analysis were done in order to investigate functional groups content (Table 47).

Table 47. XPS Analysis – Surface chemistry for pre-cleaned treated electrodes – solvent impact.

Sample	C [%]	O [%]	Na [%]
GF500	95.36	4.32	0.32
GF500E	94.8	4.96	0.25

As shown in Table 47, both samples showed similar results for oxygen content, though GF500E showed slightly higher oxygen amount. It was also noticed that other

impurities were also decreased and or eliminated, such as Na, Si and P for pre-cleaned sample.

In order to evaluate changes in the oxygen functional groups density, O_{1s} deconvolution was also analyzed (Table 48).

Table 48. XPS Analysis - O1s deconvolution for pre-cleaned treated electrodes – solvent impact.

Sample	C=O	C-O	Adsorbed O
GFPristine	1.54	1.11	-
GF500	1.86	2.16	0.30
GF500E	1.72	2.83	0.41

As it can be seen in Table 48, GF500E showed higher C-O content, which is believed to improve wettability and have catalytic activity towards vanadium reactions, which aligns with capacitance measurements. Perhaps, ethanol is cleaning the surface and creating more active surface areas to introduce functional groups during thermal treatment.

To evaluate electrodes performance, *in-situ* VRFB tests were performed to understand the impact of pre-cleaning treatment on efficiency and stability. Results for efficiencies are listed below in Table 49

.

Table 49. VRFB results for pre-cleaned treated electrodes – solvent impact.

Composition	EE [%]	CE [%]	VE [%]
GFPristine	73.1	96.4	75.8
GF500	85.2	96.2	88.5
GF500E	87.3	97.3	89.7

As it can be seen on Table 49, pre-cleaned sample showed a ~2% improvement in energy efficiency, which is mostly due to enhanced electrochemical surface area and improved kinetics shown in CV measurements. Both samples seemed stable performance and showed little or no degradation over 50 cycles.

Although it has not been fully discussed in literature, pre-cleaning process are essential to further improve electrode performance. Results has shown that pre-cleaned sample using ethanol solution showed improvements related to kinetics. Although reversibility wasn't impacted, pre-cleaned samples showed higher electrochemical surface area, which was also translated into better kinetics observed in CV results. Improvements can be explained by impurities being removed during pre-cleaning process, providing more active areas for thermal treatment and the formation oxygen functional groups. This simple and inexpensive process showed 2% improvements in EE, which was in the same magnitude of catalyst materials improvements.

4.5.2. Temperature Impact

Production leftovers are also believed to be burned off during thermal treatment in high temperatures. Thus, pre-cleaning treatment may not be needed for all temperatures. To understand the correlation between pre-cleaning treatment and temperature, different temperatures were investigated using ethanol as pre-cleaning solvent. Samples were treated at 400ºC, 450ºC and 500ºC using ethanol, and samples were denoted as GF400E, GF450E and GF500E, respectively.

SEM was used to assess changes in roughness. However, no visual changes can be seen for the samples, suggesting that ethanol had no effect on surface rather than cleaning it.

CA measurements were also performed in order to evaluate changes in pre-cleaned electrodes' wettability (Figure 52).

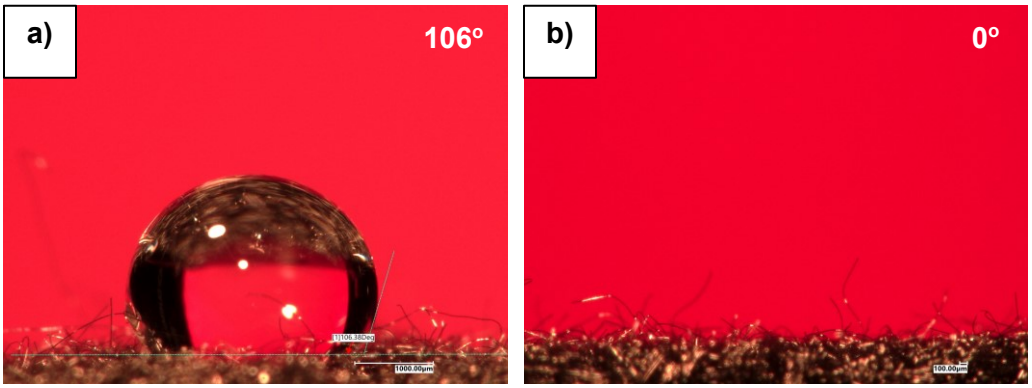

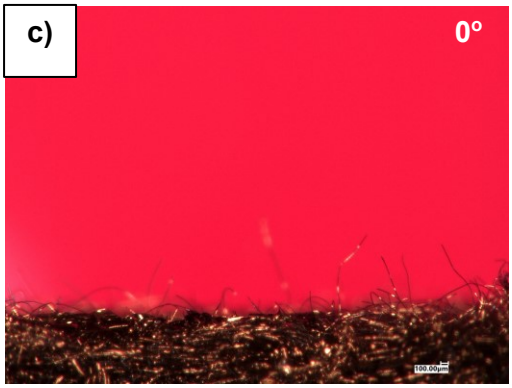

Figure 52. CA measurements for different pre-cleaned electrodes – temperature impact a) GF400E, b) GF450E and c) GF500E.

As it can be seen in Figure 52, other than GF500, which already had a hydrophilic behavior without pre-cleaning process, all samples showed improvements in wettability. Although GF400E still showed hydrophobic behavior, GF450E showed completely hydrophilic behavior, unlike no-cleaned sample, which had a CA of ~130°. Thus, pre-cleaning does have an impact on wettability. Hence, CV measurements were performed to assess wettability and improvements in electrochemical surface area (Figure 53).

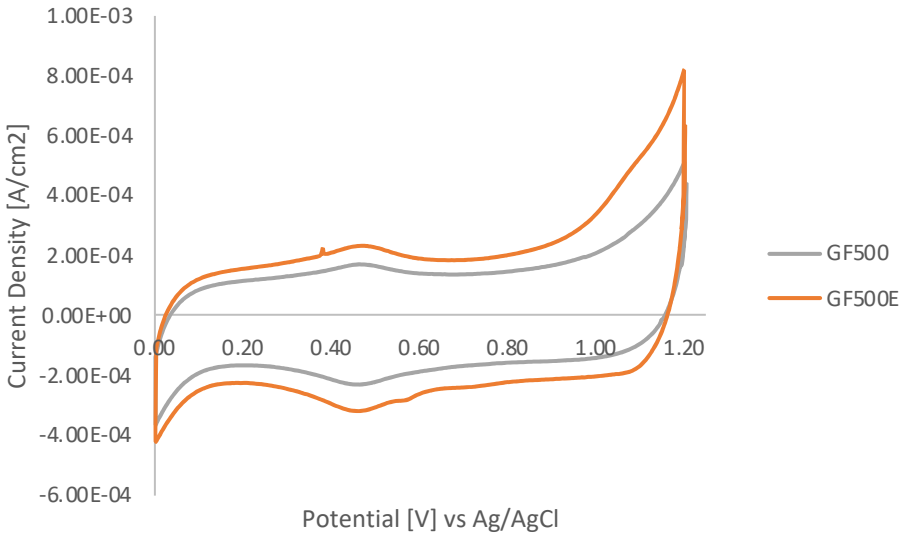

Figure 53. CV measurements in H_2SO_4 for pre-cleaned electrodes – temperature impact.

Pre-cleaning process seems to increase wettability, since all samples showed improvements in capacitance. Values for both functional group density and capacitance are listed below in Table 50.

Table 50. Capacitance and functional group density results for pre-cleaned electrodes – temperature impact.

Sample	Non-treated		Pre-treated	
	Carbolic functional group density [µmol]	**Capacitance** [µF]	**Carbolic functional group density** [µmol]	**Capacitance** [µF]
Pristine	0.000	1.06	-	-
GF400	0.001	2.31	0.187	3.40
GF450	0.003	3.74	0.005	6.17
GF500	0.009	13.43	0.151	18.16

As it can be seen in Table 50, all samples showed improvements in capacitance. As it was expected, GF400E was the least enhanced samples, while GF450 and GF500E showed significant enhancement in electrochemical surface area (~1.5x)

CV in vanadium electrolyte was also performed so that electrochemical properties can be evaluated (Figure 54)

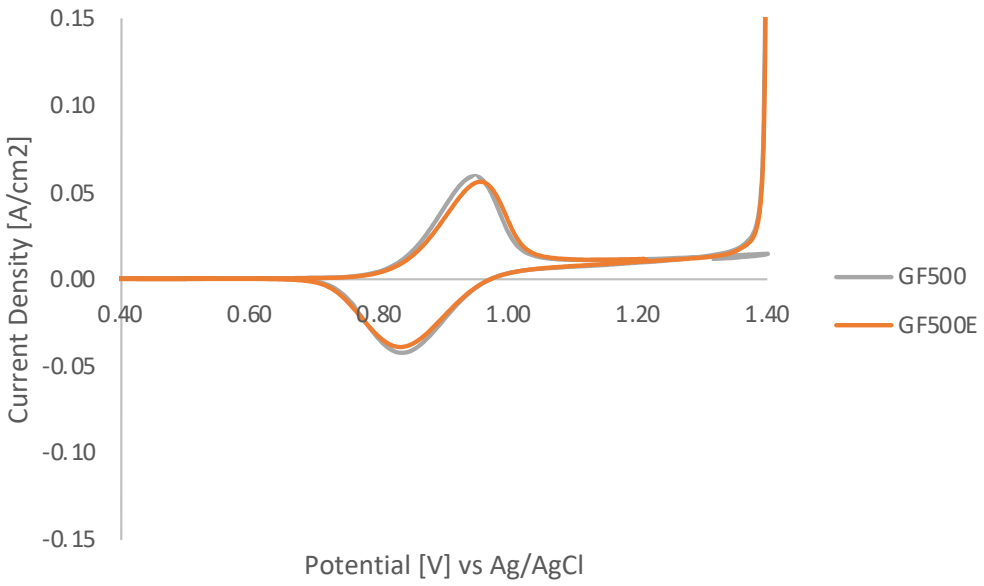

Figure 54. CV measurements for pre-cleaned electrodes – temperature impact.

CV analyses showed that peak potential separation was the least affected parameter, while peak current ratio, which is related to kinetics and active surface area was improved. Results are shown in Table 51.

Table 51. CV results for pre-cleaned electrodes – temperature impact.

Sample	Fresh		Pre-treated	
	J_{pa}/J_{pc}	ΔV [V]	J_{pa}/J_{pc}	ΔV [V]
Pristine	3.01	0.210		
GF400	2.10	0.16	2.17	0.18
GF450	1.82	0.15	1.47	0.15
GF500	1.38	0.11	1.32	0.11

As it can be seen in Table 51, while peak separation (reversibility) wasn't really improved, peak ration (kinetics) was the mainly improvement showed for most samples. Since functional groups doesn't really seem to be changed with pre-cleaning process it was shown in previous XPS data, the main and possibly the only improvement must come from kinetics (enhanced electrochemical surface area).

As it was shown, pre-cleaning process can improve wettability and consequently active electrochemical area, which is believed to be the main improvement mechanism. Samples showed higher capacitance (~1.5x higher) for all thermally treaded samples. Those improvements were also seen in electrochemical properties such as kinetics, while pre-cleaning seems to have no effect on reversibility, though changes were minor for GF400, which is not fully activated. In short, pre-cleaning process can be beneficial for thermal treatments, since it can provide more active sites for formation of functional groups and increase active electrochemical surface area.

4.5.3. Storage Time Impact

As it was discussed in chapter 4.1, functional groups may degrade over time, thus an aging investigation was proposed in this section. For that, GF500E was selected for this study since it showed the highest performance, and samples treated and stored after 4 months were analyzed as aged samples. Different physical and chemical properties were evaluated as well as their correlation to electrochemical properties.

SEM analysis was done to evaluate changes in surface morphology. However, no changes in roughness were seen after aging. Thus, changes in electrochemical properties must come from surface chemistry.

Since functional groups from the surface may degrade as it was shown for non-pre-cleaned samples, CA measurements were performed, and wettability was analyzed (Figure 55).

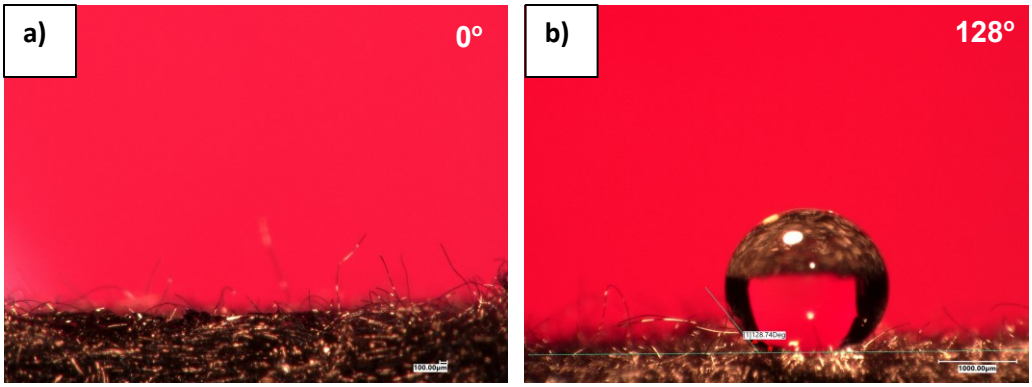

Figure 55. CA measurements for pre-cleaned electrodes a) Fresh and b) Aged.

As it can be seen in Figure 55, after 4 months, aged samples showed hydrophobic behavior like pristine samples, suggesting that functional groups get oxidized in contact with air and degraded. Wettability results are consistent with the results for aged non-pre-cleaned GF500 samples reported in section 4.1.3.

In order to evaluate changes in capacitance, CV measurements in sulfuric acid were performed (Figure 56).

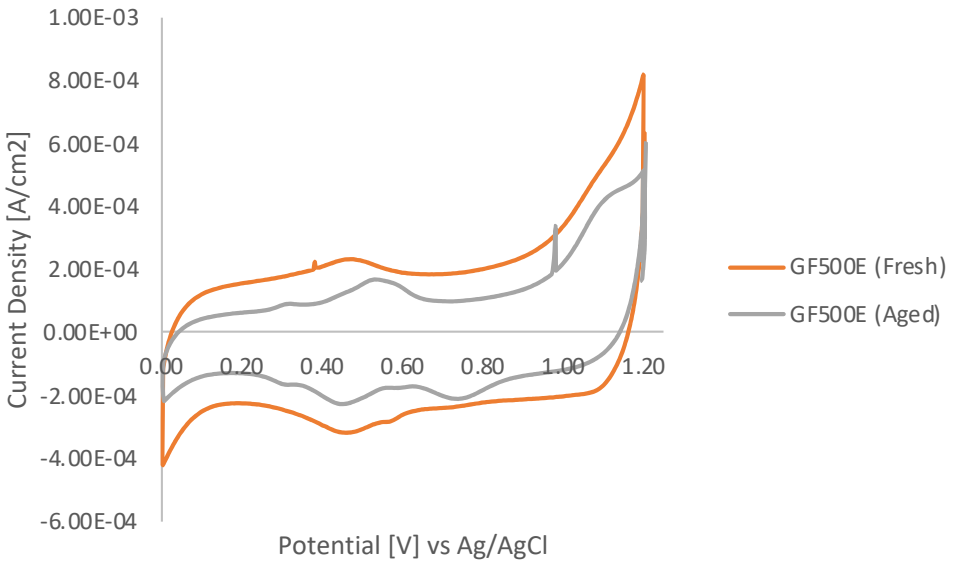

Figure 56. CV measurements in H_2SO_4 for pre-cleaned electrodes – aging effect.

Capacitance was degraded overtime and electrochemical active surface area was decreased. Values for both carbolic functional groups and capacitance are shown in Table 52. These results are also consistent and were expected, since aged non-pre-cleaned GF500 also showed decreased electrochemical active surface area. However, capacitance degradation for pre-cleaned samples were quicker compared to non-pre-cleaned samples.

Table 52. Capacitance and functional group density results for pre-cleaned GF500E electrodes – aging impact.

Sample	**Carbolic functional group density** [µmol]	**Capacitance** [µF]
Fresh	0.151	18.16
2 weeks	0.121	15.74
3 weeks	0.070	15.75
1 month	0.062	14.62
2 months	0.027	10.02
4 months	0.015	9.82

As it can be seen in Table 52, both functional groups and capacitance degrade over time. It seems that capacitance gets degraded faster than non-cleaned samples, since samples aged over 2 months and 4 months showed capacitance lower than non-pre-cleaned GF500 sample.

Other electrochemical properties were assessed during CV measurements using positive V(IV)/V(V) vanadium redox electrolyte (Figure 57) and results for peak potential separation and current ratio were listed below in Table 53.

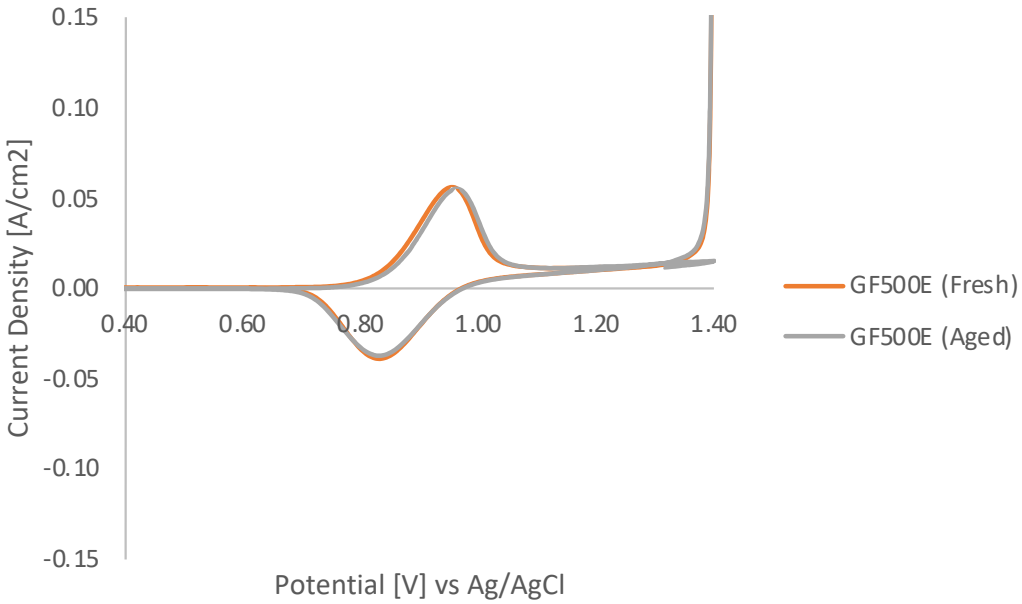

Figure 57. CV curves for pre-cleaned electrodes – aging impact.

As it can be seen in Table 53, both peak potential separation and peak current ratio were slightly worsened after aging. Minimal changes may not pose critical concerns for VRFB performances.

Table 53. CV results for pre-cleaned GF500E electrodes – aging impact.

Sample	J_{pa}/J_{pc}	ΔV [V]
Fresh	1.42	0.12
Aged (4 months)	1.49	0.13

Ideally, samples shouldn't be stored for quite long time, but understanding the impact of aging is essential to evaluate the maximum time that a treated sample can be stored before assembling new tests. Hence, *in-situ* VRFB cycling tests were also performed to evaluate the aging effect on pre-cleaned electrodes performance. For that, a single cell was assembled using aged GF500E electrodes both as positive and negative electrode. Results for both fresh and aged pre-cleaned electrodes are shown in Table 54.

Table 54. Performance of VRFB system using pre-cleaned GF500E electrodes – aging impact.

Sample	EE [%]	VE [%]	CE [%]
GF500E (Fresh)	87.3	97.3	89.7
GF500E (Aged)	87.1	97.0	89.8

As it was shown in Table 54 and discussed in section 4.1.3, functional groups stability seems not to be a concern and VRFB performance had no significant change. Results for pre-cleaned samples showed that, although capacitance degraded faster compared to non-cleaned samples and it reached similar properties compared to GF500 (no cleaning treatment), electrochemical properties such as kinetics and reversibility seem to have no impact on performance as it showed only 0.2% degradation. Thus, pre-cleaning treatment followed by thermal activation can be done in one single batch, saving time and cost, since aged samples showed little degradation in electrode performance. However, in order to avoid unwanted aging effects, freshly treated samples should always be preferred in order to ensure robust electrode performance. If aging poses a concern for electrode performance later, re-treatments can be done as a performance recovery solution, as it was shown before.

4.6. Functional Impediments Analysis

During this work, other activated graphite felt electrodes were fabricated, though performance was not improved for all of them. Some of them showed lower performance in *ex-situ* characterization, and some failure modes were expected. However, few samples showed improvements in *in-situ* characterization, such as capacitance measurements and electrochemical tests, but VRFB single cell tests showed otherwise. Hence, the pertinent functional impediments were identified and discussed to better understand the performance limitations and design engineering solutions to overcome the impediments.

4.6.1. Wettability

For ceramic materials such as metal nitrides, borides and carbides, wettability may be a concern. While metal oxides tend to be hydrophilic, some metal borides are hydrophobic. If catalyst material presents hydrophobic nature, coated area will also behave as hydrophobic areas and no longer as active sites for the reactions to take place. One example is ZrB_2, which was selected due to its high electronic conductivity and acidic stability, without taking into consideration ZrB_2 hydrophobicity. Worsened wettability was detected in CV measurements, since capacitance (electrochemical active surface area) was decreased (see Table 55).

Table 55. Capacitance and functional group density values for coated electrodes– catalyst hydrophobicity effect.

Sample	**Carbolic functional group density** [µmol]	**Capacitance** [µF]
GFE500E	0.151	18.16
ZrB_2/GFE500E	0.017	15.85

CA measurements were done to understand properties of different catalyst materials (Figure 58). ZrB_2 showed a CA of 120°, while the same metal in the oxide form (ZrO_2) showed hydrophilic behavior.

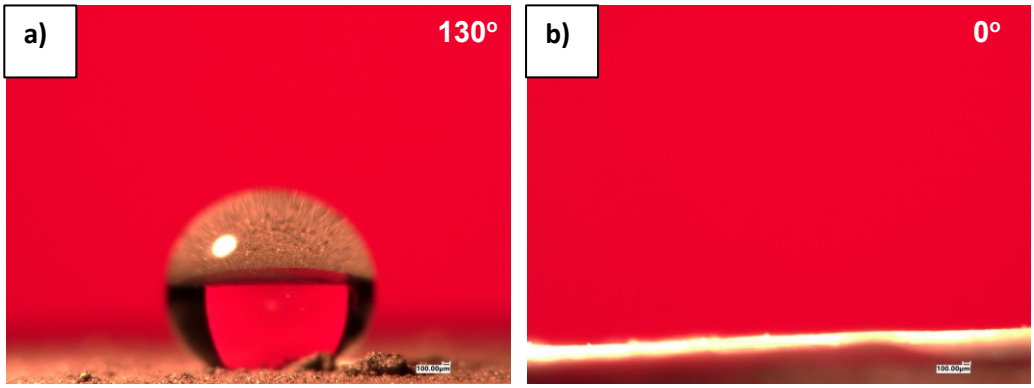

Figure 58. CA measurements for a) ZrB_2 and b) ZrO_2.

Hence, it is important to take catalyst wettability into consideration while scanning potentially candidates for catalyst materials so that active surface area does not get affected negatively.

4.6.2. Catalyst size

Catalyst hydrophilicity is one of the properties that may affect surface area. Another parameter that was not taken into consideration in few of the samples in this study was catalyst particle size. Although samples have the same catalyst loading, surface area is drastically impacted based on catalyst size, and surface area may not be improved for heavy and bigger particles. While most of the nitrides, borides and carbides were tested as micro-sized materials, metal oxides were mostly nano-sized (Table 56).

Table 56. BET Active Surface area for different catalyst materials.

Material	Catalyst Size	BET Surface Area [m^2/g]
WB_2	Macro (Commercial)	0.77
ZrB_2	Macro (Commercial)	0.32
CeO_2	Nano (Commercial)	42.93
ZrO_2	Nano (Commercial)	30.24

As it can be seen in Table 56 macro-sized catalysts have low SSA compared to nano-size materials, which may impact catalyst distribution and active surface area (Figure 59).

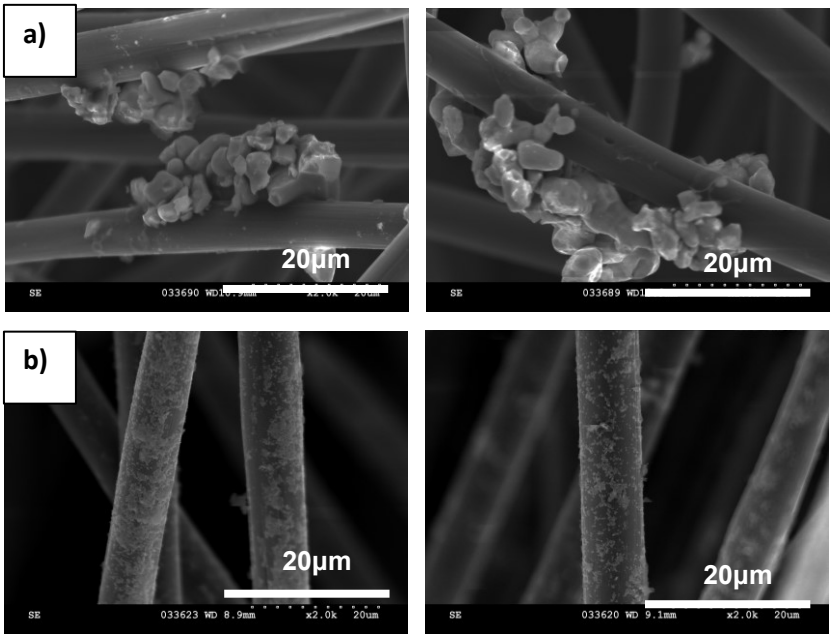

Figure 59. SEM figures for different catalyst sizes a) macro and b) nano.

Since catalyst deposition and coverage area are key parameters to improve capacitance, nano-sized catalyst is preferred, which can further increase baseline capacitance and electrical conductivity.

4.6.3. Agglomeration and blocking

Ceramic materials are heavy and tend to agglomerate if dispersion is not effective. Poor dispersion and coating can be translated into catalyst agglomeration and pores blockage. Some of the samples showed particles agglomeration, which must be avoided. One case was Ti_4O_7, which is nano-sized catalyst, but particles are heavy and showed agglomeration (Figure 60).

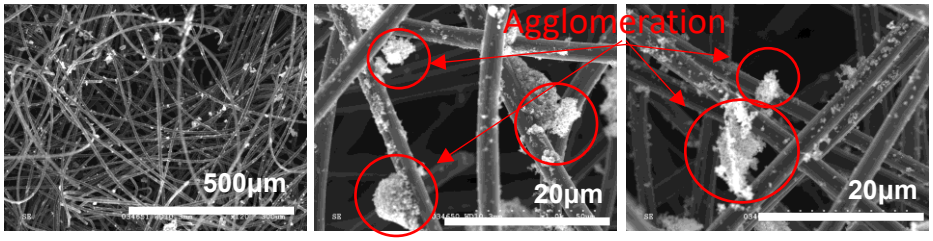

Figure 60. SEM figures for Ti_4O_7 coated sample.

As shown in Figure 60, particle agglomerations were seen, which can block pores and reduce active surface area. To mitigate this problem, acetic acid was added into catalyst ink to shift zeta potential for stronger electrostatic bond. Zeta potential was measured for both graphite and Ti_4O_7 and it was noticed that both materials showed negative zeta potentials. Thus, to shift zeta potential of the catalyst material, acetic acid was added, and zeta potential was shifted to positive values (see Table 57).

Table 57. Zeta potential measurements for different ink formulations.

Sample	Zeta Potential [mV]
GFE500	-7.54
Ti4O7	-7.02
Ti4O7 + Acetic Acid (0.01%)	-5.15
Ti4O7 + Acetic Acid (0.05%)	+7.64

GFE was then coated again using the new catalyst ink formulation and agglomeration seemed to decrease (Figure 61).

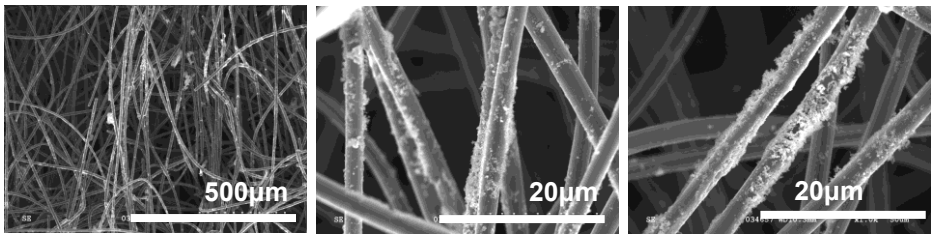

Figure 61. SEM figure Ti4O7 sample after zeta potential shift.

After using the new catalyst ink formulation, agglomeration was drastically improved compared to the sample with old formulation, though few bigger particles can still be seen, which is possibly the reason capacitance is still less than baseline, as it can be seen in Table 58.

Table 58. Capacitance and functional group density results for different ink formulation electrodes.

Sample	Carbolic functional group density [μmol]	Capacitance [μF]
GF500E	0.151	18.16
GF500E/ Ti_4O_7 (Just DMF)	0.009	11.17
GF500E/ Ti_4O_7 (Acetic Acid + DMF)	0.013	14.15

Ink formulation has a great impact on coating efficiency since catalyst dispersion and stability in the ink are important factors for coating process.

4.6.4. Solvent

During catalyst ink optimization process, different solvents were tested since different catalyst materials have different needs. While ceramic particles are heavier and should stay dispersed in solution without agglomerating, nano-sized metal oxide catalysts are lighter and showed no dispersion concerns. For metal carbides, nitrides and borides, inorganic solvent DMF was selected since it showed better dispersion compared to organic ones (see Figure 62).

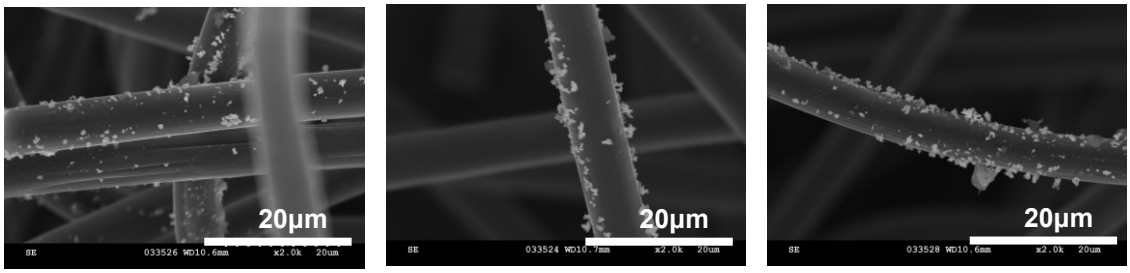

Figure 62. SEM figure macro-sized coated electrode using DMF as solvent.

Though catalyst dispersion was improved, DMF showed a trade-off between coating quality and capacitance. During thermal treatment, electrode surface gets oxidized and functional groups are introduced. However, during coating process, solvents may reduce oxygen functional groups and consequently capacitance (see Table 59).

Table 59. Capacitance and functional group density results comparison for baseline and DMF coated electrode.

Sample	Carbolic functional group density [µmol]	Capacitance [µF]
GF500E	0.151	18.16
GF500E/DMF	0.007	13.64

As it can be seen in Table 59, capacitance was drastically reduced after coating process using DMF ink, which suggests that DMF is degrading the functional groups from the surface, since functional group density was also decreased. Reduced capacitance and functional group density had an impact on *in-situ* tests, which is shown in Table 60.

Table 60. VRFB results for comparative assessment of baseline and DMF coated electrode.

Sample	Electrode	EE [%]	CE [%]	VE [%]
GFE500E	BASELINE (Positive and negative)	87.3	97.3	89.7
GFE500E - DMF	Negative	86.1	95.8	89.8

Thus, selecting solvent for catalyst ink is also an important parameter that needs to be taken into consideration so that no degradation is caused by solvent selection.

4.6.5. Additives

Another approach tested was using surfactants or binders such as Nafion and CTAB (Figure 63), which are often used in literature for ink dispersion for other electrochemical systems like fuel cells.

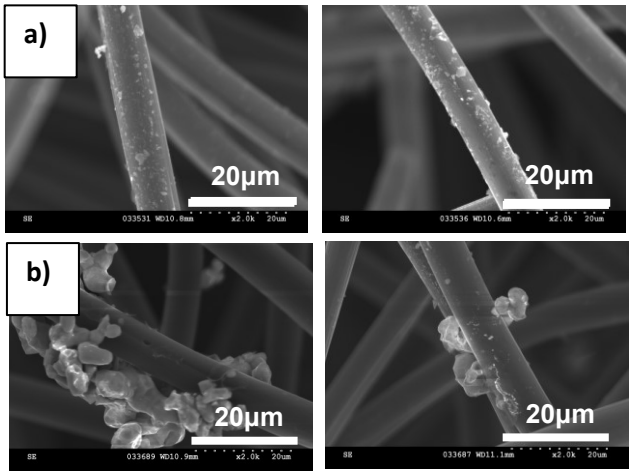

Figure 63. SEM figure for coated electrodes using a) Nafion and b) CTAB.

While CTAB sample showed bigger particles agglomeration, Nafion seems to evenly disperse particles on the fibers. SEM results align with particle size measurements for ink formulation (Figure 64), which showed that CTAB had bigger size particles compared to Nafion.

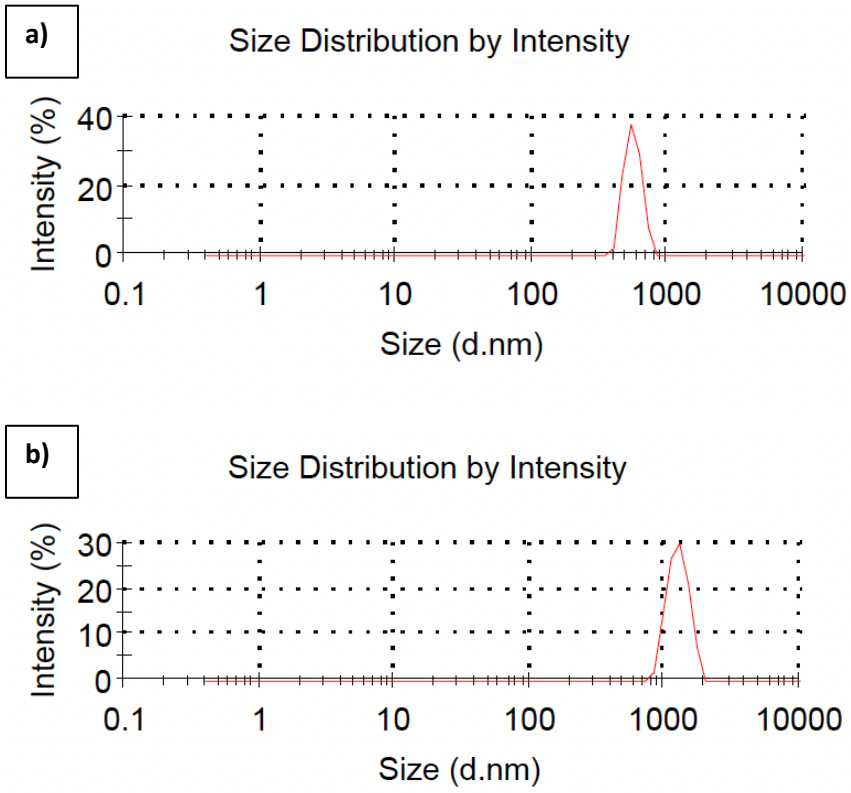

Figure 64. Particle size measurements for catalyst ink using a) Nafion and b) CTAB additives.

Both Nafion and CTAB were firstly evaluated in an isopropanol solution. Thus, after selecting DMF as a potential improvement, Nafion was added into solution to further improve deposition, which was achieved (Figure 65).

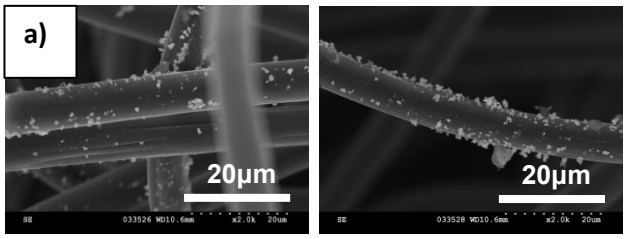

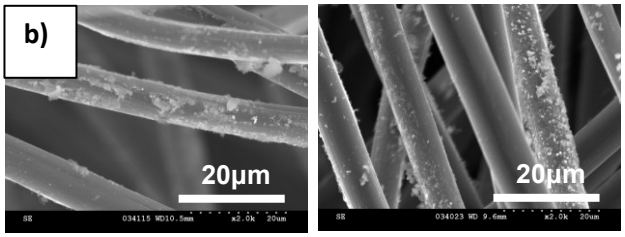

Figure 65. SEM figures for coated electrodes using a) only DMF and b) DMF + 0.1% Nafion.

However, Nafion has also a negative impact on capacitance measurements. CV were performed and results showed that capacitance values were drastically reduced (Table 61).

Table 61. Capacitance and functional group density results for Nafion additive.

Sample	**Carbolic functional group density** [µmol]	**Capacitance** [µF]
GF500E	0.151	18.16
GF500E/DMF - Nafion	0.004	12.44

Another parameter to be taken into consideration while designing catalyst ink is solvent additives since they can also impact on surface chemistry and worsen electrochemical surface area.

4.6.6. Catalyst Properties

Some of the catalysts were selected due to the fact that they showed improvements in other works reported in the literature. However, while trying to reproduce the performance improvements with few materials, results showed that performance was in fact decreased. One example was tungsten carbide (WC), both as micro-sized and nano-sized, which for both cases not only didn't show improvements, but also showed faster degradation.

Though catalyst coating was improved by using nano-size catalyst deposition, results for macro-size catalyst were considerable higher compared to nano-sized sample. Still, none of the samples showed any improvements compared to baseline (see Table 62).

Table 62. VRFB tests results for different WC coated electrodes.

Sample	Electrode	Cycle #	EE [%]	CE [%]	VE [%]
GF500 (E)	Baseline (Positive and negative)	1	86.6	96.4	89.7
		50	87.3	97.3	89.7
GFE500(E) / WC (Macro)	Negative	1	61.6	72.3	85.1
		28	61.9	90.7	68.2
GFE500(E) / WC (Nano)	Negative	1	43.6	51.9	84.0
		12	44.0	59.4	75.2

Catalyst materials properties must also play a crucial role in the performance. Catalyst materials purchased from different suppliers have different properties such as electrical conductivity, particle size, and wettability, which may also impact performance. However, it is still not clear what property has the most influence on electrode properties

and why other groups were able to show improvements using WC as catalyst material for anode applications [139].

4.6.7. Baseline Comparison

The main goal for this work is to achieve more energy efficient electrodes, regardless of the activation method. For positive electrodes, the maximum improvement was ~3%, while negative electrodes showed ~4%, which may seem little compared to other papers in literature that showed improvements up to 10% for energy efficiency. However, when analyzing those papers, they often compared activated samples to pristine electrodes. Thus, different factors play a role in improvement mechanisms. As it was showed here, wettability and electrochemical active surface area are one of the most parameters for designing activation approaches. Thus, if hydrophilic materials with high SSA, such as metal oxides nano-sized catalyst are used, hydrophilicity and electrochemical active area will be enhanced, which will then be translated into higher EE. Thus, it is hard to separate the improvements and benefits originating from the catalyst itself since different improvements were done in different aspects from baseline. Thus, even with solvent degradation, other improvements can overcome this degradation and the final enhancement will be much higher than using the same catalyst material for already enhanced baselines such as the GF500E, which showed EE higher than most of the papers presented in literature.

Table 63. VRFB Tests results for baseline and pristine electrodes.

Sample	EE [%]	VE [%]	CE [%]
GFPristine	73.1	75.8	96.4
GF500E	87.3	90.8	96.1

Thus, if we were to compare thermal treatment combined with pre-cleaned treatment, a ~14% enhancement in energy efficiency compared to pristine GF can be seen in Table 63, which follows the same trend for most of the improvements reported in literature. Thus, it's easy to achieve such high improvements comparing a hydrophobic and low SSA area sample with a higher capacitance and hydrophilic one. Thus, coating catalysts to an already highly efficient sample will only present minimum improvements, which may not be cost-effective for short term performances.

4.6.8. Current Density and Cycle numbers

For VRFB cycling tests, 80 mA/cm^2 and 50 cycles were selected for test parameters. Although most of samples were able to show improvements during short term cycles and low current density, it is possible that other samples that, although didn't show higher EE can present other advantages such as performance stability. While oxygen functional groups are believed to be degraded overtime and stability may pose a concern, during 50 cycles, stability was degraded only ~1%. However, during longer cycles (100 or even 200 cycles), degradation can be attenuated for baseline compared to coated samples, which in a longer term may be one of catalysts advantages. Another explanation for lower improvements can be lower current density. At higher current density, different overpotentials are amplified. Thus, for coated samples, which showed lower R_{ct} values, performance may not be impacted as harshly compared to baseline. Thus, performing higher current density tests and longer cycling may shine a light into other enhancements that may not be visible during lower current density and short-term cycling.

4.6.9. Catalyst Stability

SEM was also used to determine catalyst durability and adhesion after cycling. Since one of the major problems regarding catalyst deposition and system performance is catalyst degradation, samples were analyzed before and after *in-situ* cycling test to understand catalyst durability after cycling both at surface (top and bottom) and at cross-section (see Figure 66).

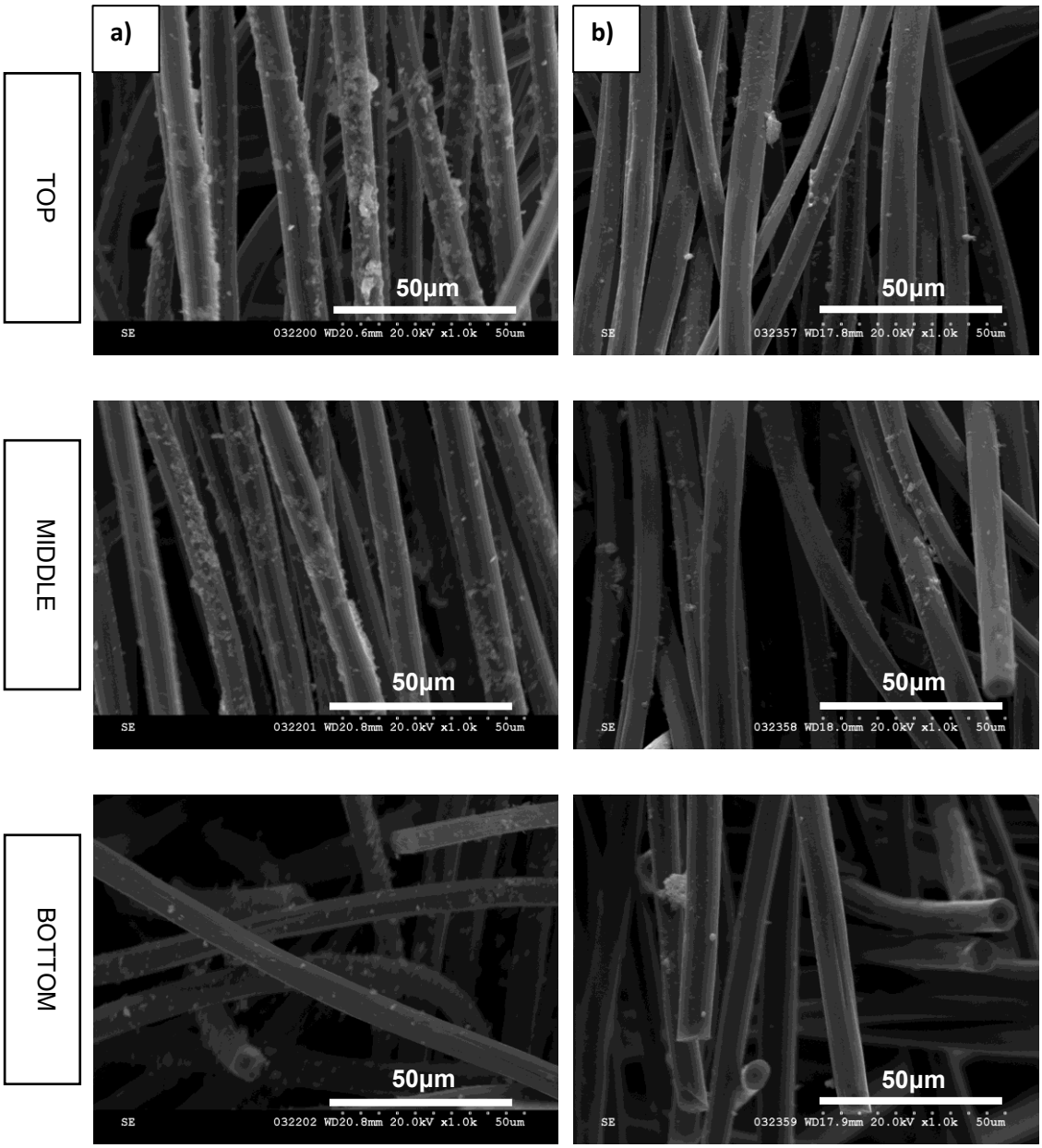

Figure 66. Degradation analysis – SEM Images. a) 40%(50%Ir40%Ru10%Se)/rGO before cycling test and b) 40%(50%Ir40%Ru10%Se)/rGO after cycling test.

SEM analysis for (40%(50%Ir40%Ru10%Se)/rGO) showed a visual change in catalyst stability. Catalyst seems to be washed off throughout the whole cross-section,

which can explain rapid degradation in the *in-situ* VRFB test. Hence, samples that didn't show any improvements compared to baseline may also present other challenges such as catalyst stability.

Chapter 5.

Conclusion and Future Work

5.1. Conclusions

For this thesis, several VRFB electrode modifications were proposed so that different physical, chemical and electrochemical properties were assessed. Understanding performance limitations are essential to design better engineering solutions and achieve higher electrode and battery performance. After carrying out a complete range of experiments, some conclusions can be made from the results presented in the past sections.

Thermal treatment process can lead to the formation of oxygen functional groups, which are believed to improve some properties such as wettability, electrochemical surface area, reversibility, and kinetics. The effect of different thermal treatment parameters was investigated, and it was seen that both temperature and time play an important role in electrode performance. Higher temperature and longer times can introduce higher content of oxygen functional groups which led to higher performance. Samples treated at higher temperature and longer time showed higher active electrochemical surface area and enhanced wettability, and consequently improved electrode kinetics.

Although thermal treatment can lead to the formation of functional groups, stability poses a concern since properties can be degraded over time. Hence, electrode aging was evaluated to understand how electrode performance is impacted. Although hydrophilicity was drastically affected on the surface, aged samples showed minor impact on electrochemical active surface area, suggesting that the external surface is mostly impacted by functional group treatment or air contamination, while the electrode bulk remains hydrophilic and electrochemical surface area is not affected. VRFB results showed that electrode performance was not reduced by aging. Thus, to save time and cost, samples can be thermally treated and then stored for later use. However, to compare

performance for activated samples, it is preferred that samples are freshly treated to ensure robust electrode properties.

Re-treatment process was also evaluated as an option to recover electrode performance and re-introduce functional groups. Results showed that re-treated electrodes not only recover their key properties such as electrochemical active surface area and wettability, but also showed improvements in reversibility and kinetics. Re-treated samples showed similar results for reversibility, which suggests that functional groups responsible for improving reversibility were re-introduced. Kinetics were further improved after re-treatment as samples showed higher capacitance, suggesting that functional groups responsible for capacitance are not degraded over time and it accumulated after re-treatment.

In order to further improve electrode performance, chemical treatments were investigated as a potential secondary treatment, since it can also introduce functional groups. However, results showed that functional groups introduced via chemical treatments showed no impact on physico-chemical properties. In fact, charge transfer resistance was increased, lowering electrode performance. Perhaps, chemical activation can be used before thermal treatment, as it can both clean electrode surface and introduce functional groups that can be possibly transformed during thermal treatments.

Catalyst materials can be coated on thermally activated samples to achieve higher efficiencies, since it can both decrease charge transfer resistance and improve active surface area. Different catalyst materials were evaluated for both positive and negative electrodes. Although noble metals showed good activity for the positive couple, other inexpensive alternative solutions such as metal oxides are also available to achieve as high performance as activated electrodes with noble metals. Results showed that WO_3 facilitates high efficiency and good catalyst stability compared to noble metals, which can be explained by enhanced wettability and improved kinetics. For the negative electrode, both metal and ceramic catalyst materials showed improvements in both electrochemical surface area and charge transfer resistance. Improvements for the negative electrode are also due to side reactions suppression, which combined with improved kinetics, can be the main mechanism for electrode performance enhancement.

Lastly, pre-cleaning treatments were evaluated and the impact of different solvents were studied. Results showed that pre-cleaned samples with ethanol had an increase in capacitance, which can provide more active sites for the electrochemical reactions. Pre-cleaning treatment showed improvements for all thermally treated samples. Enhanced performance can be explained by improvements in both electrochemical active surface area and wettability, which can enhance kinetics. Since aging may pose a concern for this treatment, sample aging studies were also performed. Although capacitance degraded faster for pre-cleaned samples compared to non-cleaned samples, VRFB performance stability was also observed. Hence, to save process cost and time, samples can be pre-cleaned, activated and then stored for later use, when needed.

In conclusion, the results showed that, in order to make a broad and comprehensive analysis, physico-chemical properties need to be assessed to make correlation to electrochemical performance, both *in-situ* and *ex-situ*. It was shown that improvements in electrode performance are primarily caused by improvements in wettability and electrochemical surface area, which leads to improvements in electrode kinetics. Combining activation methods can further improve electrode performance if key properties are targeted. Hence, understanding impediments and improvement mechanisms is essential to design viable solutions to make more robust and efficient VRFB electrodes.

5.2. Future Work

In this thesis, various VRFB electrode modification approaches were proposed, and properties were assessed by different characterization tools in order to understand improvement mechanisms and suggest better engineering solutions. While further improvements can still be achieved by combining all the conclusions from this work, other challenges arise, and a few other future works are proposed in this section.

One of the future works is the need to make realistic analysis for electrochemical assessment. Although CVs are widely used in literature, it fails to truly represent *in-situ* conditions such as compression, flow rate (mass transport), and electrolyte concentration. Thus, results may not represent the real VRFB cell performance. In order to mimic *in-situ*

performance and include all these extra parameters which are essential for further investigation of electrodes performance, especially regarding catalyst stability, a microfluidic cell was proposed for carbon paper electrodes by previous members in the group [135]. For thick electrodes such as graphite felt, a new design was proposed by the author. However, fabrication, experiments, and analysis still need to be completed to fully validate the new design. Once the design is validated, CV tests can be performed using the dynamic approach and comparison between static and dynamic performance can be evaluated.

Dip-coating process, which is often used in literature and was used for this work, have some disadvantages such as materials surplus, inefficient coating, and potential particles agglomeration. Therefore, designing better coating processes where catalyst materials can be deposited in a more efficient way is crucial to decreased process cost and increased active surface area. Moreover, coating processes use different solvents that can eventually degrade electrode properties, as it was shown in this work. Thus, a green, rapid, and cheap *in-situ* deposition process was recently proposed by our group [135]. However, they were only able to test this process in the microfluidic cell using carbon paper as working electrode, while no single cell tests were performed using graphite felt electrodes, which is hence recommended as future work.

Based on the results presented in this thesis, one of the main key parameters to improve electrode performance is electrochemical active surface area, which is linked to wettability. While static contact angle measurements give a rough estimate of hydrophilicity, it is not useful to compare hydrophilic samples, since they would all present 0º contact angle. Besides, other parameters at the electrode surface may play a role in these measurements, such as porosity, roughness, surface chemistry and others. Hence, deeper analysis and understanding is needed to evaluate different activation processes and their impact on electrode wettability. For that, dynamic contact angle can be used to give us a deeper insight on electrodes wetting properties. Moreover, method of standard porosimetry (MSP) can be combined with dynamic contact angle, wherein different liquids can be used and electrode hydrophilicity can be thoroughly assessed. While octane can be used as a soaking solvent and a total surface area can be determined, measurements using water or vanadium electrolyte as solvent can be performed so that hydrophilic surface area can be calculated and compared to the whole surface area. Thus,

hydrophobic and hydrophilic surface areas can be calculated and used to investigate the impact of different treatments and parameters on electrode wettability.

References

[1] Price A (2005) Proc Inst Civil Eng Civil Eng 158:52

[2] Y. Xiang and W. A. Daoud, Investigation of an advanced catalytic effect of cobalt oxide modification on graphite felt as the positive electrode of the vanadium redox flow battery, J. Power Sources, vol. 416, 2019.

[3] K. Amini, J. Gostick, M. D. Pritzker. Metal and Metal Oxide Electrocatalysts for Redox Flow Batteries, Adv. Funct. Mater. 2020, 30, 1910564.

[4] H. Kabir, I. O. Gyan, and I. Francis Cheng, Electrochemical modification of a pyrolytic graphite sheet for improved negative electrode performance in the vanadium redox flow battery, J. Power Sources, vol. 342, pp. 31–37, 2017.

[5] Li, W., Liu, J., and Yan, C., Graphite–graphite oxide composite electrode for vanadium redox flow battery, Electrochimica Acta. 2011.

[6] Kim, H.S. Electrochemical Properties of Graphite-based Electrodes for Redox Flow Batteries. Bull. Korean Chem. Soc. 2011.

[7] W. Wang, X. Wang. Investigation of Ir-modified carbon felt as the positive electrode of an all-vanadium redox flow battery. Electrochim. Acta 2007, 52, 6755.

[8] Wei, Z.D. and Chan, S.H. Electrochemical deposition of PtRu on an uncatalyzed carbon electrode for methanol electrooxidation. Journal of Electroanalytical Chemistry. 2004. 569(1): p. 23-33.

[9] Haddadi-Asl, V., Kazacos, M., and Skyllas-Kazacos, M. Conductive carbon-polypropylene composite electrodes for 35 vanadium redox battery. Journal of Applied Electrochemistry. 1995.

[10] X. Li, K. Huang, S. Liu, L. Chen, Electrochemical behavior of diverse vanadium ions at modified graphite felt electrode in sulphuric solution, J. Cent. South Univ. Technol. 14, 2007.

[11] B. Sun, M. Skyllas-Kazacos, Modification of graphite electrode materials for vanadium redox flow battery application-I. Thermal treatment, Electrochim. Acta 37, 1992.

[12] Jiang H, Shyy W, Zeng L, Zhang R, Zhao T. Highly efficient and ultra-stable boron doped graphite felt electrodes for vanadium redox flow batteries. J Mater Chem A 2018.

[13] Zhou X, Zeng Y, Zhu X, Wei L, Zhao T. A high-performance dual-scale porous electrode for vanadium redox flow batteries. J Power Sources 2016.

[14] Li B, Gu M, Nie Z, Shao Y, Luo Q, Wei X, et al. Bismuth nanoparticle decorating graphite felt as a high-performance electrode for an all-vanadium redox flow battery. Nano Lett 2013.

[15] Wei L, Zhao T, Zeng L, Zeng Y, Jiang H. Highly catalytic and stabilized titanium nitride nanowire array-decorated graphite felt electrodes for all vanadium redox flow batteries. J Power Sources 2017.

[16] Jiang H, Shyy W, Wu M, Wei L, Zhao T. Highly active, bi-functional and metal-free B4C-nanoparticle-modified graphite felt electrodes for vanadium redox flow batteries. J Power Sources 2017.

[17] B. Sun, M. Skyllas-Kazacos, Chemical modification of graphite electrode materials for vanadium redox flow battery application—part II. Acid treatments, Electrochim. Acta 37, 1992.

[18] S. Zhong, C. Padeste, M. Kazacos, M. Skyllas- Kazacos, J., Comparison of the physical, chemical and electrochemical properties of rayon- and polyacrylonitrile-based graphite felt electrodes, Power Sources 45, 1993.

[19] W. Li, J. Liu, C. Yan, Graphite–graphite oxide composite electrode for vanadium redox flow battery, Electrochim. Acta 56, 2011.

[20] Álvaro Cunha, F. P. Brito, Jorge Martins, Nuno Rodrigues, “Vanadium Redox Flow Batteries: A Technology Review”, International Journal of Energy Research, Elsevier International, 2015.

[21] Weber, A., Mench, M., Meyers, J., Ross, P., Gostick, J., and Liu, Q., Redox flow batteries: a review. Journal of Applied Electrochemistry. 2011

[22] Skyllas-Kazacos, M., Rychick, M., and Robins, R. All-vanadium redox battery, in US Pat., 4 786 567 1988.

[23] Skyllas Kazacos M, Kazacos G, Poon G, Verseema H. Int J Energy Res 34:182, 2010.

[24] REDT. Successful installation of REDT'S storage system in collaboration with FP7 and the European commission. 2014. Available in: <https://redtenergy.com/successful-installation-redts-storage-system collaboration-fp7-european-commission/>.

[25] Skyllas-Kazacos, M. The vanadium redox battery and fuel cell for large-scale energy storage. In: 19th World Energy Congress. [S.1.:sn.], 2004. Sydney, Australia.

[26] RICHMOND, B. C. VRB power sells two 5kW x 4hr VRB energy storage systems (TM) to Winafrique Technologies for Deployment with Safaricom, in Kenya. 2014. Available at: <http://www.marsdaily.com/reports/VRB_Power_Sells_Two_VRB_Energy_Storage_Systems_To_Winafrique_Technologies_999.html>.

[27] Vanadium Redox Flow Batteries: An In-Depth Analysis EPRI, Palo Alto, CA: 2007. 1014836. DOI.

[28] Helen Prifti, A.P., Suminto Winardi , Tuti Mariana Lim , Maria Skyllas-Kazacos. Membranes for Redox Flow Battery Applications. Membranes. 2012.

[29] Skyllas-Kazacos, M. Vanadium/polyhalide redox flow battery, in U.S. Patent 7 320 844 B22008.

[30] Ulaganathan, M.; Aravindan, V.; Yan, Q.; Madhavi, S.; Skyllas-Kazacos, M.; Mariana Lim, T. Recent Advancements in All-Vanadium Redox Flow Batteries. Adv. Mater. Interfaces 2016.

[31] Jiang H, Shyy W, Ren Y, Zhang R, Zhao T. A room-temperature activated graphite felt as the cost-effective, highly active and stable electrode for vanadium redox flow batteries. Appl Energy 2019.

[32] Q. Wu, X. Zhang, Y. Lv, L. Lin, Y. Liu, and X. Zhou. Bio-inspired multiscale-pore-network structured carbon felt with enhanced mass transfer and activity for vanadium redox flow batteries. J. Mater. Chem. A, vol. 6, no. 41, 2018.

[33] Jiaxin Zheng, Guoyu Tan, Peng Shan, Tongchao Liu, Jiangtao Hu, Yancong Feng, Luyi Yang, Mingjian Zhang, Zonghai Chen, Yuan Lin, Jun Lu, Joerg C. Neuefeind, Yang Ren, Khalil Amine, Lin-Wang Wang, Kang Xu, Feng Pan. Understanding Thermodynamic and Kinetic Contributions in Expanding the Stability Window of Aqueous Electrolytes, Chem, Volume 4, Issue 12, 2018.

[34] L. Wei, T. S. Zhao, Q. Xu, X. L. Zhou, and Z. H. Zhang. In-situ investigation of hydrogen evolution behavior in vanadium redox flow batteries. Appl. Energy, vol. 190, 2017.

[35] S. J. Yoon, S. Kim, D. K. Kim, S. So, Y. T. Hong, and R. Hempelmann. Ionic liquid derived nitrogen doped graphite felt electrodes for vanadium redox flow batteries. Carbon N. Y., vol. 166, 2020.

[36] J. Langner, M. Bruns, D. Dixon, A. Nefedov, Ch. Wöll, F. Scheiba, H. Ehrenberg, C. Roth, J. Melke. Surface properties and graphitization of polyacrylonitrile based fiber electrodes affecting the negative half-cell reaction in vanadium redox flow batteries. Journal of Power Sources, Volume 321, 2016.

[37] Gonzalez, Z.; Flox, C.; Blanco, C.; Granda, M.; Morante, J.R.; Menendez, R.; Santamaria, R. Outstanding electrochemical performance of a graphenemodified graphite felt for vanadium redox flow battery application. J. Power Sources 2017, 338, 155–162.

[38] Y. H. Wang, I. M. Hung, and C. Y. Wu. The characteristics and electrochemical performance of graphite felts with thermal and fenton's reagent treatment for vanadium redox flow battery. Ceram. Int., vol. 44, 2018.

[39] Z. Zhang, J. Xi, H. Zhou, and X. Qiu. KOH etched graphite felt with improved wettability and activity for vanadium flow batteries. Electrochim. Acta, vol. 218, 2016.

[40] Z. D. Wei and S. H. Chan. Electrochemical deposition of PtRu on an uncatalyzed carbon electrode for methanol electrooxidation. J. Electroanal. Chem., vol. 569, no. 1, 2004.

[41] H. Zhou, H. Zhang, P. Zhao, and B. Yi. A comparative study of carbon felt and activated carbon based electrodes for sodium polysulfide/bromine redox flow battery. Electrochim. Acta, vol. 51, no. 28, 2006.

[42] M. A. Goulet, A. Habisch, and E. Kjeang. In Situ Enhancement of Flow-through Porous Electrodes with Carbon Nanotubes via Flowing Deposition. Electrochim. Acta, vol. 206, 2016.

[43] Y. Liu et al.. Holey-engineered electrodes for advanced vanadium flow batteries. Nano Energy, vol. 43, 2018.

[44] D.S. Kim, D.J. Chung, H.-I. Park, M.Z. Ansari, T. Song, H. Kim, Direct nitridated graphite felt as an electrode material for the vanadium redox flow battery, Bull. Korean Chem. Soc. 39, 2018, 281–286.

[45] Flox, C.; Rubio-Garcia, J.; Skoumal, M.; Andreu, T.; Morante, J.R. Thermo-chemical treatments based on NH3/O2 for improved graphite-based fiber electrodes in vanadium redox flow batteries. Carbon 60, pp. 280 - 288. 2013

[46] Li Q, Bai A, Zhang T, Li S, Sun H.Dopamine-derived nitrogen-doped carboxyl multiwalled carbon nanotube-modified graphite felt with improved electrochemical activity for vanadium redox flow batteries. R. Soc. Open Sci. 7: 20040, 2020.

[47] Z. He, A. Su, C. Gao, Z. Zhou, C. Pan, and S. Liu. Carbon paper modified by hydrothermal ammoniated treatment for vanadium redox battery. Ionics, vol. 19, no. 7, pp. 1021–1026, 2013.

[48] Shi, L., Liu, S., He, Z. & Shen, J. Nitrogen-doped graphene: Effects of nitrogen species on the properties of the vanadium redox flow battery. Electrochim. Acta 138, 93–100, 2014.

[49] R.K. Gautam, A. Verma, Uniquely designed surface nanocracks for highly e cient and ultra-stable graphite felt electrode for vanadium redox ow battery, Mater. Chem. Phys. 251, 2020.

[50] Y. Huang, Q. Deng, X. Wu and S. Wang, N, O Co-doped carbon felt for high-performance all-vanadium redox flow battery, Int. J. Hydrogen Energy, 2017.

[51] Dixon D, Babu DJ, Bhaskar A, et al. Tuning the performance of vanadium redox flow batteries by modifying the structural defects of the carbon felt electrode. Beilstein J Nanotechnol. 2019.

[52] Z. He, L. Shi, J. Shen, Z. He and S. Liu. Effects of nitrogen doping on the electrochemical performance of graphite felts for vanadium redox flow batteries. Int. J. Energy Res., 2015.

[53] Z. He, X. Zhou, Y. Zhang, F. Jiang, Q. Yu, Low-temperature nitrogen-doping of graphite felt electrode for vanadium redox ow batteries, J. Electrochem. Soc. 166, 2019,

[54] H. J. Lee and H. Kim. Graphite felt coated with dopamine-derived nitrogen-doped carbon as a positive electrode for a vanadium redox flow battery. Journal of The Electrochemical Society, vol. 162, no. 8, pp. A1675–A1681, 2015.

[55] H.R. Jiang, W. Shyy, L. Zeng, R.H. Zhang, T.S. Zhao, Highly efficient and ultra-stable boron-doped graphite felt electrodes for vanadium redox flow batteries, J. Mater. Chem. A, 6, 2018.

[56] Shah AB, Wu Y, Joo YL. Direct addition of sulfur and nitrogen functional groups to graphite felt electrodes for improving allvanadium redox flow battery performance. Electrochim Acta. 2019.

[57] Estevez, L.; Reed, D.; Nie, Z.; Schwarz, A.M.; Nandasiri, M.I.; Kizewski, J.P.; Wang, W.; Thomsen, E.; Liu, J.; Zhang, J.-G.; et al. Tunable Oxygen Functional

Groups as Electrocatalysts on Graphite Felt Surfaces for All-Vanadium Flow Batteries. ChemSusChem 2016.

[58] Men, Y.; Sun, T. Carbon Felts Electrode Treated in Different Weak Acid Solutions through Electrochemical Oxidation Method for All Vanadium Redox Flow Battery. Int. J. Electrochem. Sci. 2012.

[59] K.J. Kim, S.-W. Lee, T. Yim, J.-G. Kim, J.W. Choi, J.H. Kim, M.-S. Park, Y.-J. Kim, A new strategy for integrating abundant oxygen functional groups into carbon felt electrode for vanadium redox flow batteries, Sci. Rep. 4, 2014.

[60] Bourke, A.; Miller, M. A.; Lynch, R. P.; Gao, X.; Landon, J.; Wainright, J. S.; Savinell, R. F.; Buckley, D. N. Electrode Kinetics of Vanadium Flow Batteries: Contrasting Responses of VII-VIII and VIVVVto Electrochemical Pretreatment of Carbon. J. Electrochem. Soc. 2016.

[61] Dixon, D.; Babu, D. J.; Langner, J.; Bruns, M.; Pfaffmann, L.; Bhaskar, A.; Schneider, J. J.; Scheiba, F.; Ehrenberg, H. Effect of Oxygen Plasma Treatment on the Electrochemical Performance of the Rayon and Polyacrylonitrile Based Carbon Felt for the Vanadium Redox Flow Battery Application. J. Power Sources, 2016.

[62] Bourke, A.; Miller, M. A.; Lynch, R. P.; Gao, X.; Landon, J.; Wainright, J. S.; Savinell, R. F.; Buckley, D. N. Electrode Kinetics of Vanadium Flow Batteries: Contrasting Responses of VII-VIIIand VIVVVto Electrochemical Pretreatment of Carbon. J. Electrochem. Soc., 2016.

[63] Xi, J.; Zhang, W.; Li, Z.; Zhou, H.; Liu, L.; Wu, Z.; Qiu, X. Effect of Electro-Oxidation Current Density on Performance of Graphite Felt Electrode for Vanadium Redox Flow Battery. Int. J. Electrochem. Sci. 2013.

[64] Zhang, W.; Xi, J.; Li, Z.; Zhou, H.; Liu, L.; Wu, Z.; Qiu, X. Electrochemical Activation of Graphite Felt Electrode for Vo2+/Vo2+ Redox Couple Application. Electrochim. Acta, 2013.

[65] Hammer, E., Berger, B. & Komsiyska, L. Improvement of the Performance of Graphite Felt Electrodes for Vanadium-Redox-Flow-Batteries by Plasma Treatment. Int. Journal of Renewable Energy Development, 2014.

[66] Kim K.J., Kim Y.J., Kim J.H., Park M.S. The effects of surface modification on carbon felt electrodes for use in vanadium redox flow batteries. Mater. Chem. Phys., 2011.

[67] Dassisti, M., Mastrorilli, P., Rizzuti, A., Cozzolino, G., Chimienti, M., Olabi, A-G., Matera, F., & Carbone, A. (2016). Vanadium: A Transition Metal for Sustainable Energy Storing in Redox Flow Batteries. In M. S. J. Hashmi (Ed.), Reference Module in Materials Science and Materials Engineering Elsevier B.V.

[68] SIGRACELL®, “SIGRACELL® Battery Felts. Retrieved from https://www.sglcarbon.com/en/markets-solutions/material/sigracell-battery-felts/.” https://www.sglcarbon.com/en/markets-solutions/material/sigracell-battery-felts/.

[69] Di Blasi A., Di Blasi O., Briguglio N., Aricò A. S., Sebastián D., Lázaro M. J., Monforte G. and Antonucci V. Investigation of several graphite-based electrodes for vanadium redox flow cell. Journal of Power Sources, 2013.

[70] Wang Y-H, Hung I-M, Wu C-Y. The characteristics and electrochemical performance of graphite felts with thermal and Fenton’s reagent treatment for vanadium redox flow battery. Ceram Int, 2018.

[71] R.K. Gautam, A. Verma, Uniquely designed surface nanocracks for highly e cient and ultra-stable graphite felt electrode for vanadium redox ow battery, Mater. Chem. Phys. 251, 2020.

[72] M. Taylor, A. Pătru, D. Streich, M. El Kazzi, E. Fabbri, T.J. Schmidt. Vanadium (V) reduction reaction on modified glassy carbon electrodes–Role of oxygen functionalities and microstructure. Carbon 109, 2016

[73] P.C. Ghimire, R. Schweiss, G.G. Scherer, T.M. Lim, N. Wai, A. Bhattarai, et al., Optimization of thermal oxidation of electrodes for the performance enhancement in all-vanadium redox flow betteries, Carbon 155, 2019.

[74] Z. He, Y. Jiang, W. Meng, F. Jiang, H. Zhou, Y. Li, et al., HF/H2O2 treated graphite felt as the positive electrode for vanadium redox flow battery, Appl. Surf. Sci. 423, 2017.

[75] Chanyong Choi, Soohyun Kim, Riyul Kim, Yunsuk Choi, Soowhan Kim, Ho-young Jung, Jung Hoon Yang, Hee-Tak Kim, A review of vanadium electrolytes for vanadium redox flow batteries, Renewable and Sustainable Energy Reviews, Volume 69, 2017.

[76] Y. Huang, Q. Deng, X. Wu and S. Wang, N, O Co-doped carbon felt for high-performance all-vanadium redox flow battery, Int. J. Hydrogen Energy, 2017.

[77] Wu, X.; Xu, H.; Xu, P.; Shen, Y.; Lu, L.; Shi, J.; Fu, J.; Zhao, H. Microwave-treated graphite felcum redox flow battery. J. Power Sources, 2014.

[78] Kabtamu, D. M.; Chen, J. Y.; Chang, Y. C.; Wang, C. H. Water activated graphite felt as a high-performance electrode for vanadium redox flow batteries. J. Power Sources, 2017.

[79] Chang, Y. C.; Chen, J. Y.; Kabtamu, D. M.; Lin, G. Y.; Hsu, N. Y.; Chou, Y. S.; Wei, H. J.; Wang, C. H. High efficiency of CO2-activated graphite felt as electrode for vanadium redox flow battery application. J. Power Sources, 2017.

[80] X. Wu, H. Xu, Y. Shen, P. Xu, L. Lu, J. Fu, H. Zhao, "Treatment of graphite felt by modified Hummers method for the positive electrode of vanadium redox flow battery", Electrochim. Acta, Vol. 138, 2014.

[81] Lee, H.J.; Kil, D.; Kim, H. Synthesis of Activated Graphite Felt Using Consecutive Post-Treatments for Vanadium Redox Flow Batteries. J. Electrochem. Soc., 2016.

[82] X. M. Cui, H. B. Ding, X. E. Chen, Z. Y. Zeng, J. Wang, Z. C. Huang, Investigations on the Thermal and Acid Treatment of Graphite Felt for Vanadium Redox Flow Battery Application, Adv. Mat. Research 953-954, 2014.

[83] Kil, D., Lee, H. J., Park, S., Kim, S. and Kim, H., "Synthesis of Activated Graphite Felts using Short-Term Ozone/Heat Treatment for Vanadium Redox Flow Batteries," Journal of the Electrochemical Society, 164, 2017.

[84] Q. H. Liu et al., High Performance Vanadium Redox Flow Batteries with Optimized Electrode Configuration and Membrane Selection. J. Electrochem. Soc. 159, A1246–A1252, 2012.

[85] Noack, J.; Tübke, J. A Comparison of Materials and Treatment of Materials for Vanadium Redox Flow Battery.ECS Trans., 2010.

[86] L. Eifert, R. Banerjee, Z. Jusys, R. Zeis, Characterization of carbon felt electrodes for vanadium redox flow batteries: impact of treatment methods, J. Electrochem. Soc. 165 (11), 2018.

[87] Li X, Huang K, Liu S, Tan N, Chen L. Characteristics of graphite felt electrode electrochemically oxidized for vanadium redox battery application. Trans Nonferrous Mat Soc Chin, 2007.

[88] Zeng L, Zhao T, Wei L. Revealing the performance enhancement of oxygenated carbonaceous materials for vanadium redox flow batteries: Functional groups or specific surface area? Adv Sustain Syst, 2018.

[89] L. Eifert, Z. Jusys, R.J. Behm, R. Zeis, Side reactions and stability of pre-treated carbon felt electrodes for vanadium redox flow batteries: A DEMS study, Carbon, Volume 158, 2020.

[90] Marc-Antoni Goulet, Maria Skyllas-Kazacos, Erik Kjeang, The importance of wetting in carbon paper electrodes for vanadium redox reactions, Carbon, Volume 101, 2016.

[91] Monteiro, R.; Leiros, J.; Boaventura, M.; Mendes, A. Insights into all-vanadium redox flow battery: A case study on components and operational conditions. Electrochim. Acta, 2018.

[92] Mazur, P.; Mrlik, J.; Benes, J.; Pocedic, J.; Vrana, J.; Dundalek, J.; Kosek, J. Performance evaluation of thermally treated graphite felt electrodes for vanadium redox flow battery and their four-point single cell characterization. J. Power Sources, 2018.

[93] Y. H. Wang, I. M. Hung and C. Y. Wu, The characteristics and electrochemical performance of graphite felts with thermal and fenton's reagent treatment for vanadium redox flow battery, Ceram. Int., 2018.

[94] Alan M. Pezeshki, Jason T. Clement, Gabriel M. Veith, Thomas A. Zawodzinski, Matthew M. Mench, High performance electrodes in vanadium redox flow batteries through oxygen-enriched thermal activation, Journal of Power Sources, Volume 294, 2015.

[95] Langner, J.; Bruns, M.; Dixon, D.; Nefedov, A.; Woell, Ch.; Scheiba, F.; Ehrenberg, H.; Roth, C.; Melke, J. Surface properties and graphitization of polyacrylonitrile based fiber electrodes affecting the negative half-cell reaction in vanadium redox flow batteries. J. Power Sources 2016.

[96] Hassan A, Tzedakis T. Enhancement of the electrochemical activity of a commercial graphite felt for vanadium redox flow battery (VRFB), by chemical treatment with acidic solution of K2Cr2O7. J Energy Storage 2019.

[97] Gao, C.; Wang, N.F.; Peng, S.; Lin, S.Q.; Lei, Y.; Liang, X.X.; Zeng, S.S.; Zi, H.F. Influence of Fenton’s reagent treatment on electrochemical properties of graphite felt for all vanadium redox flow battery. Electrochim. Acta 2013.

[98] Ali Hassan, Theodore Tzedakis. Facile chemical activation of graphite felt by KMnO4 acidic solution for vanadium redox flow batteries. Applied Surface Science 2020.

[99] Y. Wang, Y. Liu, K. Wang, S. Song, P. Tsiakaras, H. Liu, Preparation and characterization of a novel KOH activated graphite felt cathode for the electro-Fenton process, Appl. Catal. B: Environ. 165, 2015.

[100] Rajeev K. Gautam, Anil Verma, Uniquely designed surface nanocracks for highly efficient and ultra-stable graphite felt electrode for vanadium redox flow battery, Materials Chemistry and Physics,Volume 251, 2020.

[101] S. Abbas, H. Lee, J. Hwang, A. Mehmood, H.-J. Shin, S. Mehboob, J.-Y. Lee, H. Y. Ha, A novel approach for forming carbon nanorods on the surface of carbon felt

electrode by catalytic etching for high-performance vanadium redox flow battery, Carbon, vol. 128, pp. 31-37, 2018.

[102] Ertan Agar, C.R. Dennison, K.W. Knehr, E.C. Kumbur, Identification of performance limiting electrode using asymmetric cell configuration in vanadium redox flow batteries, Journal of Power Sources, Volume 225, 2013.

[103] Y. H. Wang, I. M. Hung and C. Y. Wu, The characteristics and electrochemical performance of graphite felts with thermal and fenton's reagent treatment for vanadium redox flow battery, Ceram. Int., 2018.

[104] B. Sun, M. Skyllas-Kazakos. Chemical modification and electrochemical behaviour of graphite fibre in acidic vanadium solution. Electrochim. Acta 1991, 36, 513.

[105] C. Yao, H. Zhang, T. Liu, X. Li, Z. Liu. Carbon paper coated with supported tungsten trioxide as novel electrode for all-vanadium flow battery. J. Power Sources 2012.

[106] H. M. Tsai, S. J. Yang, C. C. M. Ma, X. Xie. Preparation and electrochemical activities of iridium-decorated graphene as the electrode for all-vanadium redox flow batteries. Electrochim. Acta 2012.

[107] Y. Xiang, W. A. Daoud. Electrochemical Enhancement of Carbon Paper by Indium Modification for the Positive Side of Vanadium Redox Flow Battery J. Electrochem. Soc. 2017.

[108] Z. González, A. Sánchez, C. Blanco, M. Granda, R. Menéndez, R. Santamaría. Enhanced performance of a Bi-modified graphite felt as the positive electrode of a vanadium redox flow battery Electrochem. Commun., 2011.

[109] Li, B.; Gu, M.; Nie, Z.; Shao, Y.; Luo, Q.; Wei, X.; Li, X.; Xiao, J.; Wang, C.; Sprenkle, V.; et al. Bismuth Nanoparticle Decorating Graphite Felt as a High-Performance Electrode for an All-Vanadium Redox Flow Battery. Nano Lett. 2013.

[110] D. J. Suárez, Z. González, C. Blanco, M. Granda, R. Menéndez, R. Santamaría. Graphite Felt Modified with Bismuth Nanoparticles as Negative Electrode in a Vanadium Redox Flow Battery. ChemSusChem, 2014.

[111] T. Liu, X. Li, H. Nie, C. Xu, H. Zhang. Investigation on the effect of catalyst on the electrochemical performance of carbon felt and graphite felt for vanadium flow batteries J. Power Sources, 2015.

[112] Y. Shen, H. Xu, P. Xu, X. Wu, Y. Dong, L. Lu. Electrochemical catalytic activity of tungsten trioxide- modifiedgraphite felt toward VO2+/VO2+redox reaction. Electrochim. Acta 2014.

[113] D. M. Kabtamu, J.-Y. Chen, Y. C. Chang, C.-H. Wang. Electrocatalytic activity of Nb-doped hexagonal WO3 nanowire-modified graphite felt as a positive electrode for vanadium redox flow batteries. J. Mater. Chem. A 2016.

[114] D. M. Kabtamu, Y.-C. Chang, G. Y. Lin, A. W. Bayeh, J.-Y. Chen, T. H. Wondimu, C.-H. Wang. Three-Dimensional Annealed WO3 Nanowire/Graphene Foam as an Electrocatalytic Material for an All Vanadium Redox Flow Battery. Sustainable Energy Fuels 2017.

[115] M. Faraji, A. Hassanzadeh, M. Mohseni. Interlaced WO3-carbon nanotube nanocomposite electrodeposited on graphite as a positive electrode in vanadium redox flow battery. Thin Solid Films 2017.

[116] M. G. Hosseini, S. Mousavihashemi, S. Murcia-López, C. Flox, T. Andreu, J. R. Morante. High-power positive electrode based on synergistic effect of N- and WO3 decorated carbon felt for vanadium redox flow batteries Carbon 2018.

[117] A. W. Bayeh, D. M. Kabtamu, Y. C. Chang, G. C. Chen, H. Y. Chen, T. R. Liu, T. H. Wondimu, K. C. Wang, C. H. Wang. Hydrogen-Treated Defect-Rich W18O49 Nanowire-Modified Graphite Felt as High-Performance Electrode for Vanadium Redox Flow Battery. ACS Appl. Energy Mater. 2019.

[118] S. Mehboob, G. Ali, H.-J. Shin, J. Hwang, S. Abbas, K. Y. Chung, H. Y. Ha. Enhancing the performance of all-vanadium redox flow batteries by decorating carbon felt electrodes with SnO2 nanoparticles. Appl. Energy 2018.

[119] T. M. Tseng, R. H. Huang, C. Y. Huang, C.-H. Liu, K. L. Hsueh, F. S. Shieu. Carbon Felt Coated with Titanium Dioxide/Carbon Black Composite as Negative Electrode for Vanadium Redox Flow Battery. J. Electrochem. Soc. 2014.

[120] B. Hou, X. Cui, Y. Chen. In situ TiO2 decorated carbon paper as negative electrode for vanadium redox battery. Solid State Ionics 2018, 325, 148. flow battery Int. J. Energy Res. 2019.

[121] J. Vázquez-Galván, C. Flox, C. Fàbrega, E. Ventosa, A. Parra, T. Andreu, J. R. Morante. Hydrogen treated Rutile TiO2 shell in graphite core structure as a negative electrode for high-performance vanadium flow batteries ChemSusChem 2017.

[122] L. Wei, T. S. Zhao, L. Zeng, Y. K. Zeng, H. R. Jiang. Highly catalytic and stabilized titanium nitride nanowire array-decorated graphite felt electrodes for all vanadium redox flow batteries. J. Power Sources, 2017.

[123] D. Cheng, G. Cheng, Z. He, L. Dai, L. Wang. Electrocatalytic performance of TiO2 with different phase state towards V2+/V3+ reaction for vanadium redox. International Journal of Energy Research, 43, 2019.

[124] B. Li, M. Gu, Z. Nie, X. Wei, C. Wang, V. Sprenkle, W. Wang. Nanorod Niobium Oxide as Powerful Catalysts for an All Vanadium Redox Flow Battery. Nano Lett. 2013.

[125] A. W. Bayeh, D. M. Kabtamu, Y. C. Chang, G. C. Chen, H. Y. Chen, G. Y. Lin, T. R. Liu, T. H. Wondimu, K. C. Wang, C. H. Wang. Ta2O5-Nanoparticle-Modified Graphite Felt As a High-Performance Electrode for a Vanadium Redox Flow Battery. ACS Sustainable Chem. Eng. 2018, 6, 3019.

[126] W. Y. Li, J. G. Liu and C. W. Yan. Multi-walled carbon nanotubes used as an electrode reaction catalyst for VO2 +/VO2+ for a vanadium redox flow battery Carbon, 2011.

[127] G. Wei, C. Jia , J. Liu , C. Yan. Carbon felt supported carbon nanotubes catalysts composite electrode for vanadium redox flow battery application. J. Power Sources 220, 2012.

[128] Yang, H., Fan, C., Zhu, Q. Sucrose pyrolysis assembling carbon nanotubes on graphite felt using for vanadium redox flow battery positive electrode. J. Energy Chem. 2018.

[129] Chang, Y.-C.; Shih, Y.-C.; Chen, J.-Y.; Lin, G.-Y.; Hsu, N.-Y.; Chou, Y.-S.; Wang, C.-H. High efficiency of bamboo-like carbon nanotubes on functionalized graphite felt as electrode in vanadium redox flow battery. RSC Adv. 2016.

[130] Z. Gonzalez, P. Alvarez, C. Blanco, S. Vega-Dıaz, F. Tristan Lopez, L. P. Rajukumar, R. Cruz-Silva, A. L. Elas, M. Terrones and R. Menndez. The influence of carbon nanotubes characteristics in their performance as positive electrodes in vanadium redox flow batteries. Sustainable Energy. Technologies and Assessments, 2015.

[131] Moghim, M.H., Eqra, R., Babaiee, M., Zarei-Jelyani, M., Mohsen Loghavi, M. Role of reduced graphene oxide as nano-electrocatalyst in carbon felt electrode of vanadium redox flow battery. J. Electroanal. Chem. 2017.

[132] Z. Gonz_alez, C. Flox, C. Blanco, M. Granda, J.R. Morante, R. Menendez, R. Santamaría. Outstanding electrochemical performance of a graphene-modified graphite felt for vanadium redox flow battery application. J. Power Sources 338, 2017.

[133] G. J. Wei, C. K. Jia, J. G. Liu and C. W. Yan. Carbon felt supported carbon nanotubes catalysts composite electrode for vanadium redox flow battery applicationJ. Power Sources, 2012.

[134] Ghimire, P. C. (2019). Electrode modification and in-situ studies to enhance the performance of vanadium redox flow batteries. Doctoral thesis, Nanyang Technological University, Singapore.

[135] M.A. Goulet, O.A. Ibrahim, W.H.J. Kim, E. Kjeang. Maximizing the power density of aqueous electrochemical flow cells with in operando deposition J Power Sources, 339, 2017.

[136] Qiang Li, Qing Dong, Tianyu Zhang, Zhichao Xue, Jie Li, Zinan Wang, Hong Sun, Performance of room-temperature activated tubular polypyrrole modified graphite felt composite electrode in vanadium redox flow battery, Electrochimica Acta, Volume 409, 2022.

[137] Vázquez-Galván, J., Flox, C., Fàbrega, C., Ventosa, E., Parra, A., Andreu, T., Morante, J.R. "Hydrogen-Treated Rutile TiO2Shell in Graphite-Core Structure as a Negative Electrode for High-Performance Vanadium Redox Flow Batteries" ChemSusChem 10, 9, pp.2089 - 2098. 2017.

[138] Schneider J, Bulczak E, El-Nagar GA, Gebhard M, Kubella P, Schnucklake M, Fetyan A, Derr I, Roth C. Degradation Phenomena of Bismuth-Modified Felt Electrodes in VRFB Studied by Electrochemical Impedance Spectroscopy. Batteries. 2019.

[139] Gang Cheng, Yingqiao Jiang, Yuehua Li, Jian Chen, Zhangxing He, Wei Meng, Lei Dai, Ling Wang, Electrospun carbon nanofiber inlaid with tungsten carbide nanoparticle by in-situ carbothermal reaction as bifunctional electrode for vanadium redox flow battery, Electrochimica Acta, Volume 362, 2020.

[140] Lorenz Gubler, Membranes and separators for redox flow batteries, Current Opinion in Electrochemistry, Volume 18, 2019.

Appendix

Wettability Measurements

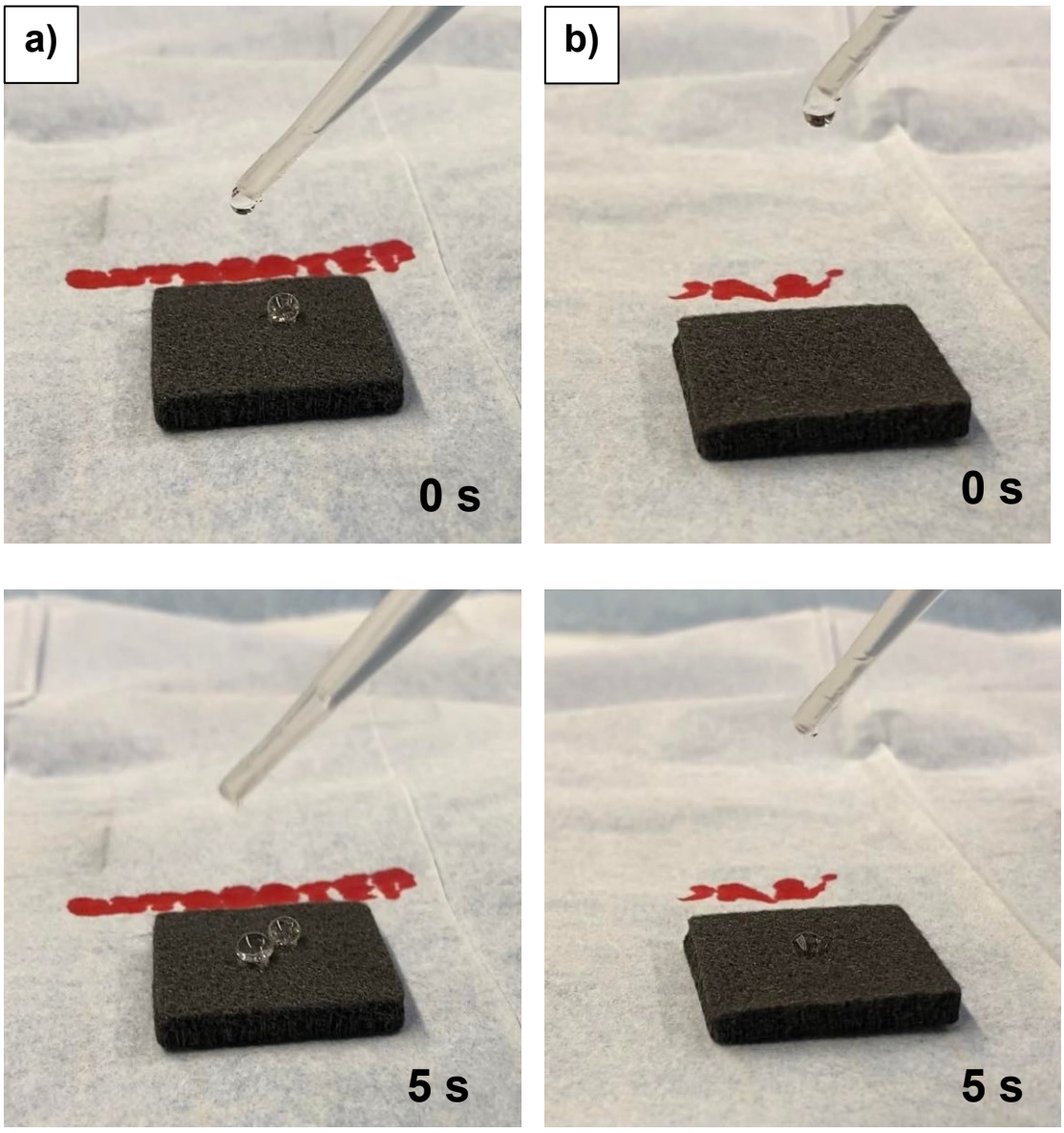

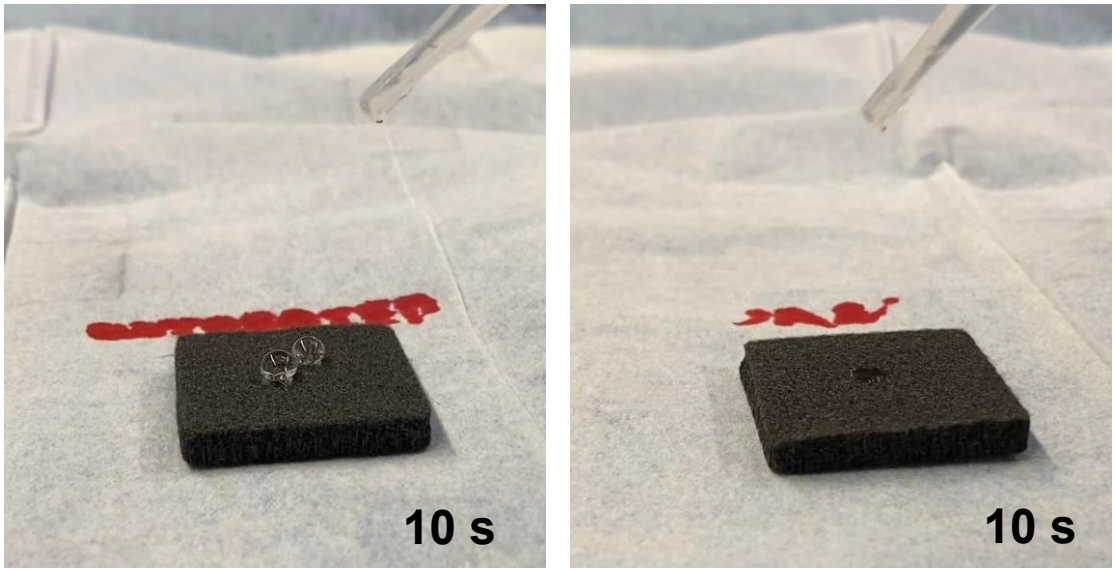

Figure 67. Wettability assessment for a) Pristine and b)Thermally treated electrodes.